Steam Gasification of Excavated Waste Residue (EWR) from a Landfill Bioreactor Operated Under Cold Climatic Conditions

by

Stephen Adewunmi Banjo

A thesis
presented to the University of Waterloo
in fulfilment of the
thesis requirement to the degree of
Master of Applied Science

in
Mechanical Engineering

Waterloo, Ontario, Canada, 2022

Author’s Declaration

This thesis consists of material all of which I authored or co-authored: see Statement of Contributions included in the thesis. This is a true copy of the thesis, including any required final revisions, as accepted by my examiners.

I understand that my thesis may be made electronically available to the public.

Statement of Contribution

Stephen Banjo is the sole author for Chapters 1, 2, 4, and 5 which are written under the supervision of Prof. Zhongchao Tan and Prof. Joseph Patrick Hettiaratchi and are not written for publication. Exceptions to sole authorship of material are as follows:

Research presented in Chapter 3:

This research methodology is conducted at the University of Waterloo by Stephen Banjo under the supervision of Prof. Zhongchao Tan and Prof. Joseph Patrick Hettiaratchi. Stephen Banjo designs this study and completes the sample preparation, data collection and analysis. The waste sample used in this research was excavated from the landfill by the research team at the University of Calgary. The procedure of the waste sample collection was written by Tina Abedi Yarandy, a student at the University of Calgary. The procedure of the waste sample collection from the landfill written by Tina Abedi Yarandy was used as a guide in writing section 3.1: Waste Sample of this thesis.

Abstract

The use of fossil fuel to generate energy has contributed to the emission of greenhouse gases, which is a leading factor in the depletion of the ozone layer. This effect of fossil fuel on the atmosphere has led to the push for a renewable source of energy with less environmental problems. Gasification of excavated landfill waste residue (EWR) is one of the promising alternatives of generating environmentally friendly energy. Steam gasification has proven to be the most favorable method among the various methods of converting waste to energy. This method enhances the quality and heating value of the produce gas.

This study examines the energy potential of converting EWR into useful gases by steam gasification. This study evaluates the effects of factors such as temperature, reaction time, and steam to feedstock ratio on the steam gasification. Optimization of the gasification process and the interaction effect of these factors on the gasification products were also investigated using the response surface methodology (RSM) based on Box Behnken experimental design. In addition, analysis of variance (ANOVA) was conducted to determine the level of confidence of the quadratic model derived from the Box Behnken method.

The products obtained during the steam gasification process include hydrogen (H_2), carbon monoxide (CO), carbon dioxide (CO_2), methane (CH_4), and tar. The optimum process conditions for the steam gasification are 1000 ^{0}C, a reaction time of 45 minutes, and a steam to feedstock ratio of 0.5. The ANOVA results show that temperature and reaction time significantly influence the steam gasification process compared to the steam to feedstock ratio.

The results also show that product gas yield increases with temperature. As the gasification temperature increases from 800 ^{0}C to 1000 ^{0}C, the product gas yield increases by 230% while the tar yield decreases by 73%, at a constant reaction time of 45 minutes, and a steam to feedstock ratio of 0.5. To obtain maximum product gas output, the steam-to-feedstock ratio and the reaction time was kept within the optimum value.

Finally, the lower heating value (LHV) of the product gas, the carbon gasification efficiency, and the cold gas efficiency of the steam gasification process all increase with

increasing gasification temperature and reaction time. The LHV increased by 450% as the temperature increased from 800 ^{0}C to 1000 ^{0}C and the reaction time from 15 to 45 minutes, with a steam to feedstock ratio of 0.5. Under the same condition, the carbon gasification efficiency and cold gas efficiency also increased by about 7% and 10%, respectively.

Acknowledgements

I would like to take this opportunity to thank the individuals and organizations that have contributed to the success of this journey, which I will always cherish.

I would like to express my deep gratitude to my supervisor, Professor Zhongchao Tan, at the University of Waterloo and co-supervisor, Professor Joseph Patrick Hettiaratchi, at the University of Calgary, for their support, guidance, and patience throughout this journey. I have been fortunate to have benefitted from their dedication to help students achieve success.

I am grateful to the examining committee, Professors John Wen and Jean-Pierre Hickey for their time and valuable feedback on this thesis.

I would like to thank the Department of Mechanical and Mechatronic Engineering, University of Waterloo, for the Graduate Research studentship (GRS) funding, and the Natural Sciences and Engineering Research Council of Canada (NSERC) CREATE IISC for their funding support.

Many thanks to all the members of the Laboratory for Green Energy and Pollution Control Research. To name a few: Yifu Li, Yi Zhang, and Jiawen Zheng, thanks for your support. I would also like to thank Joel Mills and Dr. Hesheng Yu for their intellectual input in my experimental design and data analysis.

Finally, I would like to thank my wife, Oluwakemi Amodu, for her patience, love, and encouragement along this journey. I would also like to thank my parents and my family for their unconditional love and encouragement.

Table of Contents

List of Figures

List of Tables

List of Symbols and Abbreviations

Symbol	**Definition**
μ	Micro
n	Number of moles
η	Efficiency
β	Beta
Σ	Summation
%	Percentage
Y	Response variable
Abbreviation	**Definition**
CH_4	Methane
CO	Carbon monoxide
CO_2	Carbon dioxide
ELFM	Enhanced landfill mining
EWR	Excavated waste residue
FID	Flame ionization detector
GHGs	Green house gases
CGE	Cold gas efficiency
GC	Gas chromatography
H_2	Hydrogen gas
LHV	Lower heating value
MSW	Municipal solid waste
N_2	Nitrogen gas
RDF	Refuse derived fuel

RES	Renewable energy source
RSM	Response surface methodology
TCD	Thermal conductivity detector
WM	Waste management
wt	Weight
WtE	Waste to energy
WtM	Waste to material
Subscript	**Definition**
PG	Product gas
CG	Cold gas
f	Feedstock

Chapter 1

Introduction

1.1 Background

The use of fossil fuel since the industrial revolution has contributed to climate change and led to a strong push for renewable energy sources [1]. Reducing air pollution and greenhouse gas (GHG) emissions result from fossil fuel combustion is the primary driving force of renewable energy sources (RES) [1][2]. In addition, air emissions from fossil fuel combustion contribute to the depletion of the ozone layer [3][4]. GHGs such as carbon dioxide (CO_2), methane (CH_4) and nitrous oxide (N_2O) have contributed to global warming for about 60%, 15% and 5%, respectively [4]. As a result, there is a need for renewable resources that can reduce these GHG emissions.

It is estimated that more than half of the global GHG emissions are from the G7 countries (Canada, France, Germany, Italy, Japan, the United Kingdom, and the USA) and the BRICS economies (Brazil, Russia, India, China, and South Africa) [5]**.** As shown in Figure 1.1, in 2018, China and the United States accounted for 25 and 12% of global emissions of GHGs, respectively. Canada's GHG emissions rank relatively low, accounting for less than 2% of global emissions.

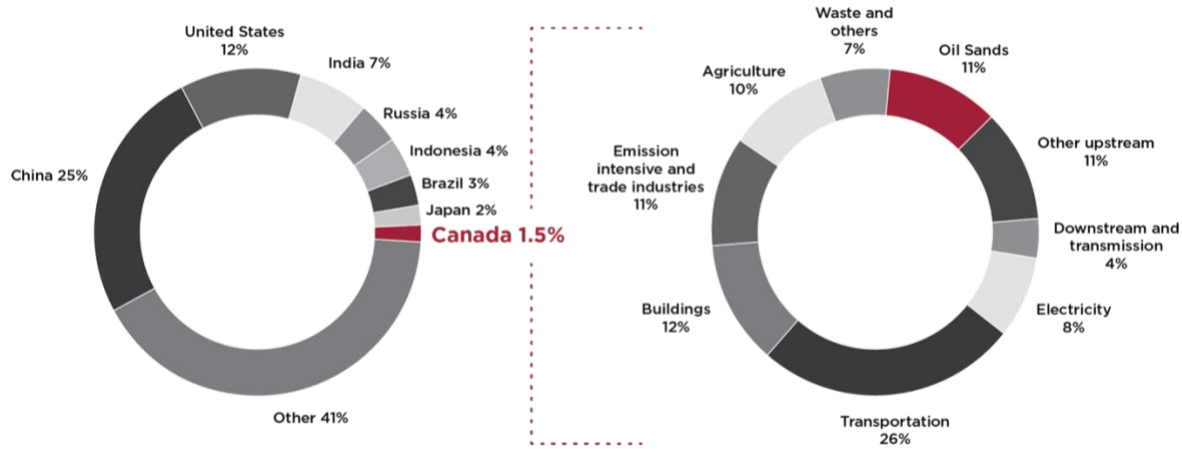

Figure 1.1. Global and Canada GHG emissions in 2018 [6]

Renewable energy is considered clean for its significantly low environmental impact [7]. In the choice of renewable resources, it is imperative to consider a wide range of factors, such as cost, cleanness, efficiency, stability, and environmental impact. Solar, wind, geothermal, hydropower, tidal, and biomass are the major resources for renewable energy production. They can also be converted into other forms of energy career, such as electricity, gas, and biofuels [8].

Municipal solid waste (MSW) is one type of biomass, which is the collection of urban wastes such as household wastes, business wastes, and waste originating from public agencies [9]. The MSW is mainly composed of wastepaper, food, wood, garden waste, cotton, and leather. It can also include plastic and fabrics. Table 1.1 summarizes the global generation of MSW. In 2016, it was 2.01 billion tons, and it is estimated to rise to 2.59 and 3.40 billion tons by 2030 and 2050, respectively [5]. Nevertheless, high-income regions like North America and Europe account for 34% of the global MSW generation, while rapid development in lower- and middle-income regions such as Sub-Saharan Africa, the Middle East, and Central Asia contribute to more than half of the total global MSW by 2050 [5].

Table 1.1. Global waste generation and projection by geographical region [5]

Geographical region	Waste generation in 2016 (millions of tons/year)	Projected waste generation in 2030 (millions of tons/year)	Projected waste generation in 2050 (millions of tons/year)
Middle East and North Africa	129	177	255
Sub-Saharan Africa	174	269	516
Latin America and Caribbean	231	290	369
North America	289	342	396
South Asia	334	466	661
Europe and Central Asia	392	440	490
East Asia and Pacific	468	602	714

Landfill and open dumps have been the primary means of disposing MSW around the world [10]. The percentages of MSW landfilled in the USA, Brazil, Saudi Arabia, Malaysia, and China are 52.6% [10], 59.1% [11], 85% [12], 94.5% [13], and 79% [14], respectively. In Venezuela, 32% of the MSW goes to sanitary landfills, controlled disposal accounts for 43%, and non-controlled disposals or open dumps take 24% of the MSW [15]. In Mexico, 65% goes to sanitary landfills and 30% to open dumps [16]. In Thailand, 27% of MSW goes to landfill [17], [18]. Studies comparing the various waste management (WM) methods (landfilling, incineration, composting, *etc*.) show that sanitary landfilling or open dumping is the most popular option in most countries because of their low technical requirement and relatively low cost [17].

Meanwhile, technologies are available to transform solid biomass into energy careers for the protection of the environment because waste-based fuels have slightly smaller carbon footprints than fossil fuels do [19]. These technologies include hydrothermal liquefaction [21], pyrolysis [22], and gasification [23]. However, it is not clear whether it is technically and economically feasible to convert MSW into energy resources.

1.2 Motivation and Challenges of the Thesis Research

The primary method of disposing of MSW in North America is landfilling for low costs and available land. About 75% of the MSW generated in Canada is landfilled [20]. On the other hand, fugitive emissions from landfill sites are one of the largest anthropogenic sources of atmospheric methane (CH_4) in developed countries. In Canada, for example, approximately 25% of anthropogenic CH_4 emissions are from landfills [20]. However, CH_4 is also an energy resource [21].

Recently, landfill space has become a challenge in Canada, particularly in urban centers like Calgary, Alberta. As a result, municipalities are examining the ways to maximize the use of available landfill space, while exploring the potential of converting landfill waste into energy resources [22]. One option is to convert the dry-tomb landfill site into a bioreactor, which expedites the biodegradation of organic compounds in the MSW by increasing microbial activity and cycling nutrients [22]. Calgary Bio-cell located in the City of Calgary is an example of this type of fully functional bioreactor [20].

Figure 1.2 shows the operation of the Calgary Bio-cell. In the first stage, the cell is operated as an anaerobic bioreactor to enhance landfill gas production. In the second stage, the bio-cell is operated in an aerobic mode to produce compost or materials that can be converted into refuse derived fuel (RDF). In the final stage, the wastes are mined, and the land space is reclaimed, ensuring the sustainable operation of the Biocell. The recovered space in the mined area can be utilized for a variety of purposes, including the creation of another bio-cell [22].

Figure 1.2. Phases of bio-cell operation with example durations [23]

On a larger scale, Enhanced Landfill Mining (ELFM) is gaining societal interest as a viable alternative to conventional remediation technique for landfill mining [24]. The ELFM involves the integration of landfill excavation, advanced materials sorting and processing, and thermo-conversion processes to recover materials and energy resources for reuse. Accordingly, the motivation of this thesis work is to investigate the energy potential of the EWR from the Calgary Bio-cell using the ELFM technique.

1.3 Research Objectives

The main objective of this research is to evaluate the energy value of the excavated waste residue (EWR) from City of Calgary Bio-cell. To achieve this main objective, this thesis

- characterizes the residual waste of the Bio-cell.
- develops a system to carry out steam gasification of the excavated landfill waste.
- evaluates the chemical composition of the gaseous product and its energy intensity
- optimizes and studies the interaction of the independent variables of the steam gasification process

- evaluates the effects of gasification temperature, steam to feedstock ratio, and residence time on product gas yield.

The residual landfill waste was excavated from the Calgary Bio-cell that has been operated for about fifteen years.

1.4 Thesis Structure

The thesis is organized into five chapters. Chapter 1, this chapter, presents the background, motivation, and objectives of the thesis work. Chapter 2 reviews recent advances in waste management and the technologies for waste conversion into energy resources. Chapter 3 presents the design of the experimental apparatus and the methodology used in this study. The methodology includes the description of the waste samples, sample preparation, sample analyses, and the product gas characterization. Chapter 4 presents the results and discussion, and Chapter 5 summarizes the conclusions of the study and recommendations for future studies.

Chapter 2

Literature Review

2.1 Waste Management

Waste is any substance that is discarded for disposal or has been required to be discarded by the holder [25]. With increasing population and urbanization, the amount of waste generate globally has been steadily increasing [26]. Various wastes originate from manufacturing processes, industries, and municipal solid wastes (MSW) [26]. Improper management of the wastes poses a long-term environmental impact, including pollution of the air, soil, and ground waters, as a well as decrease in land space because of landfilling processes [27]. A global perspective on resource management emphasizes the importance of education and awareness in waste and waste management [26].

Waste management is the process of collecting, transporting, processing, recycling, or disposing of waste [26]. The waste management practices differ between developed and developing countries, as well as between urban and rural areas and between residential and industrial sources [28]. The goal of proper waste management is to encourage the reuse of materials in society and provide sanitary living conditions while reducing the amount of waste[26].

Waste management helps achieve the following goals [28]:

- Reduction the total amount of waste
- Recycling and reintroduction of suitable substances into production cycles as secondary raw materials or energy sources
- Re-introduction of biodegradable wastes into the natural cycle
- Reducing the amount of residual waste disposed of on landfills
- Flexibility regarding the fluctuations in waste quantities and composition

2.2 Waste Management System

As shown in Table 2.1, a waste management system consists of four major elements: (1) generation, *i.e.*, how waste is generated, (2) collection and transport, *i.e.*, collection systems and how waste are being transported, (3) treatment, *i.e.*, how waste is converted into useful products, (4) final disposal, *i.e.*, recycling of waste materials or landfilling of such materials. The waste management system encompasses all the activities associated with handling, treatment, disposal, and recycling of waste materials [29].

Table 2.1. Components of waste management systems [26]

Main component	Sub-parts
Production of waste materials	Waste source
	Source separation
	Internal collection
	Production rate
	Waste types
Collection and transport	Collection
	Transport
	Transfer
Treatment	Physical reprocessing: Shredding, sorting, compacting
	Thermal reprocessing: incineration, gasification
	Biological reprocessing: Anaerobic digestion, aerobic composting
Final disposal	Recycling
	Landfilling

2.3 Waste Management Methods

Most developed countries have strict regulations regarding the management of waste, which make the remediation of waste sites an important issue, from both a safety and a site preparation perspective (*e.g* construction) [30].

Waste management methods may be divided into the following categories:

- Recycling – It refers to the process of recovering materials from products after they have been used.
- Composting - This is a type of biological method of degrading biodegradable materials.
- Sewage treatment – This involves the treatment of sewage to produce a non-toxic liquid effluent that is discharged into rivers or sea, and as a semi-solid sludge it can either be used for soil improvement or incinerated or disposed in landfills.
- Incineration – This is a means of reclaiming energy from waste while minimizing the volume of waste to be disposed.
- Landfilling – This is a special area for the disposal of waste, which consists of pre-constructed enclosure lining with an impermeable layer (natural or artificial) with controls to minimize the emissions.

2.3.1 Recycling

Recycling refers to the process of separating, collecting, processing, and reusing of a material that might otherwise be discarded [31]. Recycling as one of the strategies of minimizing waste, offers three advantages: (i) it decreases the demand for new resources, (ii) it reduces the cost of transportation and production energy, and (iii) it reuses waste materials that would otherwise be disposed into landfill sites [32].

2.3.2 Composting

The process of composting is defined as the biological breakdown of organic materials by microorganisms [33]. It is a natural process to stabilize organic waste products that can result to the development of highly nutritive materials, popularly known as compost or humus, depending on the sources of the organic waste materials [34]. For example, Bundela *et al.* [35] reported a process as one of the most cost-effective and sustainable options in municipal solid waste management, surpassing the traditional methods like landfilling and burning. It allows recycling of potential plant nutrients, which constitute the bulk of waste in most developing countries. The by-product of composting, which is either a compost or humus, can be used as agricultural productions, horticulture, and land reclamations, particularly those

relating to the reclamation of burrows pits and other areas of land depressions [36]. The sustainability of composting technologies is therefore a major driving force behind a more efficient and economically viable way to utilize related technologies, which contribute to the sustainability of both agricultural and social systems [37].

2.3.3 Incineration

Incineration refers to the process of oxidizing combustible waste to produce heat and air pollutants [38]. Incineration and other methods of treating waste at high temperatures are sometimes referred to as "thermal treatment". Despite considerable public opposition to incineration due to the emissions of pollutants, such as carbon monoxide, hydrogen fluoride, sulphur dioxide, volatile organic carbon, dioxins and furans, and heavy metals, into the air, it is often the only practical means of disposing hazardous but highly flammable, volatile, toxic, and infectious wastes. For example, clinical wastes cannot be disposed of in landfills in the United States due to their potential health risks, and any recycling and reusing must be done after sterilization [39]. On the other hand, there are problems of waste incineration, including construction and the start-up of the facilities, which may be too expensive for developing countries.

2.3.4 Landfilling

A landfill is a designated terrestrial burial site, which is usually located outside a municipality's suburban areas, for the disposal of biodegradable and non-biodegradable wastes [40]. In many countries, landfilling has been the most lucrative waste disposal method. For example, there are about 150,000 to 500,000 landfill sites in the European Union, which serve as a repository for the massive amount of municipal solid waste generated throughout Europe [41]. It is estimated that the United State and Canada have over 2000 active landfill sites to dispose of their municipal solid waste [42]. According to Giroux [42], nearly 97% of residual solid wastes in Canada are landfilled after diversion, *i.e.* recycling, composting, and energy recovery.

Landfilling is a more effective way to dispose municipal solid waste than incineration and recycling because of its cost-effectiveness and modest labor requirement. In addition, landfills can generate revenues by energy production from landfill gases. With the

implementation of efficient, integrated technologies as shown in Figure 2.1, these waste stores can be transformed from waste stores into clean energy source [40].

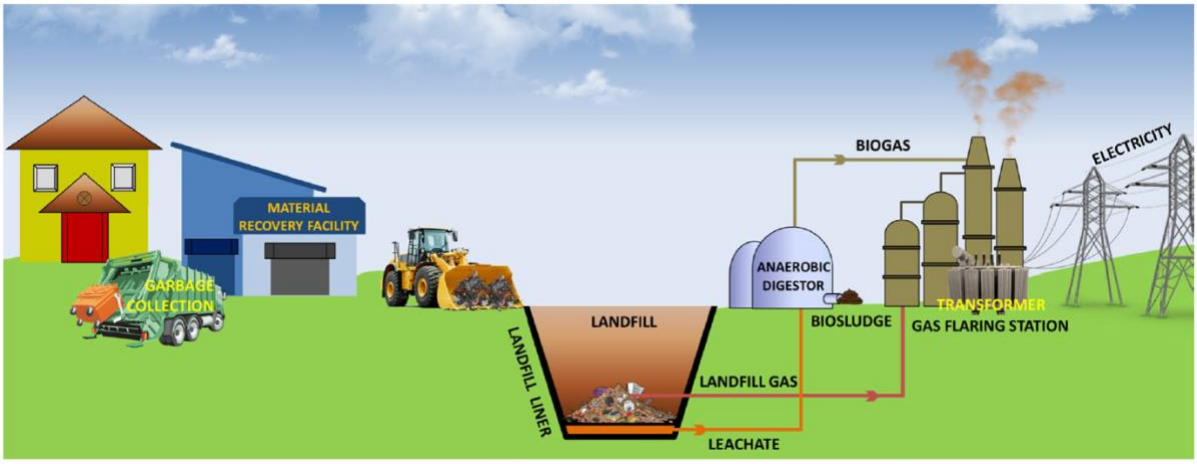

Figure 2.1. Conventional municipal solid waste landfilling system [40]

Government authorities around the world are responsible for the regulation of landfill to avoid dumping of infectious biomedical wastes from healthcare clinics, hospital, and toxic industrial residue into landfill sites [44]. Examples of developed nations that have strict landfill regulations include United States (*i.e.*, US Environmental Protection Agency, USEPA), Scotland (*i.e.*, Scottish Environmental Protection Agency), the United Kingdom (*i.e.*, Landfill Allowance Trading Scheme), the European Union (*i.e.*, Landfill Directive), Northern Ireland (*i.e.*, Northern Ireland Environmental Agency), and Canada (*i.e.*, Canadian Environmental Protection Act, CEPA)

Landfills may be classified according to the type of refuse disposed:

- Class 1: landfill use for soil disposal
- Class 2: landfill use for minerals, construction, and demolition waste disposal
- Class 3: landfill use for municipal solid waste disposal
- Class 4: landfill use for commercial and industrial waste disposal
- Class 5: landfill use for hazardous waste disposal [43].

The various classes of landfills can also be categorized into four basic types: open dumps, semi-controlled dumps, sanitary landfill, and bioreactor landfill [44].

The open dump landfill refers to a land area where municipal solid wastes are disposed of in an open environment with outdoor air circulation [43]. This type of landfill is often found in developing countries; municipal solid waste refuses in these landfill sites are disposed of indiscriminately in open areas with low ground levels. Poor management of these landfills provides a habitat for scavengers such as falcons, eagles, vultures, crows, and other birds as well as flies, mosquitoes, pests, worms, rodents, and pathogenic microorganisms [44]. The smell of persistent stench emanating from open dump landfill areas is a common problem with the type of landfill. Numerous developed countries consider open dumping as a violation of their regulatory laws and it has been banned in those countries.

Semi-controlled dump landfill is a type of landfills that is operated in designated dump location, where the municipal solid waste is sorted, shredded, and compacted before disposal. Piles of thrash are crushed and leveled and then covered with a layer of topsoil to prevent the breeding of scavenging birds, animals, pests and microorganisms. Despite the relatively less foul smell of the semi-controlled landfills due to topsoil cover, they are not designed to manage landfill gas emission and leachate discharge [44].

A sanitary landfill shown Figure 2.2 is a more advanced type of semi-controlled landfill. In addition to sorting, segregating, reducing the size of the waste, densifying and topsoil covering, the sanitary landfills have designed facilities to collect liquid leachate and landfill gas emissions. Sanitary landfills are typically located outside a regional boundary, away from residences, and they are characterized with the placement of cover soil on top of a freshly disposed waste to minimize odor, disease vectors, fires, and waste scavenging [40]. This type of landfill is common in developed countries where facilities for intercepting and treating the leachate are available.

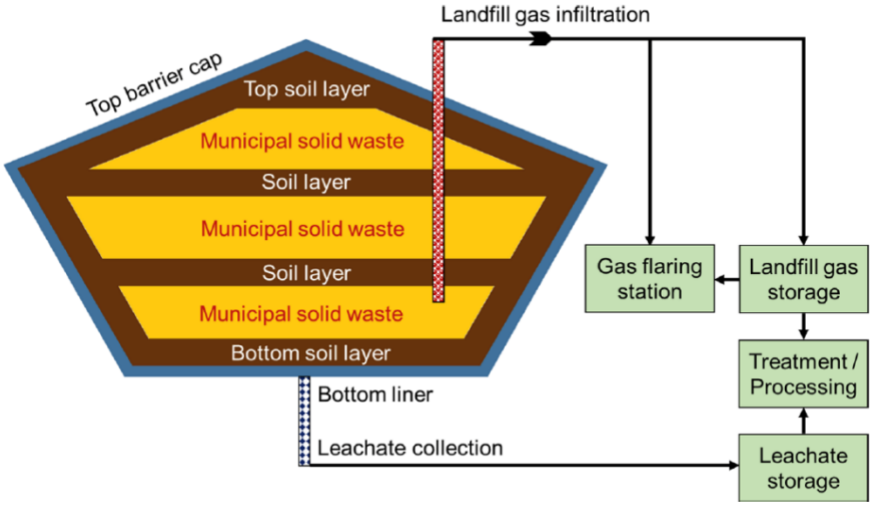

Figure 2.2. A typical sanitary landfill [40]

Even though this type of landfill minimizes groundwater contamination and the emission of landfill gas, the following residual problems still exist:

- This method is not sustainable because there is always a need to build new landfills every few years after the existing one is saturated.
- There is a long-term liability issue related to the landfill. The biodegradation process in this type of landfill is extremely slow, and it will take a long time for the waste to stabilize. In general, it may be necessary to monitor the potential environmental impacts of the landfill for a long period of time, until the waste has been fully stabilized.
- This type of landfill does not explicitly address the issue of landfill gas [45].

Recent research on sanitary landfills indicates that the operation of landfills as bioreactors may be feasible [40][40], [45]. As shown in Figure 2.3, a bioreactor landfill is an advancement in the design of sanitary landfill to enhance the degradation of the biodegradable fraction of the waste by micro-organisms, leading to faster mineralization and stabilization. A conventional sanitary landfill hinders the biodegradation by reducing the moisture content in the landfill, whereas a bioreactor expedite the biodegradation process by controlled moisture input in the landfill, leachate recirculation and increasing cycling of nutrients and bacterial populations.

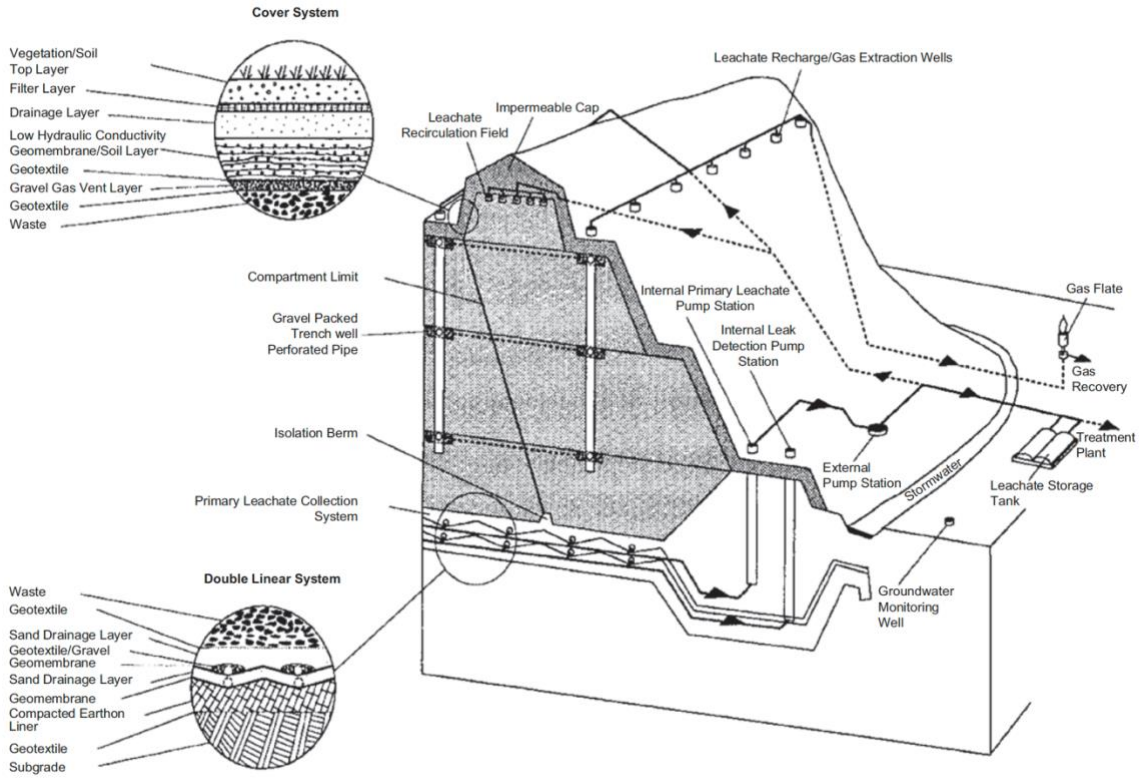

Figure 2.3. Operational features of a bioreactor landfill system [46]

Compared to the conventional sanitary landfill, the bioreactor landfill has several advantages as follows. [46]

- Improved leachate quality
- Leachate storage and treatment
- High productivity and yield of landfill gases
- Accelerated waste stabilization
- Increased biodegradation rate of the waste
- Increased possibility of converting waste to energy

Despite these advantages, the bioreactor landfill fails to address one of the most critical issues related to conventional sanitary landfills, that is, lack of space and the need to continuously locate new landfills. To address these problems, a bioreactor variation is proposed, termed "Sustainable Biocell" or "Biocell" [45].

A Biocell entails the operation of a waste cell in three stages. In the first stage, the cell operates under anaerobic conditions with leachate recirculation to maximize the recovery of the energy potential from the waste. In the second stage, the Biocell is operated aerobically, and compost is produced. In the third or final stage, the Biocell is mined to recover resources [45]. The process of extracting the remains of disposed materials, and possible energy resources from a landfill is called landfill mining [47]. The incorporation of landfill excavation, advanced materials sorting and processing, and thermal conversion processes for the recovery of materials and energy resources for reuse in society is the start-of-art in landfill mining, and it is called "Enhanced Landfill Mining (ELFM)" [48].

2.4 Enhanced Landfill Mining (ELFM)

The concept of ELFM is beneficial to both old and new landfills. This makes landfills the future mines for materials that are yet viable for recycling economically or have a potential of being recycled effectively with the current technologies. In fact, incineration process eliminates the possibility of reusing certain waste streams. To ensure more materials being recycled or transformed to other useful forms rather than being burned or buried, the concept of ELFM becomes valuable [48]. Enhanced landfill mining (ELFM) is driven by the value-added nature of the waste materials.

Generally, there are two types of recovery processes in which valuable resources can be recovered from excavated landfills. These recovery processes include: (i) Waste to Material (WtM), a process creating new materials depending on the characteristics of the excavated landfill, and (ii) Waste to Energy (WtE), a process of extracting energy from excavated waste as an alternative to fossil fuels. ELFM prevents the emissions of carbon dioxide and other pollutants during material valorization. [49].

The rest of this section overviews the WtE technologies using excavated landfill waste (usually MSW) as feedstock.

2.5 Municipal Solid Waste (MSW) as Energy Feedstock for WtE

There are two broad categories of waste in the MSW stream: inorganic and organic [50]. The organic fraction includes food waste, yard waste, paper, wood, and process residues, while the inorganic fraction includes plastic, textile, leather, rubber, and metals [51].

There are numerous technologies available for treating MSW; however, knowing the exact compositions of the MSW is important to determining the most appropriate and effective technology for the treatment of MSW [51]. The characteristics of MSW feedstock depend on many factors, such as storage method (the humidity influence), maturity (age of the excavated landfill waste), and sorting procedure (varies from country to country) [52]. To emphasize, the successful implementation of WtE technologies in the concept of ELFM depends on the efficiencies of the WtE processes, which fundamentally depend on the feedstock quality. To meet the WtE input requirements, the MSW excavated from landfills (possibly processed into RDF) fulfill the WtE process requirement.

Table 2.2 shows the composition of MSW and RDF in the Phyllis database [53]. The mean value and range of values of different types of MSW and RDF are given in the Phyllis database. The range of values of MSW and RDF on the Phyllis database is shown in paratheses. The data indicate that the content and calorific value can vary widely. For example, in an experimental study performed on excavated municipal solid waste MSW) from a landfill in Belgium [54], the MSW was processed into RDF using conventional pre-treatment techniques, including shredding, screening, sorting, drying, and pelletizing. The result of the processed RDF listed shows that the waste composition of the processed RDF from the Belgium landfill is within the range of values found in the Phyllis database.

Table 2.2. Composition of MSW and RDF: mean values, and [min – max] value [53]

Content	Unit	MSW by (Phyllis, 2011)	RDF by (Phyllis, 2011)	RDF processed from Belgium landfill
Moisture content	wt% wet	32.4 [31.0 – 38.5]	10.8 [2.9 – 38.7]	14.4
Volatiles	wt% daf[a]	87.1 [87.1]	88.5 [74.6 – 99.4]	80.4
Ash	wt% dry	33.4 [16.6 – 44.2]	15.8 [7.8 – 34.5]	27.1
NCV[b]	MJ/Kg	18.7 [12.1 – 22.5]	22.6 [16.1 – 29.3]	22.0
C	wt% daf	49.50 [33.9 – 56.8]	54.60 [42.5 – 68.7]	54.9
H	wt% daf	5.60 [1.72 – 8.46]	8.37 [5.84 – 15.16]	7.38
O	wt% daf	32.40 [22.4 – 38.5]	34.40 [15.8 –15.16]	NA[c]
N	wt% daf	1.33 [0.7 – 1.95]	0.91 [0.22 -2.37]	2.03
S	wt% daf	0.51 [0.22 – 1.40]	0.41 [0.01 – 1.27]	0.36

C: Carbon, H: Hydrogen, O: Oxygen, N: Nitrogen, S: Sulphur

a: dry ash free, b: Net calorific value, c: Not available

2.6 Methods of Converting Landfill Waste to Energy

Waste-to-energy involves recovering energy from waste in the form of electricity or heat [54]. Due to its heterogeneity, MSW is composed of materials of varying sizes, shapes, and compositions. If MSW is fed into the WtE processes as “excavated” it may result in unstable operating conditions, leading to quality variations in the product. As a result, refuse derived fuel (RDF), a processed form of the MSW, is often used in WtE systems. MSW is generally converted to RDF by shredding, screening, sorting, drying and/or palletisation to improve the handling characteristics and homogeneity of the waste. There are several advantages to converting MSW to RDF, including enhanced calorific value, improved homogeneous physical and chemical compositions, reduced pollutant emissions, reduced ash content, improved ease of storage, handling, and transportation [53].

As shown in Figure 2.4, the available technologies of converting landfill waste to energy can be categorized into biochemical or thermochemical processes. The biochemical process includes anaerobic digestion, and the thermochemical process includes incineration, pyrolysis, and gasification [55]. They are introduced as follows.

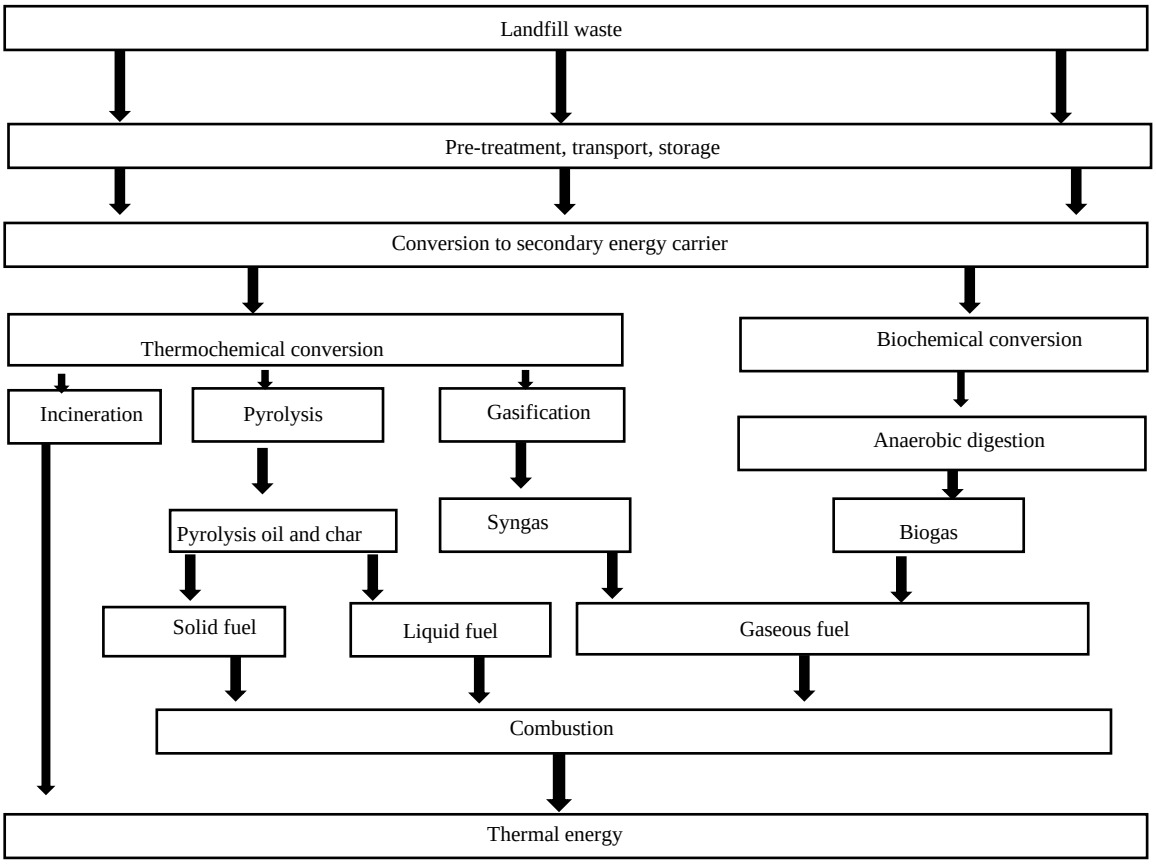

Figure 2.4. Landfill waste-to-energy technologies [53]

2.6.1 Biochemical Conversion of Landfill Waste to Energy

Biochemical conversion of landfill waste to energy is the biological decomposing of landfill waste into useful energy carriers. The process consists of different metabolic reactions such as hydrolysis, acidogenesis, and methanogenesis [56]. As an example, anaerobic digestion is described as follows.

In anaerobic digestion, the feedstock (usually MSW or biomass) is decomposed by bacteria in the absence of oxygen. It is typically a fermentation process, in which the major gas products are methane and carbon dioxide [57]. Anaerobic digestion is a useful technology from an environmental point of view. As described by Ward *et al*. [58], this process provides two distinct benefits for reducing environmental pollution:

- The process of decomposition is contained within a sealed environment, thus preventing potentially methane from entering the atmosphere.

- The use of methane separated from the landfill gas can help reduce the emissions of greenhouse gases.

2.6.2 Thermochemical Conversion of Landfill Waste to Energy

Table 2.3 shows the characteristics of the thermochemical process conversion of landfill waste. Thermochemical conversion of landfill waste to energy is carried out at high temperatures (usually above 200 ^{0}C) to produce useful gaseous products. The advantage of this process includes reduction of waste volume and weight, recovery landfill space, and reduction of landfill gas emissions. The major types of this waste to energy conversion process are incineration, pyrolysis, and gasification [5].

The term incineration refers to the combustion of waste materials in excess air or oxygen without material recovery [59]. MSW incineration has become popular because it requires little processing before it is incinerated or directly burned. The heat from this process can be used to produce high pressured steam, which can then be used to run a steam turbine power plant to generate electricity. One of the major environmental drawbacks of this process is the generation of ash from the boiler's grate and these ashes are usually disposed in landfills. A variety of other emerging incineration technologies are also capable of obtaining energy from waste and generating controlled levels of emissions. As a result, such advanced technologies should be more publicly accepted than conventional incineration processes.

Pyrolysis refers to the thermal decomposition process that take place in the absence of oxygen to transform a feedstock (usually MSW or biomass) into carbon rich solid (biochar), liquid (pyrolysis oil) and a mixture of combustible gases [60]. The pyrolysis process usually occurs in three stages. The first stage occurs between 120 to 200°C, and this stage is called the pre-pyrolysis stage where bond breakage occurs, free radicals appear and carbonyl groups are formed, resulting in the release of water (H_2O), carbon monoxide (CO) and carbon dioxide (CO_2). The second stage is the main pyrolysis process (200^{0}C to 900^{0}C), where the thermal decomposition results in significant weight loss. In the last stage, the char produced from the second stage is devolatilized by the further breakdown of C-H and C-O bonds [61]. Pyrolysis can be classified based on the reaction temperature, heating rate, and residence

time. They are slow pyrolysis (convectional pyrolysis), fast pyrolysis, and flash pyrolysis [60].

Table 2.3. Characteristics of the thermochemical process conversion of landfill waste technologies [62]

	Incineration	**Pyrolysis**	**Gasification**
Aim	Maximize waste conversion into high temperature flue gas	Maximize thermal decomposition of solid into coke, gases, and condense phases	Maximize waste conversion into high calorific gases
Temperature (^{0}C)	800 – 1450	250 – 900	500 - 1800
Pressure (bar)	1	1	1 - 45
Atmosphere	Air	Inert	Gasifying agent: O_2, air, H_2O
Stoichiometric	> 1	0	< 1
Products from the process:			
Gas phase	CO_2, H_2O, O_2, N_2	H_2, CO, H_2O, N_2, hydrocarbons	H_2, CO, CO_2, CH_4
Solid phase	Ash	Ash, coke	Ash, slag
Liquid phase	-	Pyrolysis oil, water	-

As shown in Figure 2.5, gasification is a thermochemical process that involves the conversion of energy in carbon-based feedstock into gaseous fuel rich product called syngas [5][63]. The conversion process is achieved by partial oxidation of the feedstock at a high temperature (500 – 1800^{0}C) in an inert atmosphere [62]. As shown in Table 2.3, the syngas or synthesis gas produce majorly contains hydrogen (H_2), carbon monoxide (CO), carbon dioxide (CO_2), and methane (CH_4). Trace amount of higher hydrocarbons, inert gases due to the gasifying agent and various types of contaminants such as char residues can also be found in the gasification product [64]. The syngas produced can be used as feedstock for chemical

industry (through certain reforming procedure); it can also be used to produce power and energy [65].

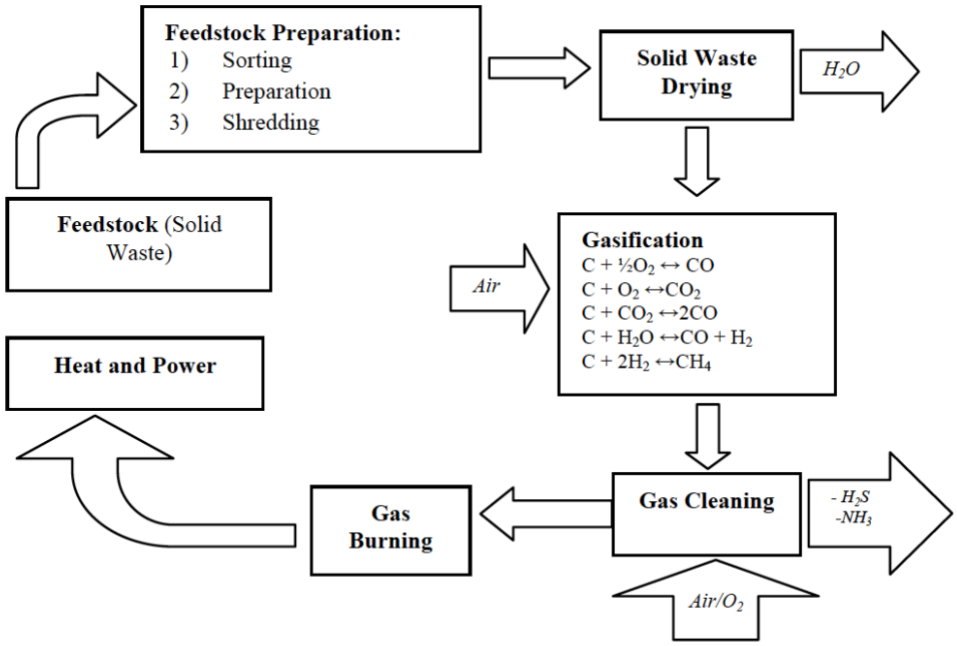

Figure 2.5. Schematic diagram of gasification process [66]

Table 2.4 compares different types of gasifying agents, including oxygen, air, steam, or mixtures of these agents. The simplicity of air gasification and its low cost make it an attractive alternative to oxygen. As a result, air is the most popular gasifying agent for the gasification process. However, because of nitrogen dilution, it has a major disadvantage of yielding a gas with low calorific value (4 - 7MJNm^{-3}). Another popular gasifying agent is steam, which is usually employed if the main purpose is to product H_2 and CO-enriched product gas [62]. Steam gasification also enhances the quality of the gas and significantly increases its heating value. According to the experiment conducted by Wu *et al.* [67], for example, adding steam to a two-stage gasification of plastic increased product gas yields while reducing solid and oil yields. The increase in product gas is due to the improvement of thermal cracking of large molecules.

Table 2.4. Comparison of different types of gasifying agents [62]

Gasifying agent	Advantages	Limitation	Product gas
Oxygen	Higher calorific value and cleaner product than air, enhances combustion reactions in gasification, and reduces cost of preheating the reactor	Generation of pure oxygen is capital and energy intensive	Enhances formation of combustible gases while reducing N_2 content in the syngas
Air	Simplicity and low cost	Diluted syngas, low calorific value gas, possibility of NOx formation	Significant amount of N_2 in the product gas
Carbon dioxide	Direct conversion of greenhouse gas (CO_2), reduces cost of carbon capture and storage, enhances adjustment of H_2/CO ratio for various applications	Requires external heating and catalytic tar reforming	CO-enriched syngas
Steam	Enhancement of gas quality and heating value. Improvement of reforming and Water gas shift reactions	Requires external heating and steam generation plant. Therefore, may be energy intensive. Higher tar formation than air and oxygen	Syngas with enhanced H_2 and CO concentrations

In order to understand the gasification process, it is necessary to understand the basic chemical reactions that take place during the different phases of the gasification process. The reaction is either endothermic or exothermic in nature and their rate depends on the temperature, pressure and the gasifying agent employed [68]. The gasifier is divided into

different zones: drying, pyrolysis, combustion, and reduction zones. The process and chemical reactions that takes place in each zone are presented in Equations (2-1) – (2-8) [66].

- **Drying zone*:***

Table 2.5 shows the moisture contents of different types of feedstocks [69]. A feedstock with a moisture content between 10% and 20% is generally recommended for producing syngas with a high calorific value [70]. Therefore, the quality of the gasification product is largely determined by the feedstock. Prior to gasification, feedstock with high moisture content is dried in the drying zone of the gasifier. However, feedstock with high moisture content results in energy loss and degrades product gas quality [71][72].

Table 2.5. Moisture content of different types of feedstocks [69]

Feedstock	Moisture content on wet basis (%)
Wheat straw	8 - 20
Rice straw	50 - 80
Corn stalks	40 – 60
MSW	15 - 60
Saw dust	25- 55
Wood bark	30 - 60
Rice husk	7 – 10

- **Pyrolysis zone:**

This zone is characterized by the reduction of large molecular groups into smaller hydrocarbons to form biochar, liquids, and gaseous molecules [73] . The cellulose present in feedstock decomposes by forming tar, char, and gaseous products. In other words, pyrolysis temperature has the great impact on the selectivity of products in pyrolysis. Above 773 K, little tar is formed, and a large proportion of biodiesel and bio-oil are produced [74]. Feedstock pyrolysis usually occur at temperatures between 398 and 773 K, resulting in different types of products according to the temperature selected [69].

- **Combustion zone:**

The combustion zone is characterized by exothermic chemical reactions, by increasing the temperature to the range of 1373 - 1773 K [72]. The final product in this zone are carbon monoxide, carbon dioxide, and water as presented in Eqs. (2-1) to (2-3) [75].

$$C + \frac{1}{2}O_2 \rightarrow CO \qquad -110\ {}^{MJ}/_{Kmol} \qquad 0\text{-}1$$

$$CO + \frac{1}{2}O_2 \rightarrow CO_2 \qquad -282\ {}^{MJ}/_{Kmol} \qquad 0\text{-}2$$

$$H_2 + \frac{1}{2}O_2 \rightarrow H_2O \qquad -241\ {}^{MJ}/_{Kmol} \qquad 0\text{-}3$$

- **Reduction zone:**

As the name implies, the reduction zone reduces the content of tar particles in the product gas by bringing them to a high temperature of about 1273 K [76]. The major problem caused by gasification process is the generation of tar. Excessive amount of tar in the product gas will decrease the overall efficiency of feedstock and increase the overall separation cost of the product gas [77]. There are two methods of tar reduction: (1) *in situ* tar reduction (Primary Process) and (2) *ex situ* tar reduction (Secondary Process) [78]. The *in situ* process involves the removal of tar through optimization and designing the gasifier to alter the temperature and pressure conditions of the gasification process and incorporating catalysts into the process. The *ex situ* process employs post-gasification equipment such as wet scrubbers, wet electrostatic precipitators, and filters [69]. The chemical reactions that take place during *in situ* process are presented in Eqs. (2-4) to (2-6).

- Boudouard reaction:

$$C + CO_2 \rightarrow 2CO \qquad +171\ {}^{MJ}/_{Kmol} \qquad 0\text{-}4$$

- Water-gas shift reaction:

$$C + H_2O \rightarrow CO + H_2 \qquad +130\ {}^{MJ}/_{Kmol} \qquad 0\text{-}5$$

- Methanation reaction:

$$C + 2H_2 \rightarrow CH_4 \qquad -75\ {}^{MJ}/_{Kmol} \qquad 0\text{-}6$$

The product gas composition of the gasification process is affected by several operation factors. Among these factors are temperature, pressure, type of feedstock, catalyst, residence or reaction time, and gasifying agent used. These factors must be considered when deciding the desired product gas composition and applications. The factors affecting the gasification process are discussed below:

The gasification temperature is one of the most important factors to be considered in the gasification process because the main reactions are endothermic in nature. Zaini *et al.* [24] reported their steam gasification of landfill experiment. BIncreasing the temperature of the gasifier from 800^0C to 1000^0C increases the product gas yield from 0.73 to 0.78 g/g-fuel, and the H_2 content of the syngas also increases linearly with temperature from 0.029 g/g-fuel at 800^0C to 0.046 g/g-fuel at 1000^0C. The yield of CH_4 gas also increases linearly with the increase in temperature. They also carried out steam co-gasification of landfill waste with 35 wt% biomass. There was about 45% tar reduction when the gasification temperature increased from 800^0C to 900^0C. Tar compounds are cracked down into smaller non-condensable gases or molecules at higher temperatures [79].

Residence time is the time it takes the feedstock to completely breakdown in the reactor [80]. The residence time can be regulated by varying the feed rate or product discharge time. An increase in the residence time results in more reactions, which promotes the formation of char and other stable products. Nanda et al., found that at 650^0C, the total syngas yield increases from 10.2 mol/kg at 15 min residence time to 14.1 mol/kg at 45 min residence time. Chen *et al.* [81] also confirms that longer reaction times favor thermal cracking reactions, which in turn increases the product gas yield.

A steam to feedstock ratio refers to the amount of steam that is introduced into a gasifier in relation to the feedstock input [1]. According to Li et al., [82] the optimum steam to feedstock ratio was 1.33 during their steam gasification of palm oil waste. They found that

the introduction of steam increased the yield of H_2 gas and total product gas by steam reforming reaction in the gasifier. When the quantity of steam introduced into the system was more than the optimum ratio, they notice a decrease in syngas and H_2 yields due to excess steam in the system, which lowers the reaction temperature. Therefore, it is important to determine the optimum steam to feedstock ratio in order to get the maximum output of product gas.

A catalyst is used to amplify the chemical reactions in the gasification process and to enhance the quality of the product gas. This is because catalytic cracking occurs at a much faster rate, and it requires less energy compared to the conventional thermal cracking. The catalyst used in the gasification process can be classified in two different types according to phase in which they are used. A homogeneous catalyst is the catalyst that is in the same phase as a reaction feedstock, *e.g.* sodium hydroxide and potassium hydroxide; heterogeneous catalysts are usually in different phase as the feedstock, *e.g.* zirconium dioxide [83]. For example, Nanda et., [81] found that, at a temperature of 650^0C, 45 min residence time and 3% potassium hydroxide (KOH), the total syngas yield was 44% higher than non-catalytic gasification of timothy grass.

2.6.3 Types of gasifiers

Gasifiers are classified into fixed or moving bed gasifiers, fluidized bed gasifers, and entrained flow gasifiers, depending on how the gas and fuel interact in the gasifier. The gasification process can be divided into different zones: drying, pyrolysis, combustion or oxidation, and reduction regardless of the type of gasifier. The type of gasifier employed is determined by several factors, including product demand, moisture content, and fuel availability.

2.6.3.1 Fixed bed gasifier

The fixed bed gasifier is the most frequently used gasifier in industry due to its simplicity and ease of operation. These gasifiers are also called moving bed gasifiers because the fuel moves downward in the gasifiers in form of a plug. A fixed bed gasifier operates within the pressure range of 1-70 bars. Fixed/moving bed gasifiers may be classified as up-draft, down-draft and

cross-draft gasifier depending on the nature of contact between the gasifying agent and the feedstock [84].

- **Up-draft gasifier**

As shown Figure 2.6, the feedstock enters the up-draft gasifier through the top while the gasifying agent enters through the bottom of the gasifier, hereby making it appear as a counter flow movement. As a result, up-draft gasifiers are also referred to as counter-flow gasifiers. There is a combustion zone in the lower portion of the gasifier, where the gas products are formed because of drying and pyrolysis. These raise the temperature of the combustion zone and the product gas to about 1000 K [73]. The hot gases from the combustion are immediately reduced in the reduction zone to facilitate feedstock drying and steam generation. These types of gasifiers have the highest thermal efficiencies because the product gases exit the gasifiers at low temperatures [85]. This type of gasifier is also susceptible to several limitations, including sensitivity to tar and moisture content of feedstock, low syngas production, long engine start-up time, and poor response capability [86].

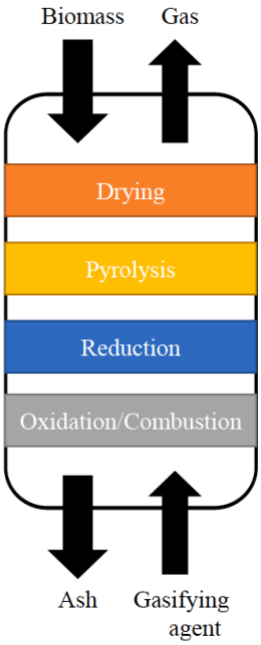

Figure 2.6. Schematic diagram of up-draft gasifier [1]

- **Down-draft gasifiers**

In contrast to updraft gasifiers, the gasifying agent in a down-draft gasifier is fed to the combustion zone through the mid-section of the gasifier; see Figure 2.7. The feedstock is fed through the top into the drying section where it is dried and further moved to the pyrolysis zone, where it is transformed into char and gases. All the decomposition products are then forced to pass through the combustion zone for thermal cracking of volatile compounds to produce the high-quality product gas with less tar content [87]. The interaction of the gasifying agent and the feedstock occur in the downward direction results in the ash and product gas to flow in the same direction. Therefore, the down-draft gasifiers are also referred to as co-current gasifiers [61].

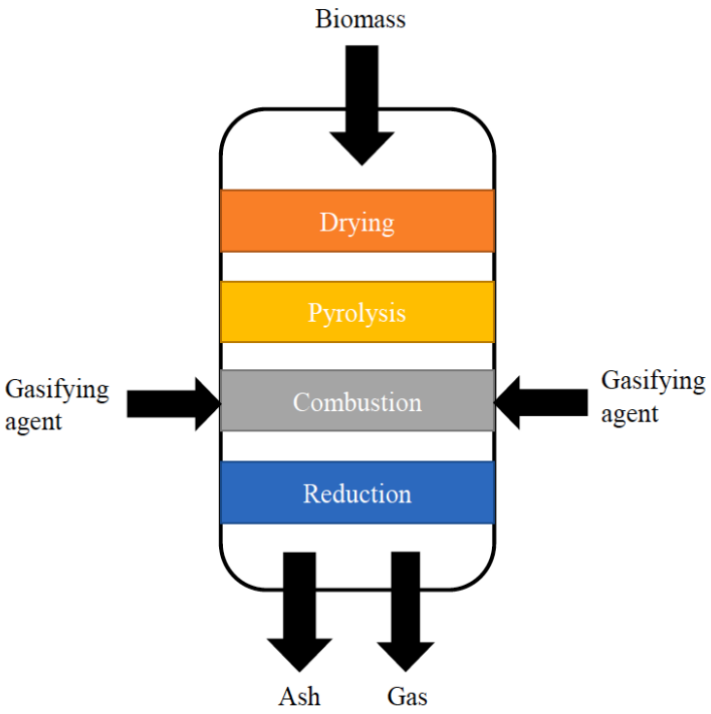

Figure 2.7. Schematic diagram of down-draft gasifier [1]

- **Cross-draft gasifier**

The cross-draft gasifier is one of the simplest gasifiers in which the gasifying agent is supplied through the side nozzles, while the feedstock enters through the top nozzle as shown in Figure 2.8. A cross-draft gasifier, however, has a separate ash bin and reduction zone, thus reducing the amount of fuel needed for its operation. Additionally, it produces less ash in the product gas [88]. This type of gasifier is also known as side-draft gasifiers [89]. Table 2.6 compares the advantages and disadvantages of the up-draft, down-draft and cross-draft gasifiers.

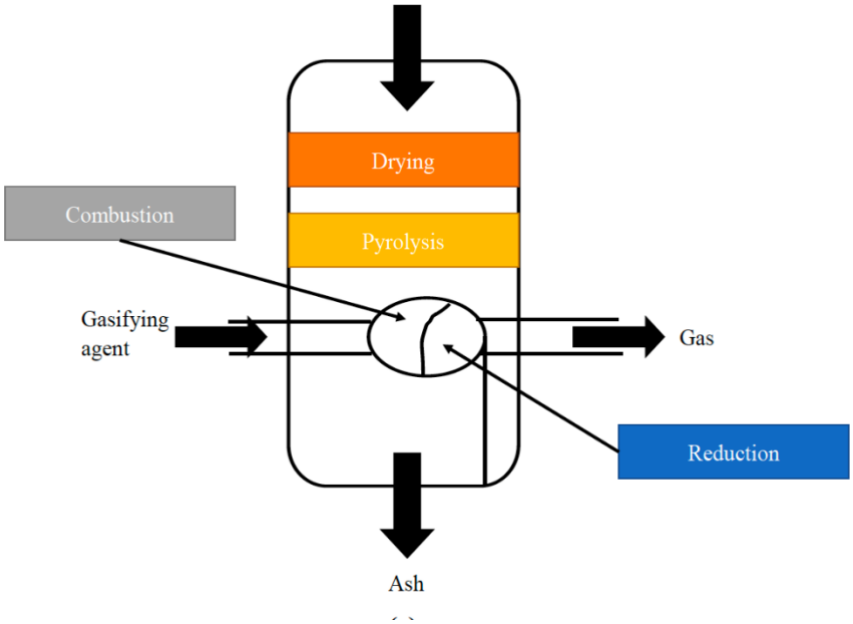

Figure 2.8. Schematic diagram of cross-draft gasifier [1]

Table 2.6. Advantages and disadvantages of different types fixed bed gasifiers [90][91][92]

Type of gasifier	Advantages	Disadvantages
Up-draft gasifier	• good thermal efficiency • Utilizes heat of combustion effectively because of counter-flow operation • Less pressure drop • Little tendency towards slag formation	• Not suitable for high volatility feedstock • Low production of syngas • Ideal only for scale uses • Poor reaction capability • It takes long time to start up • High tar yield
Down-draft gasifier	• Low sensitivity to tar, and dust in feedstock • Low tar yield compared to updraft gasifiers • Less time to ignite	• Low thermal efficiency due to high temperature outlet of product gas • High particulate matter content
Cross-draft gasifier	• Low tar yield • fast response time • Flexible product gas yield	• High pressure-drop • High sensitivity to formation of slag

2.6.3.2 Fluidized gasifiers

Fluidized gasifiers are gasifiers that gasify feedstocks in a bed of small particles such as sand, silica, and dolomite with the gasifying agents. A fluidizing gas is used to make the bed of the gasifier behave like a fluid. The process is characterized by high output, improved gas and solid reactions with enhanced heat and mass transfer, longer reaction time, better char conversion, and high calorific value of the product gas. Thus, fluidized beds are an effective option for gasifying plastic wastes due to their excellent gas solid mixing and uniform temperature distribution. Typically, fluidized bed gasifiers are operated at temperature ranging between 923 and 1223 K [93] and at pressures ranging between 0 and 70 bar [94].

There are two main categories of fluidized bed gasifiers based on the velocity of the gasifying medium: (1) bubbling bed gasifier and (2) circulating bed gasifier [69].

- **Bubbling bed gasifier**

Bubbling bed gasifiers are the oldest type of fluidized bed gasifier [96]. As shown in Figure 2.9, the bubbling bed gasifier consists primarily of inert particles such as sand and silica. Wheeldon *et al*. [95] observed in their experiment that the tar conversion rate of the bubbling bed gasifier was significantly enhanced when the bed material was imparted with catalytic activity. Particles of the feedstock reaching the top of the bed experience increased cross-sectional area, decreasing their velocities (usually 1 m/s) [69]. This promotes the formation of particulate matter. As a result, the bubbling bed gasifier requires a network of cyclone separators at the gasifier's exit [96]. Feedstocks with high ash contents may be converted by bubbling bed gasifier due to their flexibility in fuel processing and loading. The downside of these gasifiers is their conversion efficiencies lower than those of circulating bed reactors [97].

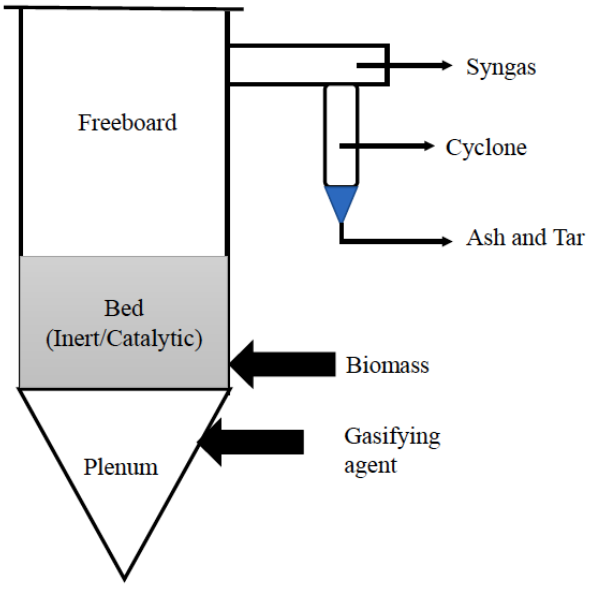

Figure 2.9. Schematic diagram of a bubbling bed gasifier [1]

- **Circulating fluidized bed gasifier**

As shown in Figure 2.10, the feedstock into a circulating bed gasifier flows outside the gasifier followed by recycling back into the gasifier to increase the conversion efficiency. Circulating bed gasifiers become more attractive due to the extended reaction time they offer. The fluidization velocity (3.5 – 5.5 ms^{-1}) of this type of gasifier is much higher than that of a bubbling bed gasifier [85]. The circulating bed gasifier can provide high gas yields and higher calorific value of product gas. Additionally, circulating bed gasifier have several advantages over other types of gasifiers, including the ability to process a large volume of feedstock, a low tar yield, a greater efficiency of carbon conversion, and an optimal residence time [97]. However, the initial and operating cost of this system is expensive. The main application of this type of gasifier can be found in the power sector, cement industry, and paper industry [69][76].

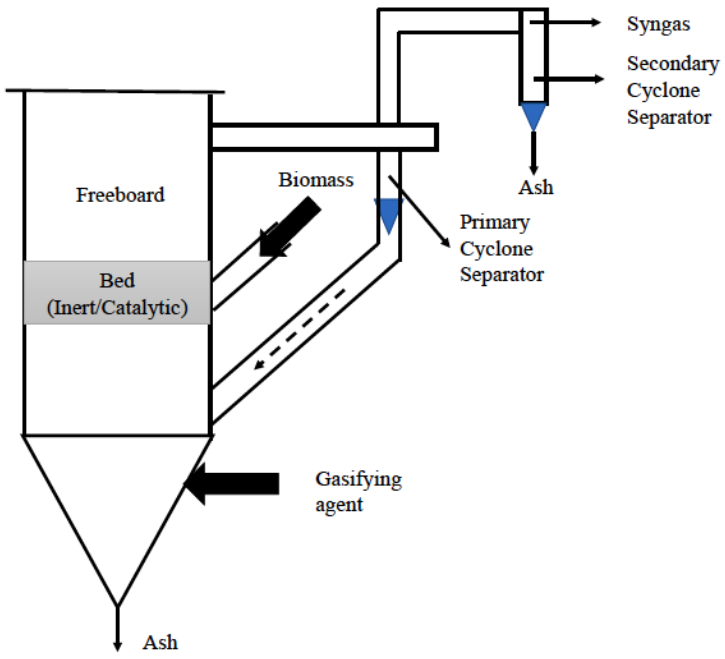

Figure 2.10. Schematic diagram of circular bed gasifier [1]

2.6.3.3 Entrained flow gasifier

In an entrained flow gasifier, the feedstock (usually < 1 mm) and the gasifying agent are fed into the gasifier in a co-current; see Figure 2.11. This type of gasifier operates at a pressure of

23 to 30 bar and at a temperature of 1273 K, which makes them suitable for tar cracking [98]. They are usually employed in coal and mixed plastic waste gasification [70]. This type of gasifiers has a carbon conversion efficiency of almost 100%, which makes them appropriate for large-scale applications. Although these gasifiers operate at high temperatures, they still pose difficulties in terms of material selection and ash melting [99].

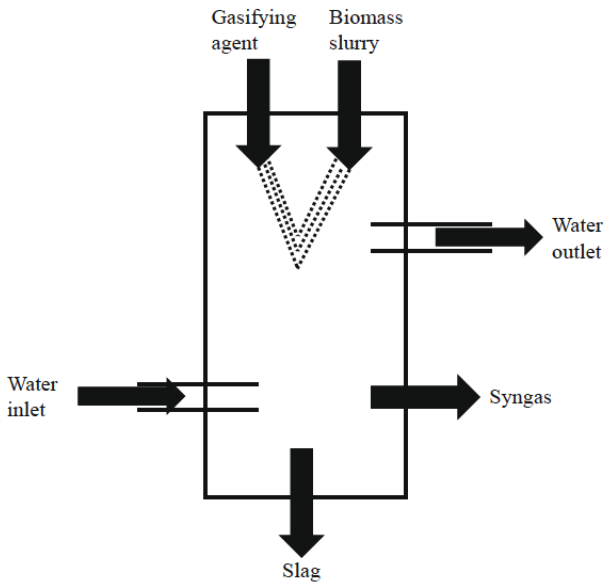

Figure 2.11. Schematic diagram of entrained gasifier [1]

2.7 Syngas Utilization and Cleanup

2.7.1 Syngas utilization

The syngas can be used in several ways, either in an external or internal combustion engine. There are several thermodynamic systems that can utilize the syngas such as gas engines, gas turbines, or heating system such as steam turbines, and absorption chillers.

2.7.2 Syngas cleanup

Syngas cleanup is the process of removing pollutants or pollutant-forming traces from the syngas. A variety of pollutants are produced during the gasification process, and the pollutants produced are determined by the operational parameters of the gasifier (e.g., temperature, gasifying agent, and particle size) as well as the composition of the feedstock.

The pollutants include phenol, heavy tars, sub-micron particulate matter, cresol, ammonia (NH_3), sulfides, and hydrochloric acid (HCl). If not managed properly, these compounds can reform to produce dioxins and furans [66]. These pollutants maybe controlled by applying the following methods:

- By excluding PVC and Teflon from the feedstock is one of the strategies to control chlorine and fluorine.
- By drying high moisture content waste before gasifying to lower the tar yield.
- Catalytic conversion of phenols, cresols, ammonias, and heavy tars into light gases under anoxic conditions (the scrubber must be heated to over 400°C).
- Fine dusts are removed from the syngas through light compression and cooling in a liquid.

2.8 Comparison of Methods of Converting Landfill Waste to Energy

Figure 2.12 illustrates the WtE technologies that are available for treating MSW and RDF [53]. The main advantages and disadvantages of the three main types of thermochemical technologies (*i.e.* incineration, pyrolysis, and gasification) for MSW and/or RDF (Refuse derived fuel) are discussed below. The discussion emphasizes the possibilities these technologies offer in WtE valorization route - which is essential in ELFM.

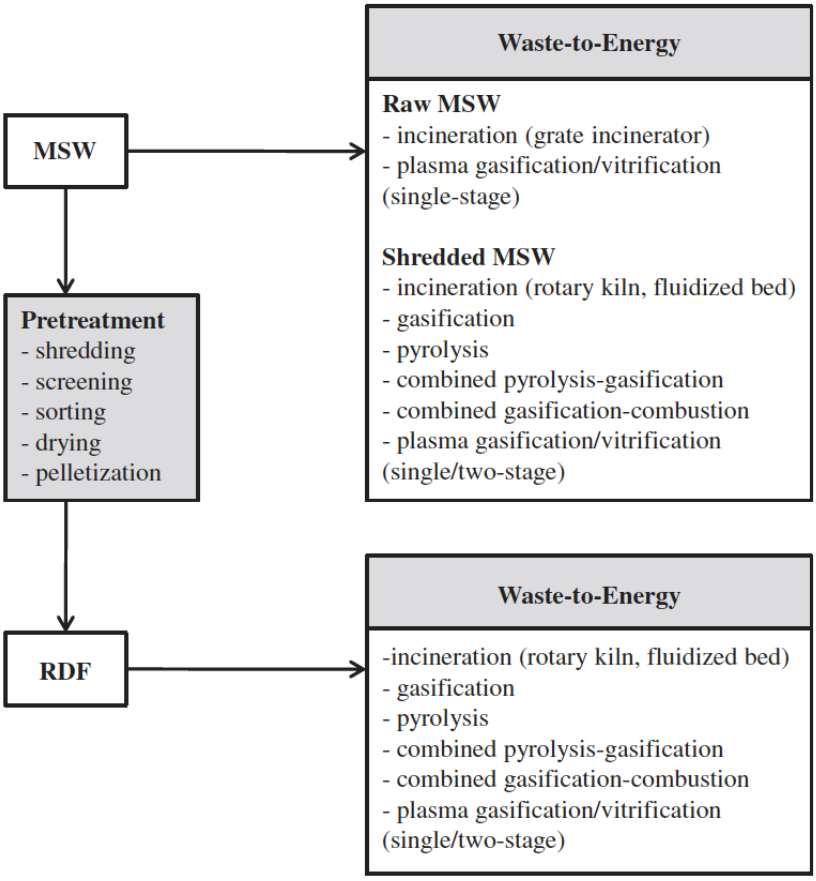

Figure 2.12. Thermochemical WtE technologies for MSW and RDF [53]

It is possible to recover energy from wastes through incineration. MSW incinerators offer a great deal of potential as a source of heat/electricity. As shown in Figure 2.13, using steam turbines to generate electricity is one of the WtE possibilities for MSW incineration. However, the flue gas from steam turbines does not meet the required quality standard for gas turbines; gas engines that are more efficient than steam turbines in producing electricity. Although solid waste incinerators can reduce the volume of waste significantly to about 90%, a high volume of the residues must still be disposed of on landfills [100].

Incinerator bottom ash is composed of slag, ferrous and non-ferrous metals, ceramics, glass, and other non-combustibles and residual organic matter in a highly heterogeneous mixture. This composition of a bottom ash is closely dependent on the composition of waste being incinerated. There are multiple sources of various elements in MSW, and these elements influence the bottom ash characteristics [100]. As a result of the potential risk of

heavy metal leaching, bottom ash is largely disposed in landfills and not suitable for reuse. MSW incinerator bottom ash needs to be treated with advanced thermal technology to make eco-friendly products. Therefore, MSW incinerators can generate a considerable amount of WtE, but not so much suitable for WtM.

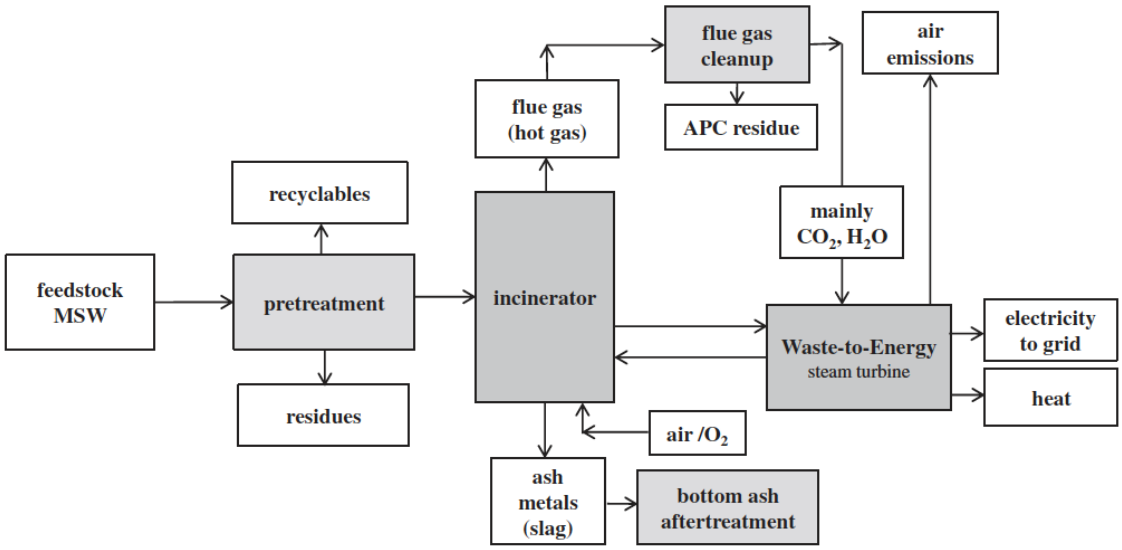

Figure 2.13. WtE – from MSW to electricity (heat) through incineration [53] (*APC= Air Pollution Control)*

Depending on the process design, pyrolysis may produce a combustible gas, a solid product, or a liquid product. As shown Figure 2.14, the gaseous stream of the pyrolysis process is mainly CO and H_2, which can be used in gas turbines, gas engines, and even useful in fuel cells after purification. Although pyrolysis has been proven to be viable for specific feedstock (*e.g.* tires, electronics waste), it is not a perfect replacement for MSW incineration. The main reason is that it needs pre- and after-treatment of feedstock. Pyrolysis products could become useless, or at less useful if pollutants are present, making additional treatment steps necessary. For example, the residual solid (char) from pyrolysis of MSW is usually disposed in landfills, and this become a major environmental issue [59]. Excavated landfill waste (usually MSW) is a highly heterogeneous material, and processing it into a stream that meets the stringent pyrolysis process requirements may reduce the process commercial viability.

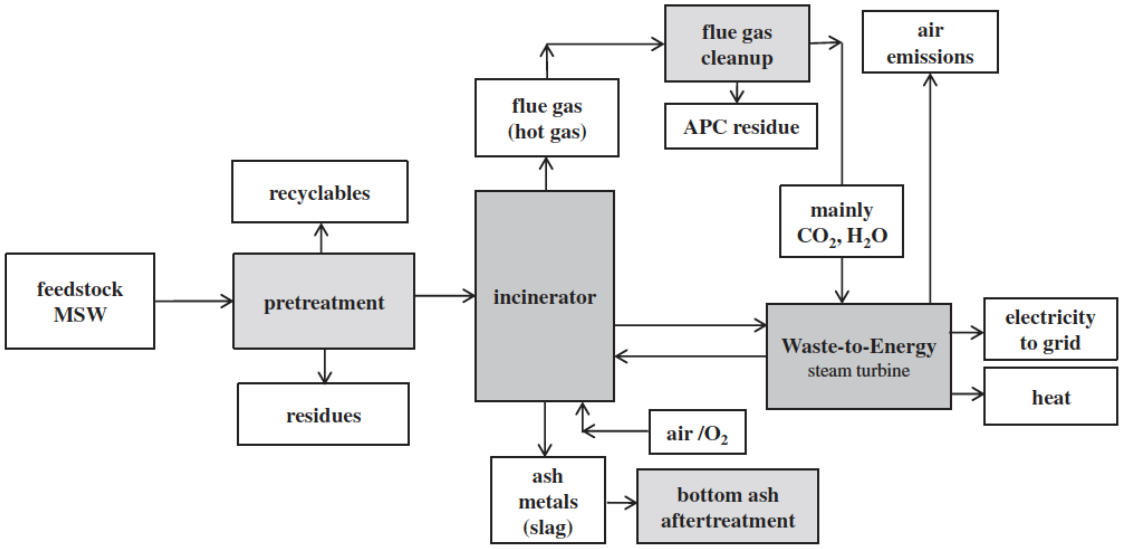

Figure 2.14. WtE – from MSW to electricity (and heat) through pyrolysis [53]

Comparing to incineration of MSW, gasification offers a number of advantages. The oxygen requirement is much lower when compared to incineration. As a result, the formation of dioxins, SO_2, and NOx is limited, and the volume of process gas is less, resulting in less expensive equipment for gas cleaning. In addition, gasification produces combustible gases that can be utilized in combination with combined cycle turbines, gas engines, and potentially fuel cells for electric (and heat) generation [101]. Since the tar generated in the gasification process is burned in the combustion zone, then extensive gas cleaning equipment is not needed, which will significantly reduce the capital costs. Figure 2.15 presents the WtE gasification process schematic with MSW as feedstock.

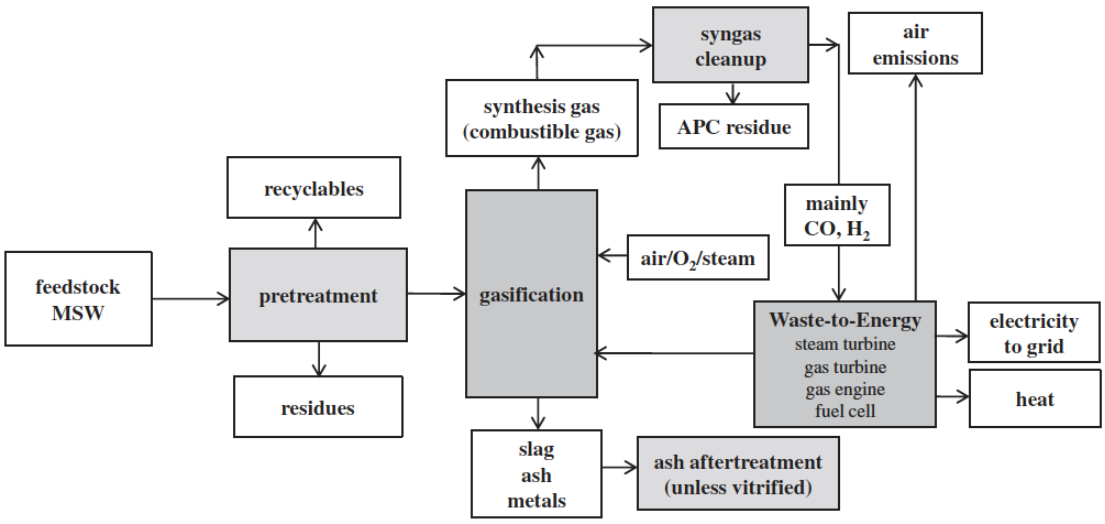

Figure 2.15. WtE – from MSW to electricity (and heat) through gasification [53]

Table 2.7 lists the key findings of the comparison among the available technologies of converting landfill waste to energy.

Table 2.7. Comparison of the three main thermochemical waste treatment technologies [53]

Waste treatment technology	Suitable for MSW/RDF (incl. excavated landfill waste)	WtE potential	Commercially proven
Incineration	++	-	+
Pyrolysis	--	-	-
Gasification	++	+	+

2.9 Economic Comparison of Methods of Converting Landfill Waste to Energy

As shown in Table 2.8, an economic analysis of waste to energy thermal processes was performed [59] for three thermal processes (i.e., incineration, pyrolysis, and gasification). They estimated the economic effects of a facility with a capacity of 500 tons of MSW per

day. Table 2.8 shows that incineration requires the highest capital expenditure of about $116 million, followed by pyrolysis and then gasification, which is only about 80 million. Even though incineration requires the most capital for investment, it is the least preferred technology because it shows a net negative annual revenue (before taxes), while pyrolysis and gasification process has a net positive annual revenue (before taxes). Gasification has the highest net positive annual revenue.

Among the three thermochemical processes converting wastes to energy, gasification has been the most efficient with a production of about 685 kWh/ton of MSW [59]. Based on the characteristics of waste to energy technologies, incineration produces the largest amount of ash as by-product, which is environmentally unfriendly. Among various gasifying agents available, steam has proven to be the most efficient and commercially available. As a result, it can be concluded that steam gasification is the most attractive process to convert waste to energy due to the following characteristics:

- High thermal efficiency
- Enhanced product gas quality and heating value
- Various syngas for energy sources
- Eco-friendly products

Thus, the motivation of this thesis work is to investigate the energy potential of the Calgary Bio-cell waste residue through steam gasification process.

Table 2.8. Parameter for economic assessment of waste to energy thermal processes [59]

Parameters	Incineration	Pyrolysis	Gasification
Investment @6% for 20 years	~$116,000,000	~$87,000,000	~$80,338,000
MSW capacity (tons/days)	500	500	500
Power generation (kWh/ton)	~545	~570	~685
Operation and maintenance	~$8,217,000	~$7,194,000	~$6,872,000
MSW tipping fee ($/ton)	$35	$35	$35
Green tags	$0.02/kWh	$0.02/kWh	$0.02kWh
Energy sales	$0.065/kWh	$0.065/kWh	$0.065/kWh
By-products	~$0.2	~$0.2	~$0.2
Residue (tons/ton MSW)	Ash	Ash and char	Ash and slag

Chapter 3

Methodology

This chapter describes the experimental methods and materials, including waste sample, waste characterization, and apparatus, used to carry out the steam gasification tests. The methods used for the product gas characterization and evaluation of the gasification performance are also discussed in this chapter.

3.1 Waste Sample

Figure 3.1 shows the excavated waste residue (EWR) sample collected from the Calgary Bio-cell located in Shepard landfill site in Calgary, Alberta, Canada. The excavated waste residue was stored in the Calgary Bio-cell for about 15 years between 2006 and 2020 [22]. The EWR was collected in October 2020 from the Calgary Bio-cell by borehole drilling using grab sampling method. Three pilot boreholes were drilled by Earth Drilling Co. Ltd. using a track-mount R-45 LS MiniSonic drill rig equipped with a sonic corer (180 millimeter outside diameter) at three spatially distributed points on the Calgary Bio-cell surface. Based on the maximum depth available at each point, boreholes were drilled to depths ranging from 9 m to 10.6 m. In total, 8 containers of 10 litres of EWR samples were collected from all the three locations selected. Each point of the sample collection was identified as $P_{1\text{-}1}$, $P_{1\text{-}2}$, and so on. The Calgary Bio-cell was built with three waste lifts and each lift was divided with a 500 mm thick intermediate cover layer. The topmost layer was named lift 1 and the bottom layer lift 3.

Table 3.1 shows the name, point number and depth of the boreholes for the excavation of the EWR sample. Point 1 elevation in the Calgary Bio-cell is 9 m deep, while point 2 and 3 were 10. 6 m each. However, since point 1 has the smallest total depth, only two sample were collected from point 1. This excavation process was carried out by the research team at the university of Calgary and their written procedure for the sample collection was used as a guide in writing this section. The EWR sample collected from each of the three locations were chosen to collect EWR data that represent the total waste deposited in the Calgary Bio-cell. The EWR sample collected was shipped to Energy Research Center (ERC), Room 2006, University of Waterloo for gasification experiment.

Figure 3.1. Excavated Waste Residue (EWR) from Calgary Bio-cell

Table 3.1. Name, point number and depth of each EWR sample

Name	Point #	Depth (m)
P_{1-1}	1	0 - 6
P_{1-2}	1	6 - 9.1
P_{2-1}	2	0 – 4.5
P_{2-2}	2	4.5 – 7.6
P_{2-3}	2	7.6 - 10.6
P_{3-1}	3	0 – 4.5
P_{3-2}	3	4.5 – 7.6
P_{3-3}	3	7.6 – 10.6

3.2 Physical Characterization of EWR Sample

As shown in Figure 3.2, the physical characterization of the EWR sample was carried out by hand sorting the waste sample into different categories. The same sorting method was used by Lopez *et al*. [102] during their characterization of excavated landfill waste after ballistic separation to evaluate material and energy recovery potential of the waste. After the manual hand sorting, the EWR sample was then categorized into the 11 different categories which

includes: wood, paper, textile, plastic 2D, plastic 3D, glass, ferrous metals, non-ferrous metals, inert, soil, and others. The percentages of each category were calculated and recorded. There is no category for organic waste (*e.g.* food waste) because they were not distinguishable from the soil. It is likely that the organic materials have decomposed to soil-like material [102], [103]. After the categorization, the glass, ferrous metals, non-ferrous metals, and inert materials were removed from the EWR sample because they cannot be gasified.

Figure 3.2. Different categories in EWR samples

3.3 Chemical Characterization of the EWR Sample

The chemical characterization of the EWR sample was conducted by NERSIC International Laboratory, Waterloo, Ontario Canada to determine the elemental chemical composition and properties of the sample. It is important to conduct these analyses, *i.e.*, quantitative (elemental chemical composition) and qualitative (moisture content, ash content, volatile matter, and calorific value) analyses on the EWR sample because it helps to determine the energy recovery potential of the waste [104]. According to Kaartinen *et al.* [105] in their sampling, processing, and characterization of landfill waste experiment, the moisture content in excavated waste did not hinder the processing of the waste, but it reduces the processing efficiency. Quaghebeur *et al.* [106] also observed that to assess the efficiency of waste to

energy (WtE) process, the characteristics such as calorific value, ash content, chemical composition such as of carbon, nitrogen, hydrogen, oxygen, and sulfur content of the waste sample must be determined. These values quantify the energy that can be recovered from the waste and the residue that can be produced [107]. The results of the quantitative and qualitative analyses of the EWR sample used in this study are discussed in Chapter 4.

3.4 Steam Gasification Experiment

3.4.1 Sample preparation for steam gasification

Enhanced landfill mining (ELFM) technique was used in this study to prepare the waste samples. This technique involves the integration of landfill excavation, advanced materials sorting and processing, and thermochemical conversion processes to recover energy resources from waste. The main purpose of ELFM technique is to recover high quality materials and fuels from the heterogenous EWR samples. The heterogeneity of the EWR from landfill requires the waste to be separated and treated to enable the production of valuable materials [106].

There are various treatment and separation methods available for the treatment of heterogeneous waste. Many of these methods employ a combination of dry and wet mechanical separation techniques, including milling, crushing, sieving, magnetic separation, and eddy current separation. The EWR samples used in this study were first reduced in size using a mechanical blender (model: BC701CCO, Ninja), then the sample was screened to a particle size of about 3 mm using an aluminum sieve. After that, the samples were dried in a 1100 ^{0}C Box furnace (model BF51800 series from Thermo Scientific, Canada) at 105 ^{0}C for 24 hours. This treatment enhances the surface area and homogeneity of the EWR sample for better reaction and reduces its moisture content. As a result, the EWR sample is transformed into refuse derived fuel (RDF) *i.e.*, processed form of excavated waste, which is often used in WtE systems. There are several advantages of converting excavated waste to RDF, this includes higher calorific value, more homogeneous of physical and chemical compositions, less pollutant emissions, less ash content, easier storage, and easier transportation [53].

3.4.2 Experimental setup

Figure 3.3 shows the schematic of the experimental setup used for steam gasification. This setup consists of a horizontal lab-scale tube reactor, a gas control system, a steam generation system, a gas cooling system, and a gas storage system.

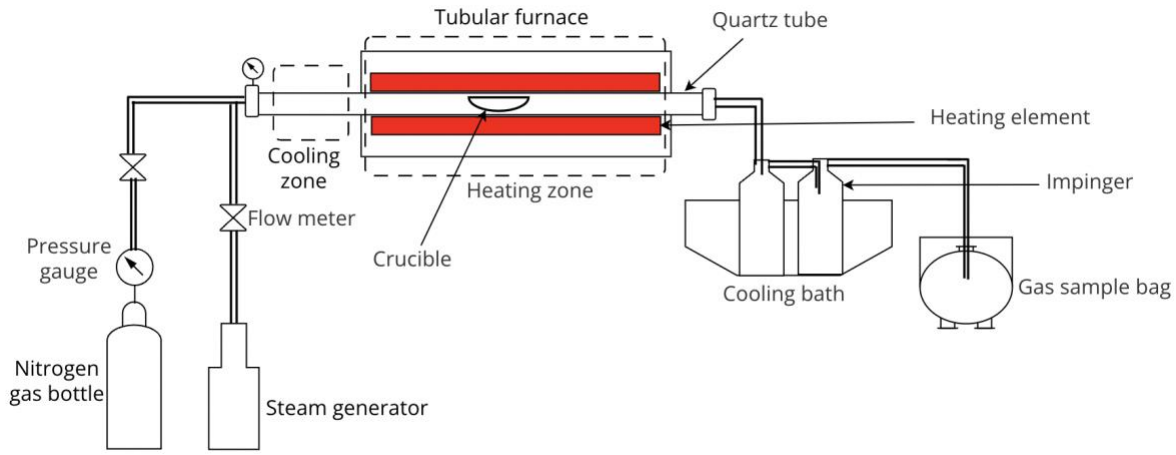

Figure 3.3. Schematic diagram of horizontal lab-scale reactor used for steam gasification experiment

The horizontal lab-scale reactor (model OTF-1200X-S-UL from MTI corporation USA) consists of a horizontal furnace body, alumina crucible of 50 x 20 x 20 mm, and a 1000 mm long quartz tube with an inner diameter of 44 mm, which is heated using a uniformly arranged resistance wire (Fe-Cr-Al alloy) in the heating area of the reactor. The reactor is rated with a maximum heating rate of 20 ^{0}C/min with a maximum temperature of 1200^{o}C and a maximum pressure of 3 PSI.

The nitrogen gas (Grade: 4.8, Purity: 99.99%) used for this experiment was purchased from Praxair; the flow meters used for measuring the flow rate of nitrogen (model: OF-03217-12) and steam (model: OF-03217-00) were purchased from Cole Parmer, Canada. The steam used in this experiment was generated by heating deionized water in a beaker. Some nitrogen gas from the nitrogen gas cylinder passed through the steam bottle to increase the steam pressure. The heater used for heating the deionized water is Barstead/Thermolyne Cimarec 3 (model SP47235) magnetic hot plate (America Laboratory, ATL Inc. USA). The cooling bath used was prepared in a plastic drum by putting pure ice cubes in salt water to

attain a temperature of -15 ^{0}C. The temperature of the cooling bath was monitored using a thermometer (range: -50 to 100^{0}C) from the Chem Store at the University of Waterloo, Canada. Gas sample bags (model: OF-01410-14, Cole Parmer, Canada; size: 20 liters) were used to collect and store the product gases.

3.4.3 Steam gasification procedure

For each test, the furnace was heated to the target temperature (800, 900, or 1000) with a constant nitrogen flow rate of 160 ml/min to purge the reactor [24], [108]. After the furnace has reached the targeted temperature, preheated steam was metered into the reactor to control the steam-to-feedstock ratio, with the aid of a flow meter [109]. After that, 4 g of the pretreated EWR sample contained in an alumina crucible, which was originally kept in the cooling zone [24], [110] during the heating of the furnace, was pushed into the heating zone for gasification. The gasification process was maintained at this condition for 15, 30, or 45 minutes.

During the gasification process, the gas generated is cooled at -15^{o}C by passing through series of impingers filled with acetone placed in a cooling bath to trap its tar content (see Figure 3.3). After gasification, the steam flow was shut off, and the nitrogen flow rate increased to 320 ml/min for 30 minutes to ensure all the product gas generated were collected [24] into the 20-litre gas sample bag. The waste residue after gasification was weighted using an electronic balance and recorded for further analysis.

3.5 Statistical Design of Experiments

3.5.1 Response surface method

Response surface methodology (RSM) based on Box Behnken statistical experimental design was used to study the influence of three factors on the output response, *i.e.*, product gas yield (g/g of dry feedstock). RSM is a statistical tool for multiple regression analysis to determine the relationship between process variables and its response [111]. The major objective of RSM is to optimize this response. RSM based on Box Behnken statistical experimental design was used because it can help observe the nonlinear effects and interactions between the independent variables, and it also requires less runs than the Central Composite Design (CCD) and full factorial design [112].

The variable conditions considered in RMS based on Box Behnken design using Minitab software are temperature (X_1), steam to feedstock ratio (X_2), and reaction time (X_3) with three levels of factors. After identifying the optimal conditions for the temperature, steam to feedstock ratio, and reaction time of the gasification process, the effects of these independent variables on the steam gasification product were also investigated under the optimal condition [3].

The temperature for this experiment was set within the range of 800-1000 ^{0}C. This temperature range was selected based on the steam co-gasification of excavated landfill waste experiment carried out by zaini *et al.* [24], who found that an increase in gasification temperature led to an increase in product gas yield. In their experiment, increasing the gasification temperature from 800^{0}C to 1000^{0}C increased the product gas yield by 58.6% or so. In order to achieve a high carbon gasification efficiency, Saidi *et al.* [113] recommended that the reactor should be operated at a temperature above 1350^{0}C and a pressure of 0.5MPa. However, due to the limitation of the reactor and quartz tube used in this experiment, the maximum recommended temperature was 1000^{0}C and a pressure of 0.02 MPa.

The steam to feedstock ratio for this experiment was in the range of 0.5 – 2.6 according to Xiao *et al.* [114]. They observed that the highest product gas and H_2 gas yields occur at a steam to feedstock ratio of 1.33 with a reactor temperature of 800 ^{0}C, and that a steam to biomass ratio of 2.67 under the same condition resulted in a lower yield of product gas and H_2 gas because excess steam lowered the reaction temperature. The reaction time ranged from 15 min to 45 min, according to Nanda *et al.* [115].

Table 3.1 shows the experimental factor levels used for the design of experiment. The factors considered in this study includes three independent continuous variables: temperature, steam to feedstock ratio and reaction time, which are coded X_1, X_2 and X_3, respectively. Three level factors were considered in this experimental design to help determine any curvature in the response variable. The highest level is termed (+1) and the lowest is (-1) while the centre point is (0).

Table 3.2. Experimental factor levels used for design of experiment

Independent variable	**Factors**	**Coded levels**		
		-1	0	+1
Temperature (^{0}C)	X_1	800	900	1000
Reaction time (min)	X_2	15	30	45
Steam to feedstock ratio	X_3	0.5	1.55	2.6

Table 3.2 shows the experimental design output based on Box Behnken method; the output is used for the steam gasification experiment in this research work. The design approach generated 15 experiments that comprises of 3 centre points or replicates. This centre points help optimise the results based on the experimental output of response variables. To understand the interaction effect among the three factors considered, the polynomial of the second order is the best method to fit the surface response model as shown in Equation (3-1). Several one-at-a-time experimental tests were also carried out to better understand the interactions among the variables. Analysis of variance (ANOVA) was also performed on the experimental output of the response variables to verify the significance of the model.

$$Y = \beta_0 + \sum_{i=1}^{p} \beta_i X_i + \sum_{i=1}^{p} \sum_{j=1}^{p} \beta_{ii} X_i X_j + \sum_{i=1}^{p} \beta_{ii} X_i^2 \qquad (0\text{-}1)$$

where i≠j

Y is the response variable

β_0 is the overall mean response

β_i is the main effects for each factor (i=1, 2 …., p)

β_{ij} is the two-way interaction between the ith and jth factors

β_{ii} is the quadratic effect for the ith factor [112].

Table 3.3. Experimental design

Number of Test	(X_1) Temperature (^{0}C)	(X_2) Steam/feedstock ratio	(X_3) Reaction Time (min)
1	900	1.55	30
2	900	0.5	45
3	900	1.55	30
4	800	0.5	30
5	1000	1.55	15
6	1000	2.6	30
7	900	0.5	15
8	800	1.55	15
9	1000	1.55	45
10	1000	0.5	30
11	900	2.6	45
12	800	1.55	45
13	900	1.55	30
14	800	2.6	30
15	900	2.6	15

3.6 Product gas Characterization

3.6.1 Analysis of the product gas

Agilent 6890 gas-chromatograph (GC) was used to analyse the composition of the product gases, which is typically composed of H_2, CO, CO_2 and CH_4 gases [24], [82], [116]. The GC is equipped with two columns. The two columns installed in the GC includes the following:

- Packed column: Carboxen 1000 with dimension 15ft x 1/8 in x 2.1 mm and part number 141624 from Sigma Aldrich
- Capillary column: GS-CARBONPLOT with dimension 30m x 0.320 mm x 3.0 μm, serial number USC410821H and part number 113-3133 from Agilent technologies inc.

The GC is also equipped with Flame Ionization Detector (FID) and Thermal Conductivity Detector (TCD). The FID was used to detect CH_4 while TCD to detect CO, CO_2, and H_2. The product gas from steam gasification of other landfill waste is mainly composed of hydrogen (H_2), carbon monoxide (CO), carbon dioxide (CO_2), methane (CH_4) and traces of

hydrocarbon gas [109]. Thus, only H_2, CO, CO_2, and CH_4 were analyzed for the product gas [109]. The volume of the generated gas was also measured.

The gas yield was calculated as the molar amount of each gas generated per gram of feedstock. The total gas yield was calculated by adding up the mole fraction of each product gas generated per gram of the feedstock. The lower heating value (LHV) of the product gas was calculated using Equation (3-2) [3], [115].

$$LHV\ \left({}^{KJ}/_{m^3}\right) = [(25.7\ \times\ n_{H_2}) + (30\ \times\ n_{CO}) + (85.4\ \times\ n_{CH_4}] \times\ 4.2 \qquad (3\text{-}2)$$

where n_{H_2}, n_{CO}, and n_{CH_4} are the moles H_2, CO and CH_4 gas respectively.

3.6.2 Analysis of the solid phase

An acetone solution was used to trap the ash content and impinge the product gas. The acetone solution was filtered using a filter paper (retention size: 8 -10 um) and the filtered solution was evaporated at 40 ^{0}C for 12 hours following the procedure as described in the literature [24]. The tar yield of the gasification process was determined by adding the weight of the tar yield during the filtration process and that of the evaporation process.

3.7 Evaluation of Steam Gasification Performance

3.7.1 Carbon gasification efficiency

The carbon gasification efficiency (CGE) is defined as the ratio of the amount of carbon leaving the reactor through the product gas to that of carbon fed into the reactor as fuel [117]. It is estimated as the total moles of carbon in gas yield per total mole of carbon in the feedstock [11], [13].

$$\text{CGE (\%)} = \left(\frac{\sum_i M_i\ \times C_{gas,i}}{M_f \times C_f}\right) \times 100 \qquad (0\text{-}3)$$

where $C_{gas,i}$ is the carbon content of the *i*th gas component (mol), M_f is the mass of the feedstock (kg), C_f is the carbon content of the feedstock (mol), and M_i is the mass of the ith gas component (kg).

3.7.2 Cold gas efficiency

The cold gas efficiency (η_{CG}) is defined as the chemical energy in the product gas in relation to the chemical energy in the feedstock [117]. It is estimated as the ratio of the total Lower Heating value (LHV) of the product gas to the total LHV of the feedstock:

$$\eta_{CG}(\%) = \frac{V_{PG} . LHV_{PG}}{M_f . LHV_f} \times 100 \qquad (0\text{-}4)$$

where V_{PG} is the volume of the product gas (Nm^{-3}), LHV_{PG} is the lower heating value of the product gas ($MJNm^{-3}$), M_f is the mass of the feedstock fed into the reactor (kg), and LHV_f is the lower heating value of the feedstock ($MJ.kg^{-1}$).

Chapter 4

Results and Discussions

This chapter presents the results of the physical and chemical characterization of the excavated waste residue (EWR) and the produce gas. The effects of temperature, reaction time and steam to biomass ratio on the gasification process are also discussed. In addition, the steam gasification performance, efficiency, and the optimization of the gasification process is also discussed.

4.1 Physical Characterization of Excavated Waste Residue (EWR)

Table 4.1 shows the physical characteristics of the EWR from Calgary Bio-cell. The EWR was classified according to the material type and its weight fraction in the total sample. The largest weigh fraction is soil (25%); this may be due to impurities in the EWR, which appears as soil. This may also be because of the organic materials (food waste, yard waste, *etc*.) in the waste residue that has decomposed into soil like materials due to the operation of the bioreactor under anaerobic condition to enhance the biodegradation of the waste. The second largest fraction is the 2D plastic (16%), followed by 3D plastic materials (14%). According to literature, the level of income of a country determines the composition of waste generated in such a country [5]. The lowest fraction is non-ferrous metals (1%), followed by the ferrous metals (2%); this may be due to the type of waste the deposited the bioreactor is designed to take. The bioreactor was design to take municipal solid waste such as household waste and agricultural waste. Therefore, wastes such as ferrous and non-ferrous metals are expected to be of low quantity.

Table 4.1. Classification of excavated waste residue (EWR) from Calgary Bioreactor

Category	Material	Type	% Weight
1	Wood	All types of wood	5
2	Paper	Paper, cardboard,	10
3	Textile	All type of textile	8
4	Plastic 2D	Bags, Foils	16
5	Plastic 3D	PET, PCV	14
6	Glass	Colorless glass, green glass, *etc*.	3
7	Fe metals	Ferrous metals: iron	2
8	NFe metals	Non-ferrous metals: copper, aluminum, *etc*.	1
9	Inert	Stones, ceramics	5
10	Soil	Soil-like materials	25
11	Others	Foam, rubber, sandpaper, composite,	11

4.2 Chemical Characterization of Excavated Waste Residue EWR

Table 4.2 shows the results of the elemental composition and chemical properties of the EWR samples. The lower heating value (LHV) of the EWR sample is 6650 BTU, which is 15.5MJ/kg; this is quite low when compared to the 22.9 MJ/kg of similar sample that was not subjected to enhanced biodegradation [24]. This means that part of the useful energy in the waste sample deposited in the bioreactor has been withdrawn during the enhanced biodegradation stage of the bioreactor.

The moisture content of the EWR sample is 42.4 % wt, this amount is high when compared to other types of waste like coconut shell and timothy grass, which are 5.7 and 6.2 %wt, respectively [82][115]. This high moisture content reduces the gasification efficiency.

The volatile matter and ash content of the EWR sample are 46.7 and 41.4 % wt, respectively. These values are considered high and may be due to the high amount of plastics and impurities in the waste samples. High amount of impurities in the feedstock tends to reduce the gasification performance by lowering the thermal output and increasing the formation of ash clinker [118]. It has also been demonstrated by Zaini *et al.* [119] that the presence of impurities significantly reduced the reactivity of the feedstock during steam gasification of excavated landfill waste. A fuel with ash content above 40% wt is considered as a low quality fuel [120].

The fixed carbon content of the EWR sample is 11.9 % wt. This value is quite low when compared to the raw biomass (beech wood), which is 15 % wt [24]. This might be due to the high amount of plastics in the EWR sample: according to Zhou *et al.* [121] landfilled plastics contains less fixed carbon and higher ash contents than fresh plastic waste, and the magnitude of theses difference increases with the age the landfill.[24] This low amount of fixed carbon in the EWR sample is the reason for its low calorific value because a fuel with high concentration of fixed carbon should have a higher calorific value [24].

Table 4.2. Chemical composition of EWR sample

Composition	Unit	Result
Fixed carbon (C)	%, OD basis	11.9
Carbon (C)	%, OD basis	37.4
Hydrogen (H)	%, OD basis	4.46
Nitrogen (N)	%, OD basis	1.09
Sulfur (S)	mg/kg, OD basis	4050
Oxygen (O)	%, OD basis	15.2
Moisture content	%, as recvd	42.4
Calorific value (LHV)	BTU/lb, OD basis	6650
Volatile matter	%, OD basis	46.7
Ash content at 575^0C	%, OD basis	41.4

OD = oven dried
as-recvd = As received
LHV = lower heating value

4.3 Product Gas Characterization

4.3.1 Product gas composition

Table 4.3 shows the product gas composition and the product gas yield from the EWR steam gasification. The two detectors installed in the GC are thermal conductivity detector (TCD) and flame ionization detector (FID). The thermal conductivity detector (TCD) was used to identify inorganic elements such as the hydrogen, carbon dioxide, carbon monoxide and Nitrogen in the gas sample. The flame ionization detector (FID) was used to identify hydrocarbons in the gas sample.

The gaseous product detected by the TCD are hydrogen (H_2), carbon monoxide (CO), and carbon dioxide (CO_2) while the FID detects methane (CH_4). According to Zhai *et al.* [109], the product gas from steam gasification of landfill waste is mainly composed of hydrogen (H_2), carbon monoxide (CO), carbon dioxide (CO_2), methane (CH_4) and a traces of hydrocarbon gas such as acetylene (C_2H_2), ethene (C_2H_4), and ethane (C_2H_6). Therefore, the GC was calibrated to analyse only H_2, CO, CO_2, and CH_4 gases in this study.

Table 4.3. Steam gasification result with product gas yield composition and the total product gas yield

Test	(X_1) Temperature (^{0}C)	(X_2) Reaction Time (min)	(X_3) Steam/feed stock ratio	H_2 yield (mol/kg)	CO yield (mol/kg)	CO_2 yield (mol/kg)	CH_4 yield (mol/kg)	Total product gas yield (mol/kg)
1	900	30	1.55	0.39	3.49	5.63	2.12	11.64
2	900	45	0.5	0.60	3.16	5.77	7.20	16.72
3	900	30	1.55	0.55	3.37	5.21	2.39	11.53
4	800	30	0.5	0.21	0.14	4.81	2.52	7.68
5	1000	15	1.55	0.51	2.45	2.05	4.76	9.77
6	1000	30	2.6	1.39	3.24	4.17	6.81	15.60
7	900	15	0.5	0.26	1.66	2.73	3.79	8.44
8	800	15	1.55	0.19	1.99	3.60	4.31	10.09
9	1000	45	1.55	3.37	8.04	7.37	11.70	30.48
10	1000	30	0.5	1.65	4.13	3.90	7.30	16.98
11	900	45	2.6	0.46	1.95	4.33	4.66	11.39
12	800	45	1.55	0.29	1.85	5.01	3.12	10.26
13	900	30	1.55	0.44	2.68	3.49	3.08	9.68
14	800	30	2.6	0.22	1.47	4.43	4.14	10.26
15	900	15	2.6	0.34	1.85	3.16	2.75	8.10
16	1000	45	2.6	1.14	4.56	6.31	4.83	16.83
17	800	45	0.5	0.24	1.05	4.06	1.95	7.29
18	900	45	1.55	1.54	5.32	5.81	9.33	22.00
19	800	45	2.6	0.20	1.18	2.96	0.44	4.78
20	1000	45	0.5	2.36	6.34	5.37	10.45	24.52
21	1000	30	1.55	0.60	5.95	3.19	5.06	14.80
22	1000	15	0.5	0.60	1.7116	1.45	3.17	6.93

4.3.2 Analysis of the product gas yield results

Table 4.4 shows the experimental design with the response variable. The independent variables considered for the experimental design are temperature (^{0}C), reaction time (min), and steam to feedstock ratio while the response variable is the product gas yield.

Table 4.4. Box Behnken experimental design and product gas yield results

Test	(X_1) Temperature (^{0}C)	(X_2) Reaction Time (min)	(X_3) Steam/feedstock ratio	Product gas yield (mol/kg)
1	900	30	1.55	11.64
2	900	45	0.5	16.72
3	900	30	1.55	11.53
4	800	30	0.5	7.68
5	1000	15	1.55	9.77
6	1000	30	2.6	15.60
7	900	15	0.5	8.44
8	800	15	1.55	10.09
9	1000	45	1.55	30.48
10	1000	30	0.5	16.98
11	900	45	2.6	11.39
12	800	45	1.55	10.26
13	900	30	1.55	9.68
14	800	30	2.6	10.26
15	900	15	2.6	8.10

Table 4.5 shows the analysis of variance (ANOVA) result of the total product gas yield for the response surface methodology (RSM) based on Box Behnken model. The level of significance of this model can be determined by the F-value and p-value with confidence level of 95%. The F-value is determined by the ratio of variation between the variables (*i.e.*, temperature, reaction time, and steam to feedstock ratio) and the variation within these same variables. The higher the F-value, the more the difference between the variables than the difference within the same variables. The F-value of the overall model is observed to be 10.83 in the ANOVA result, and this indicates that there is more variation between the considered variables than within the variables itself.

The p-value is defined as the probability of getting results that are closer to an actual experimental data. In the study, p-value ($p \leq 0.05$) signifies that the RSM model is significant with a confidence level of 95%. The p-value of the overall model is observed to be 0.009 and this indicates that our model is significant. The "lack of fit" for this model has a p-value of 0.155, which is considered statistically insignificant because its p-value is greater than 0.05. Therefore, there is no visible lack of fit between the RSM model and our experimental data for the total product gas produce during the steam gasification process.

In addition, this study also examined the significance of each variable and their interactions. The results of the p-value of 0.002 and the corresponding F-value of 32.94 of temperature shown in Table 4.5 indicate that temperature is the most significant variable influencing the yield of product gas in the steam gasification process. Another significant variable influencing the yield of product gas is the reaction time with a p-value of 0.003 with an F-value of 29.10. The steam to feedstock ratio is not a significant factor influencing the yield of product gas because it has a p-value of 0.392 with an F-value of 0.55. Similarly, the significant model interaction variables influencing the yield of product gas is temperature and reaction time with a p-value of 0.005 and a corresponding F-value of 23.29.

The regression coefficient (R^2) and adjusted regression coefficient (Adj-R^2) are also used to evaluate the precision of the RSM model in relation the experimental data. The regression coefficient is usually within the range of (0 to 1). The closer the regression coefficient value is to (1), the better the accuracy of the model's prediction for the output response. The value of R^2 increases as the number of variables increases. The Adj-R^2, on the other hand, offers more appropriate results than R^2 because it decreases as insignificant variables are added to the model fit [122]. The regression coefficient (R^2) observed is 0.95, this value indicates that the RMS model can be fitted to our experimental results with an acceptable degree of precision. Also, the value of Adj-R^2 which is 0.86 agrees with the value of R^2.

Equation (4-1) shows the final model equation in terms of the independent variables considered for product gas yield in the steam gasification experiment. This equation represents the second order degree polynomial regression equation.

$$syngas\ yield\ \left(\frac{mol}{kg}\right) = 273 - 0.56X_1 - 3.05X_2 + 13.55X_3 + 0.00028{X_1}^2 + 0.0061{X_2}^2 - 1.05{X_3}^2 + 0.0032X_1X_2 - 0.0094X_1X_3 - 0.079X_2X_3 \quad (0\text{-}1)$$

where X_1 = Temperature (^{0}C),

X_2 = reaction time (min),

X_3 = Steam to feedstock ratio.

Table 4.5. ANOVA results of total gas yield for RSM model

Response variable	Degree of freedom	Sum of squares	Mean squares	F-value	P-value
Model	9	441.44	49.05	10.83	0.009
X_1	1	149.16	149.16	32.94	0.002
X_2	1	131.77	131.77	29.10	0.003
X_3	1	2.49	2.49	0.55	0.392
X_1^2	1	29.67	29.67	6.55	0.051
X_2^2	1	6.90	6.90	1.52	0.272
X_3^2	1	4.92	4.92	1.09	0.345
X_1X_2	1	105.46	105.46	23.29	0.005
X_1X_3	1	3.90	3.90	0.86	0.396
X_2X_3	1	6.20	6.20	1.37	0.295
Error	5	22.64	4.53		
Lack of fit	3	20.24	6.75	5.61	0.155
Total	14	464.08			
R^2		0.95			
Adj R^2		0.86			

X_1 = Temperature, X_2 = reaction time, X_3 = Steam to feedstock ratio

Another important contribution of the analysis of variance (ANOVA) is to study the interaction of two independent variables towards the output response. The interaction of two variables was carried out using three-dimensional plots by means of surface response. This graphical information can be further used to interpolate these interactions to intermediate points, which have not been studied experimentally.

Figure 4.1 shows the three-dimensional surface plot of the total gas yield *vs* temperature, and reaction time. This three-dimensional surface plot is used to visualize the interaction between the two independent variables (temperature and reaction time) on a specific output response (total gas yield). Based on the result from the ANOVA, there are two variables that has significant influence on the product gas yield. These variables are temperature and reaction time.

The interaction of temperature and reaction time on product gas yield was investigated at steam to feedstock ratio of 1.55 as shown in Figure 4.1. When the temperature increased from 800 ^{0}C to 1000 ^{0}C at a constant reaction time of 45 min, the total product gas yield increases by about 66%. Similarly, when the reaction time increases from 15 min to 45 min, at a constant temperature of 1000 ^{0}C, the total product gas yield increases by about 67%. This might be due to that the tar compounds present in the product gas were broken down at temperature into smaller hydrocarbon molecules or non-condensable gases [24]. At a high temperature, a longer reaction time favors thermal cracking reactions, which result in a higher product gas yield [115].

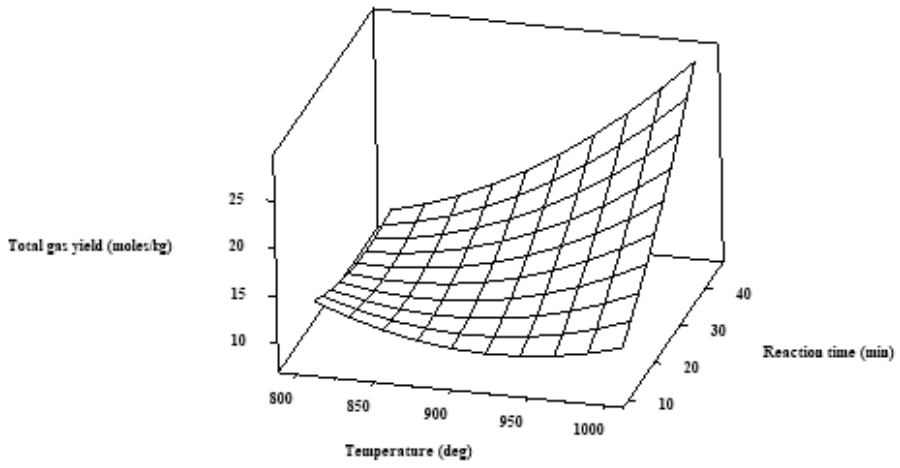

Figure 4.1. Surface plot of representing the combine effect of temperature (^{0}C) and reaction time (min) on the total gas yield (mol/kg) during steam gasification process

4.3.3 Optimization of the steam gasification process

The ANOVA analysis indicates the quadratic model that best fit the experimental results based on the p-value, F-value, and lack of fit as regression coefficients. After the best fitting of the model, the optimum operating conditions based on operating parameters considered for the steam gasification process based was determined. The optimization process was carried out using Minitab software.

Table 4.6 shows the optimum operating conditions based on the operating parameters considered. The optimum operating variable condition for the steam to feedstock ratio is 0.5 at temperature of 1000 ^{0}C, reaction time of 45 min, and steam to feedstock ratio of 0.5.

Table 4.6. Optimum operating parameter values

Parameters	Optimum value
Temperature (^{0}C)	1000
Reaction time (min)	45
Steam to feedstock ratio	0.5

A comparison was made between the experimental result at the optimum conditions and the optimal values predicted by the model. The total product gas yield at the optimum condition during the experimental run is 24.52 mol/kg, while the total product gas yield predicted by the model is 30.30 mol/kg. The difference between the predicted value and our experimental value is 5.78 mol/kg. This value is known as residual error, and it might be because of errors within the experimental setup during the gasification process.

4.4 Effects of Temperature on Gasification Product

4.4.1 Effect of temperature on product gas product composition

In Figure 4.2, the gasification temperature was plotted against the product gas product composition at the constant steam to feedstock ratio of 0.5 and the reaction time of 45 minutes. The steam to feedstock ratio and reaction time were held constant at these values because the optimal conditions predicted by the optimization model in this study are reaction time of 45 min and steam to feedstock ratio of 0.5. The gas products (H_2, CO, CO_2, and CH_4) are represented in Figure 4.2 by different hatch patterns.

As shown in Figure 4.2, the highest product gas product yield observed is CH_4 (10.45 mol/kg) at a temperature of 1000 ^{0}C. An increase in the gasification temperature from 800 to 1000 ^{0}C increases CH_4 yield from 1.94 mol/kg to 10.45 mol/kg. This might be because of the high amount of 2D and 3D plastic content in the feedstock (see Table 4.1). According to the literature [123], thermal cracking of plastics typically contains heavy hydrocarbons such as CH_4 along with smaller amount of H_2, CO and CO_2. The amount of H_2 and CO also increases from 0.24 to 2.35 mol/kg and 1.1 to 6.34 mol/kg respectively as the temperature increase. This might be due to high temperature favoring H_2 yield from the waster-gas shift (WGS) reaction [3]. The WGS is the reaction between CO and water vapor to form CO_2 and H_2 (see equation 2-5). However, a different trend was observed for CO_2. At a temperature of 800 ^{0}C,

the highest product gas yield is CO_2 (4.1 mol/kg). The yield increase by about 40% from 4.1 to 5.77 mol/kg as the temperature increases from 800 ^{0}C to 900 ^{0}C, but later it decreases by 6.9% from 5.77 to 5.37 mol/kg as the temperature further increase from 900 ^{0}C to 1000 ^{0}C.

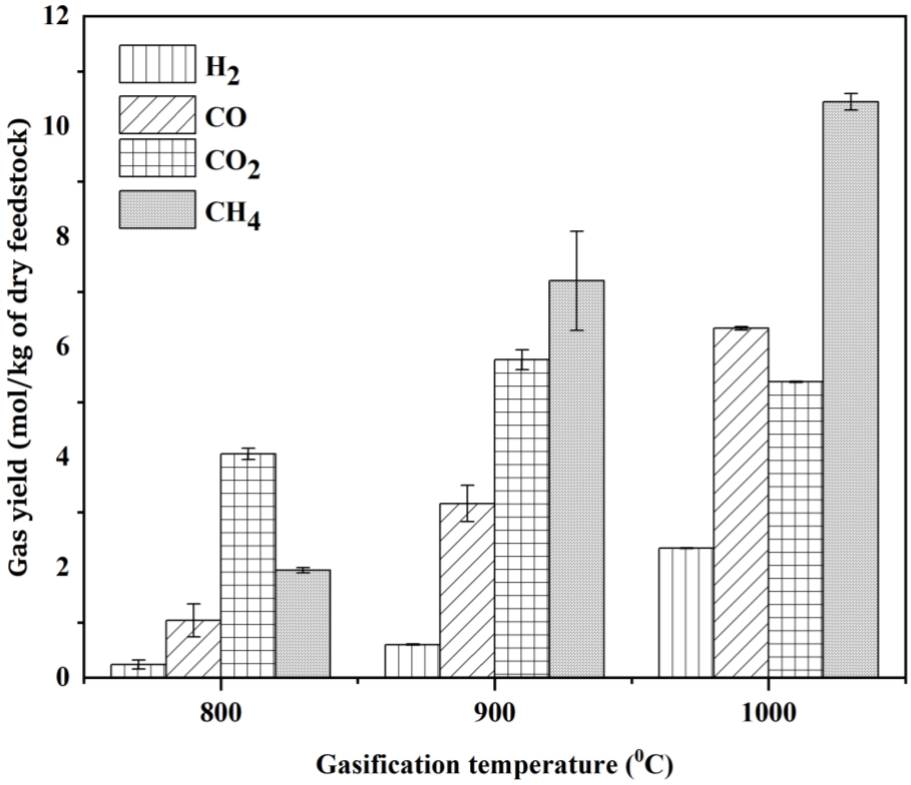

Figure 4.2. Effect on temperature on product gas product composition at reaction time 45 min and steam to feedstock ratio of 0.5

4.4.2 Effect of temperature on product gas yield and tar yield

Figure 4.3 shows the effects of temperature on the product gas yield and tar yield during steam gasification process. The gasification temperature was plotted against the product gas yield and tar yield at constant steam to feedstock ratio of 0.5 and reaction time of 45 minutes.

As shown in figure 4.3, the total product gas yield, which is the summation of all the product gas product yield for each experimental test, increases as the gasification temperature increases. The total product gas yield increase by about 230% from 7.3 mol/kg to 24.52 mol/kg as the gasification temperature increases from 800 to 1000 ^{0}C. This might be due to the high temperature and longer reaction time favoring thermal cracking reactions, resulting in higher product gas yields [115]. This result agrees with the data reported by Zaini *et al.*

[24], who investigated the effects of temperature on product gas yield from excavated landfill waste through steam co-gasification of biochar. They observed that product gas yield increases with temperature.

However, the tar yield decreases as the temperature increases. The tar yield decreases by 73% from 18.9 to 5.03 g/kg as the temperature increases from 800 to 1000 ^{0}C. At a higher temperature, tar compounds are broken down into smaller non-condensable gases, increasing the product gas yield [24].

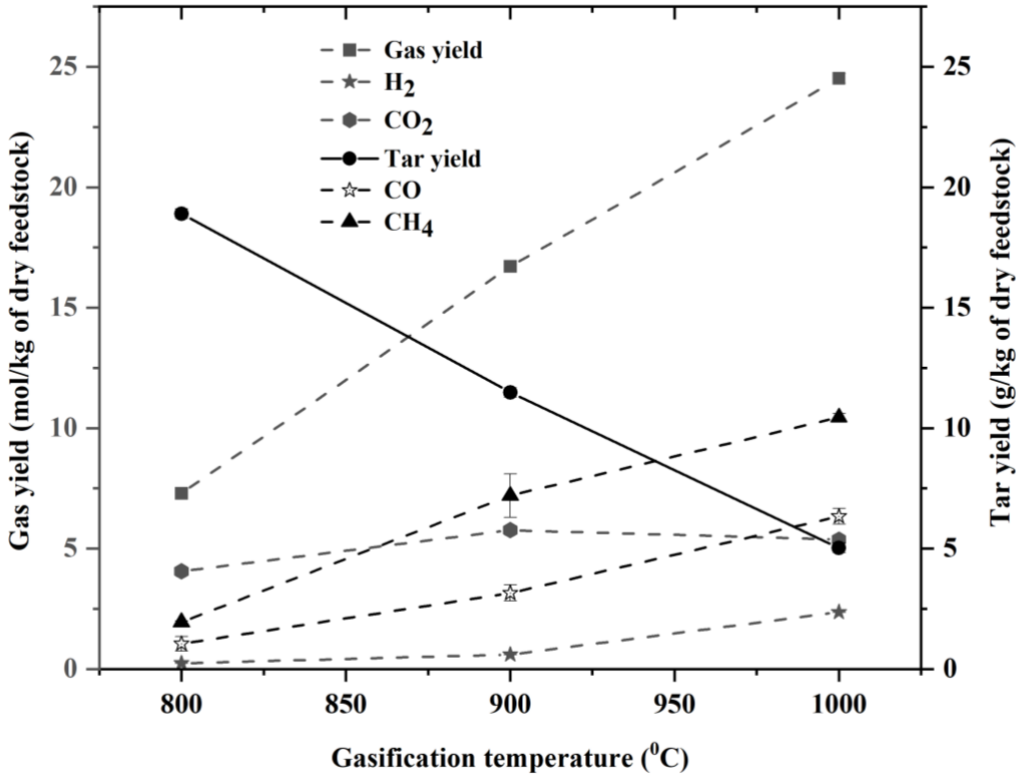

Figure 4.3. Effects of temperature on product gas yield and tar yield at a reaction time of 45 min and steam to feedstock ratio of 0.5

4.4.3 Effect of temperature on lower heating value (LHV)

Figure 4.4 shows the effects of temperature on the lower heating value (LHV) of the steam gasification process. The gasification temperature was plotted against the lower heating value at a constant steam to feedstock ratio of 0.5 and a reaction time of 45 minutes. Table 4.7 also shows the lower heating value, carbon gasification efficiency, cold gas efficiency and tar

yield of the steam gasification. The lower heating value increases by about 450% from 2.06 to 11.53 KJ/Nm^3 as the gasification temperature increases from 800 to 1000 ^{0}C. This is because the lower heating value of the product gas is calculated from the mole fraction of the combustible gases such as H_2, CO and CH_4 in the product gas yield. Therefore, the lower heating value follows the same trend as H_2, CO and CH_4. In this study, the yield of H_2, CO and CH_4 increases as the gasification temperature increases (see 4.4.1). This result agrees with that reported by Saebea *et al.* [124]. Their result showed that increasing the gasifier temperature from 650 to 1100 ^{0}C increased the mole fraction of the product gas product yield.

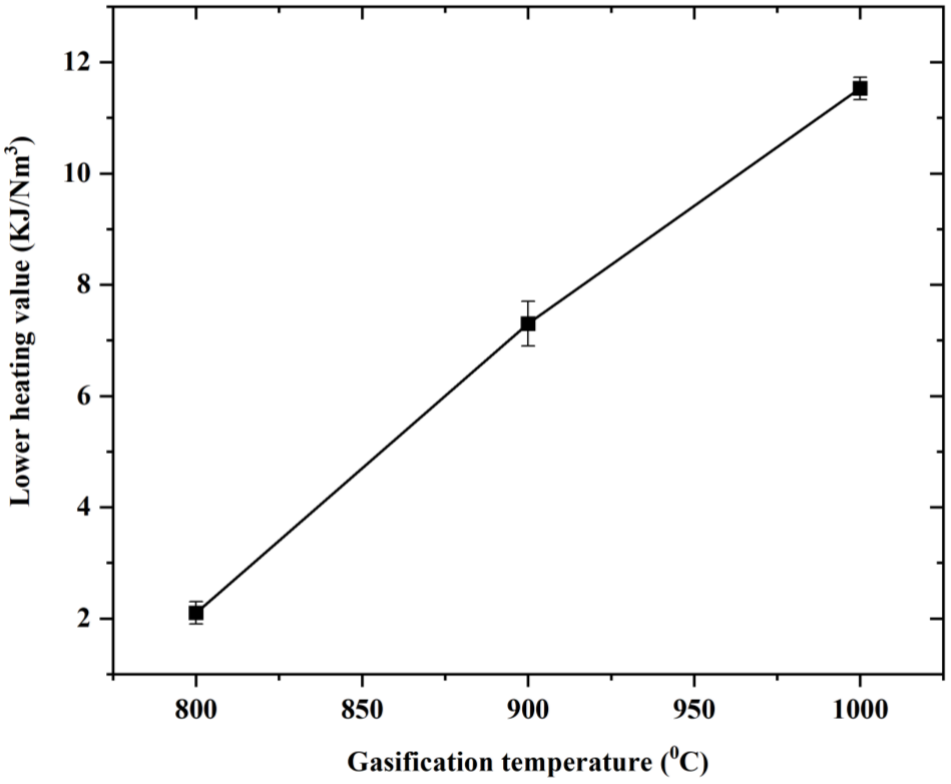

Figure 4.4. Effect of temperature on the heating value of steam gasification at reaction time 45 min and steam to feedstock ratio of 0.5

Table 4.7. Steam gasification results

Test	(X_1) Temperature (^{0}C)	(X_2) Reaction Time (min)	(X_3) Steam/feedstock ratio	LHV (KJ/Nm^3)	Carbon gasification efficiency (%)	Cold gas efficiency (%)	Tar yield (g/kg)
1	900	30	1.55	2.98	5.40	2.31	6.95
2	900	45	0.5	7.30	7.74	8.48	11.48
3	900	30	1.55	3.22	5.27	2.49	7.10
4	800	30	0.5	2.26	3.59	1.75	20.15
5	1000	15	1.55	4.97	4.44	1.92	8.98
6	1000	30	2.6	7.20	6.83	5.57	11.45
7	900	15	0.5	3.83	3.93	1.48	3.38
8	800	15	1.55	4.36	4.75	1.69	3.20
9	1000	45	1.55	13.38	13.01	15.54	2.25
10	1000	30	0.5	7.96	7.36	6.16	5.98
11	900	45	2.6	4.72	5.25	5.48	0.73
12	800	45	1.55	3.32	4.79	3.85	1.73
13	900	30	1.55	3.57	4.44	2.70	7.23
14	800	30	2.6	4.06	4.82	3.15	27.00
15	900	15	2.6	3.01	3.72	1.17	14.53
16	1000	45	2.6	5.83	7.53	6.77	9.45
17	800	45	0.5	2.05	3.39	2.38	18.90
18	900	45	1.55	10.04	9.82	11.66	8.93
19	800	45	2.6	0.79	2.20	0.91	24.23
20	1000	45	0.5	11.53	10.64	13.38	5.03
21	1000	30	1.55	6.31	6.81	4.89	6.48
22	1000	15	0.5	3.40	3.04	1.32	6.73

4.4.4 Effect of temperature on carbon gasification efficiency and cold gas efficiency

Figure 4.5 shows the effects of temperature on carbon gasification efficiency and cold gas efficiency. The gasification temperature was plotted against the carbon gasification efficiency and the cold gas efficiency at a constant steam to feedstock ratio of 0.5 and a reaction time of 45 minutes. The carbon gasification efficiency and the cold gas efficiency increase as the gasification temperature increases. The carbon gasification efficiency increases from 3.39 to 10.6 % (see Table 4.7), while the cold gas efficiency increases from 2.39% to 13.38% as the gasification temperature increases from 800 to 1000 ^{0}C.

The carbon gasification efficiency and cold gas efficiency in this study are lower than those reported by others. For example, Zaini *et al.* [24] used biochar to enhance the gasification performance of excavated landfill waste through steam co-gasification. The carbon gasification efficiency and cold gas conversion efficiency reported were approximately 44% and 69%, respectively [24]. Since landfill wastes are known to contain high amounts of silica [125], the low carbon conversion and cold gas efficiencies reported in this study might be because of high amount of silica in the EWR. As reported in the literature, the presence of inorganic elements such as silicon (Si) could slow down the reactivity of the feedstock during steam gasification [126][125].

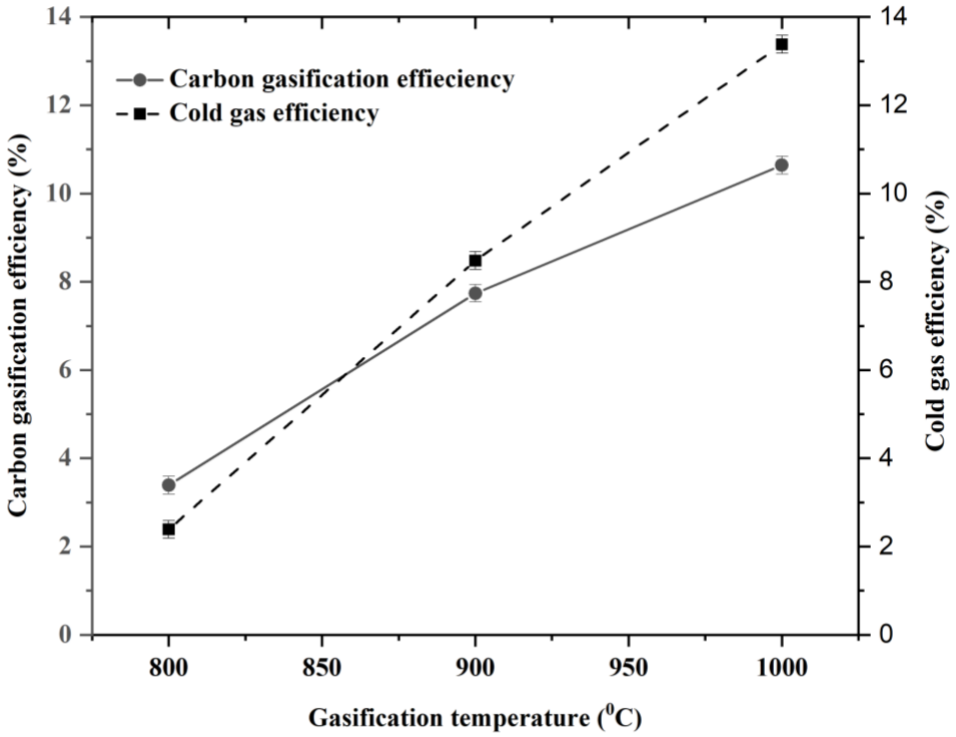

Figure 4.5. Effect of temperature on carbon gasification efficiency and cold gas efficiency at a reaction time of 45 min and steam to feedstock ratio of 0.5

4.5 Effects of Reaction time on Gasification Product

4.5.1 Effect of reaction time on product gas product composition

Figure 4.6 shows the effects of reaction time on product gas product composition. The gasification reaction time was plotted against the product gas yield at a constant temperature of 1000 ^{0}C and a steam to feedstock ratio of 0.5. The steam to feedstock ratio and reaction time were held constant at these values because the optimal conditions determined for this steam gasification process was the temperature of 1000 ^{0}C, the reaction time of 45 min and the steam to feedstock ratio of 0.5. The gas products (H_2, CO, CO_2, and CH_4) are represented by different hatch patterns on the graph.

As shown in Figure 4.6, the highest product gas product yield is CH_4 (10.45 mol/kg) at the reaction time of 45 min. The gas products (i.e., H_2, CO, CO_2, and CH_4) increases as the gasification reaction time increases from 15 min to 45 min. The hydrogen (H_2) yield increases by about 290 % from 0.60 to 2.36 mol/kg, while carbon monoxide (CO) and carbon

dioxide (CO_2) increases by 270 and 260 %, respectively. The highest product gas yield, which is for CH_4, increases by about 220 % as the reaction time increases from 15 to 45 minutes. This might be because a longer reaction time improves the gasification yield by favoring thermal cracking reactions at a higher temperature [3]. High temperatures and long reaction times favors methanation and water-gas shift reaction (see Equations 2-5 and 2-6) [3].

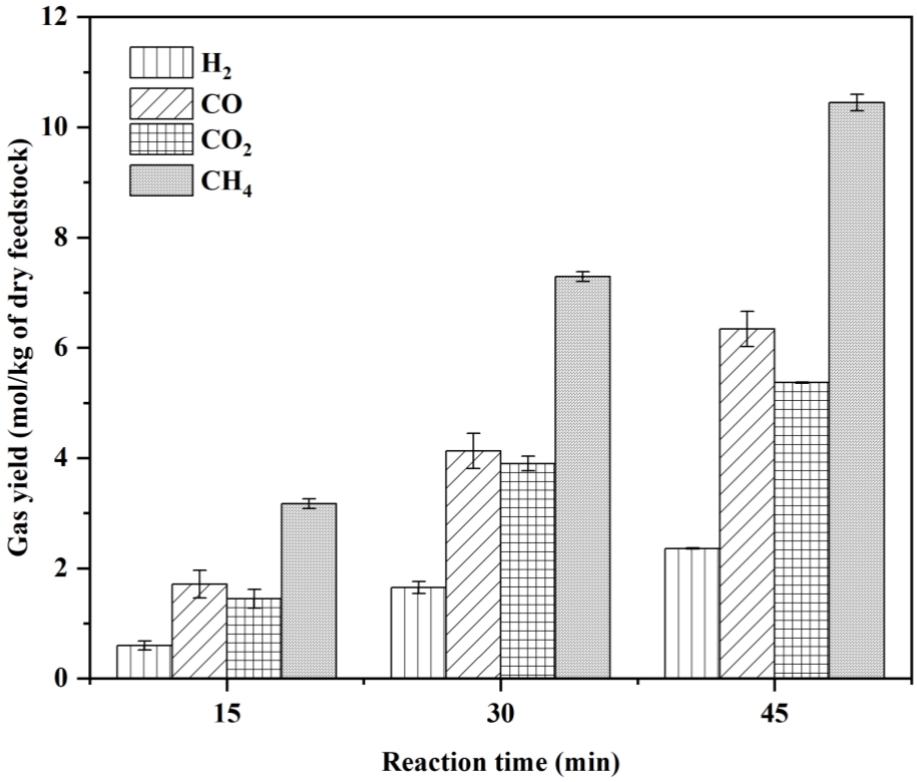

Figure 4.6. Effect of reaction time on product gas product composition at a temperature 1000 ^{0}C and steam to feedstock ratio of 0.5

4.5.2 Effect of reaction time on product gas yield and tar yield

Figure 4.7 shows the effects of reaction time on product gas and tar yield on steam gasification product. The gasification reaction time was plotted against the product gas and tar yield at constant temperature of 1000 ^{0}C and steam to feedstock ratio of 0.5.

All the product gas products (i.e., H_2, CO, CO_2, and CH_4) increase as the gasification reaction time increases from 15 to 45 minutes. The total product gas yield also follows

similar trend as it increases by about 230 % from 7.29 to 24.52 mol/kg as the reaction time under the same condition. However, the tar yield decreases as the gasification reaction time increases. The tar yield decreases by about 25 % from 6.73 to 5.03 g/kg as the reaction time increases from 15 to 45 minutes. This might be due to tar compounds been broken down into smaller non-condensable gases at high temperature and longer reaction time which results in an increase in the product gas yield [24].

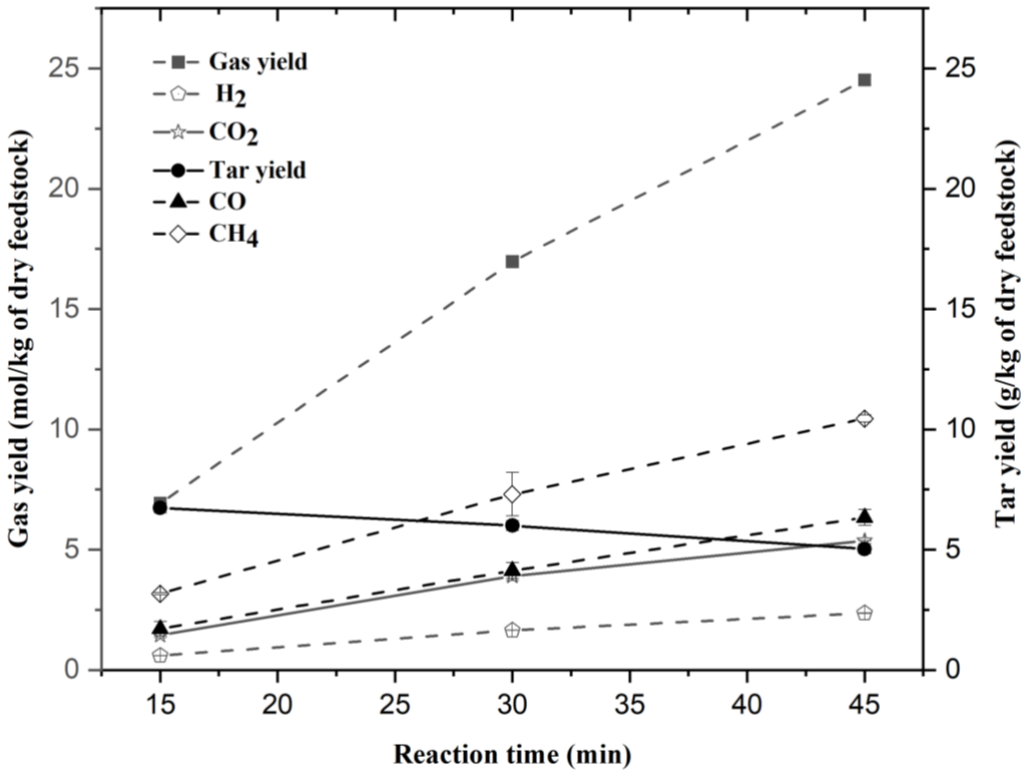

Figure 4.7. Effect of reaction time on product gas yield and tar yield on steam gasification product at a temperature of 1000 ^{0}C and steam to feedstock ratio of 0.5

4.5.3 Effect of reaction time on lower heating value

Figure 4.8 shows the effects of reaction time on lower heating value on steam gasification product with the gasification reaction time plotted against the lower heating value at constant temperature of 1000 ^{0}C and steam to feedstock ratio of 0.5. The lower heating value of the product gas increases as the reaction time increases. The lower heating value increases by about 220 % from 3.40 to 11.53 KJ/Nm^3 as the reaction time increases from 15 to 45 min.

This is because all the product gas products (H_2, CO, CO_2, and CH_4) increase with longer reaction time (see 4.4.1), and the lower heating value of the product gas is determined from the composition of the combustible gases such as H_2, CO and CH_4 in the product gas product.

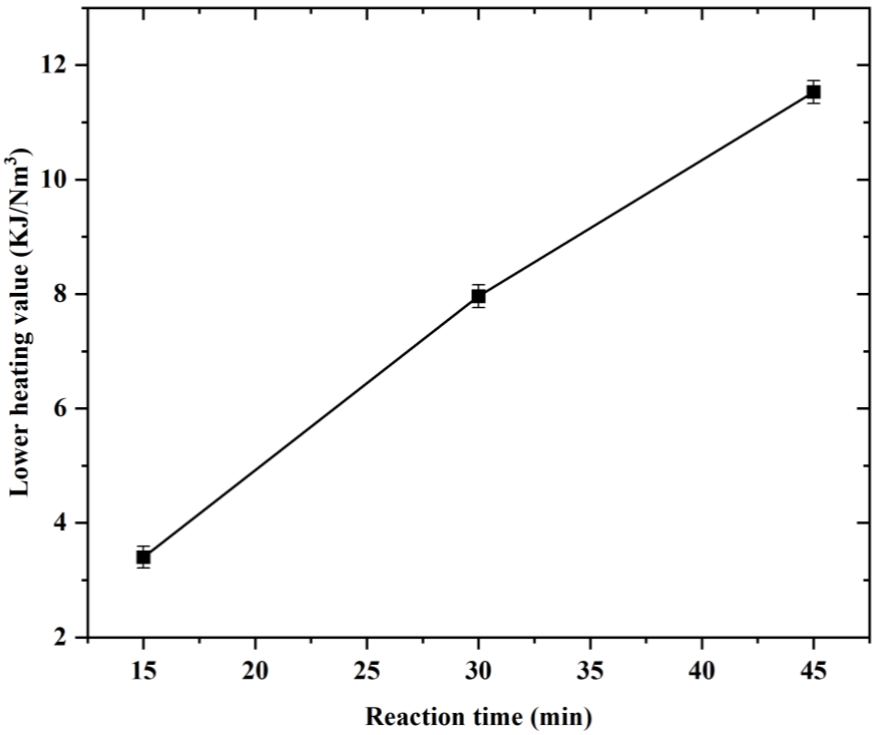

Figure 4.8. Effect of reaction time lower heating value on steam gasification product at a temperature of 1000 ^{0}C, and steam to feedstock ratio of 0.5

4.5.4 Effects of reaction time on carbon gasification efficiency and cold gas efficiency

Figure 4.9 shows the effect of reaction time on carbon gasification efficiency and cold gas efficiency on the steam gasification product. The gasification reaction time was plotted against the carbon gasification efficiency and the cold gas efficiency at constant temperature of 1000 ^{0}C, and steam to feedstock ratio of 0.5. The carbon gasification efficiency and the cold gas efficiency increases as the gasification reaction time increases. The carbon gasification efficiency increases by from 3.04 to 10.64 %, while the cold gas efficiency increases from 1.32% to 13.38% as the gasification reaction time increases from 15 to 45 min. In comparison with the literature [24], our data agree with that of the literature that

carbon gasification and cold gas efficiency increases as the reaction time of the steam gasification increases.

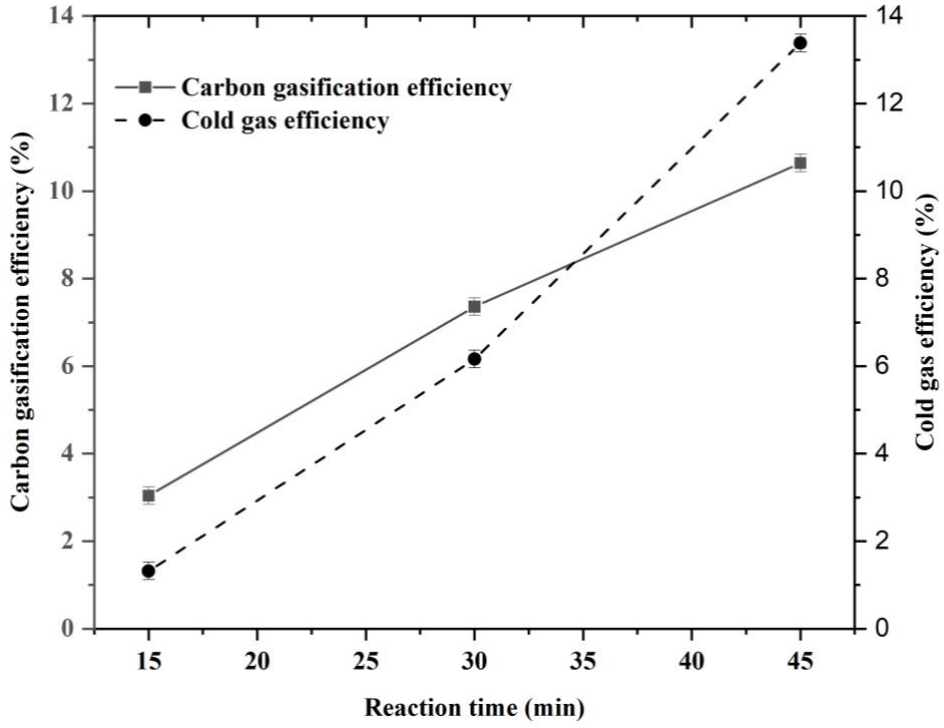

Figure 4.9. Effect of reaction time on carbon gasification efficiency and cold gas efficiency on steam gasification as a temperature of 1000 ^{0}C, and steam to feedstock ratio of 0.5

4.6 Effect of Steam to Feedstock Ratio on Gasification Product

4.6.1 Effect of steam to feedstock ratio on product gas yield

Figure 4.10 shows the effect of steam to feedstock ratio on product gas yield. The steam to feedstock ratio was plotted against the product gas yield at constant temperature of 1000 ^{0}C and reaction time of 45 minutes. The steam to feedstock ratio and reaction time was held constant at these values because the optimal conditions determined for this steam gasification process is temperature (1000 ^{0}C), and reaction time (45 min). The product gas products (H_2, CO, CO_2, and CH_4) are represented by different hatch patterns.

As shown in Figure 4.10, the highest product gas product yield is CH_4 (11.70 mol/kg) at a steam to feedstock ratio of 1.55. The product gas highest product yield (CH_4) increases by 11

% from 10.45 to 11.70 mol/kg as the steam to feedstock ratio increases from 0.5 to 1.55. After that, a sharp decrease of about 58 % was observed as the steam to feedstock ratio increases from 1.55 to 2.6. The yield of H_2, CO and CO_2 yield also increases by 42 %, 26 %, and 37 % respectively under the same condition. But later decreases to about 66 %, 43 %, and 14 % respectively as the steam to feedstock ratio increases from 1.55 to 2.6. This might be because excess steam quantity lowers the reaction temperature, which results to reduction in the quality of the product gas [82]. At a steam to feedstock ratio of 2.6, CO_2 (6.31mol/kg) yield was observed to be highest yield. This result agrees with the results from the literature [82].

The highest product gas yield (30.48 mol/kg) was observed at steam to feedstock ratio of 1.55. But, during the optimization of the steam gasification process, the optimal steam to feedstock is 0.5. The experimental results observed for the optimum condition for product gas yield is 24.52 mol/kg and the optimization model prediction result for the product gas yield is 30.30 mol/kg. The optimization process was carryout to achieve the best design for the steam gasification process in terms of temperature, steam to feedstock ratio, reaction time and the product gas yield. Since excess steam lowers the product gas yield and product gas grade, since steam production come at a cost, then optimal steam to feedstock ratio is an important factor in steam gasification process.

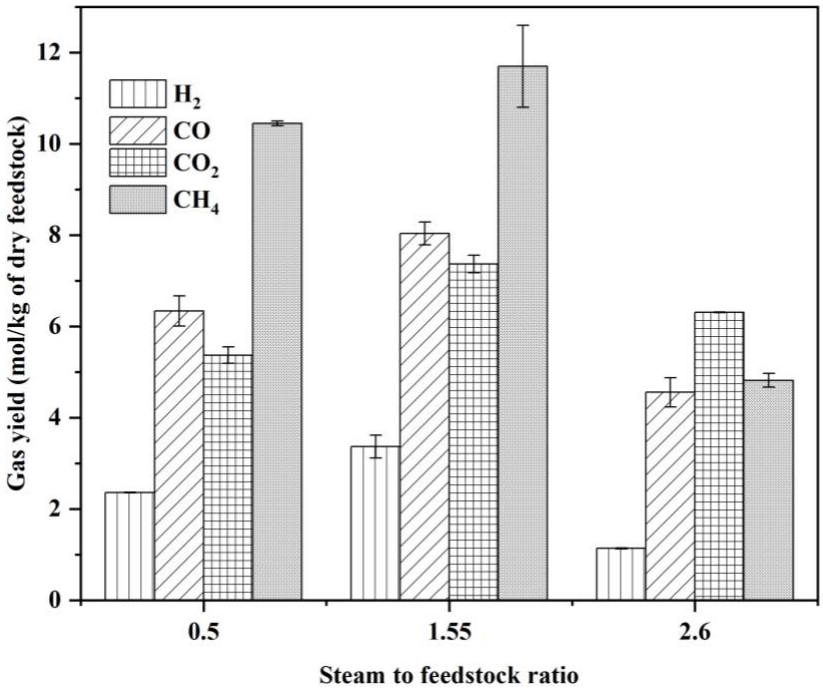

Figure 4.10. Effect of steam to feedstock ratio on gasification product composition on steam gasification at a temperature of 1000 ^{0}C, and reaction time of 45 minutes

4.6.2 Effect of steam to feedstock ratio on product gas yield and tar yield

Figure 4.11 shows the effect of steam to feedstock ratio on product gas and tar yield on steam gasification. The steam to feedstock ratio was plotted against the product gas and tar yield at constant temperature of 1000 ^{0}C and reaction time of 45 minutes.

The product gas yield increases as the steam to feedstock increase from 0.5 to 1.55 but later decrease sharply as the steam to feedstock ratio further increase to 2.6. The total product gas yield for the steam gasification process also follows the same trend since it is determined by the summation of all the product gas yield. The total product gas yield increases by about 24 % from 24.52 to 30.48 mol/kg as the steam to feedstock ratio increase from 0.5 to 1.55 and later decrease by about 44 % from 30.48 to 16.83 mol/kg when the steam to feedstock ratio further increase to 2.6.

As shown in Figure 4.11, the tar yield reduces by about 55 % from 5.03 to 2.25 g/kg as the steam to feedstock ratio increases from 0.5 to 1.55 but later increases to about 300 % from

2.25 to 9.45 g/kg as the steam to feedstock increases from 1.55 to 2.6. This might be because excess steam lowers the reaction temperature, and this results in low quality of product gas yield.

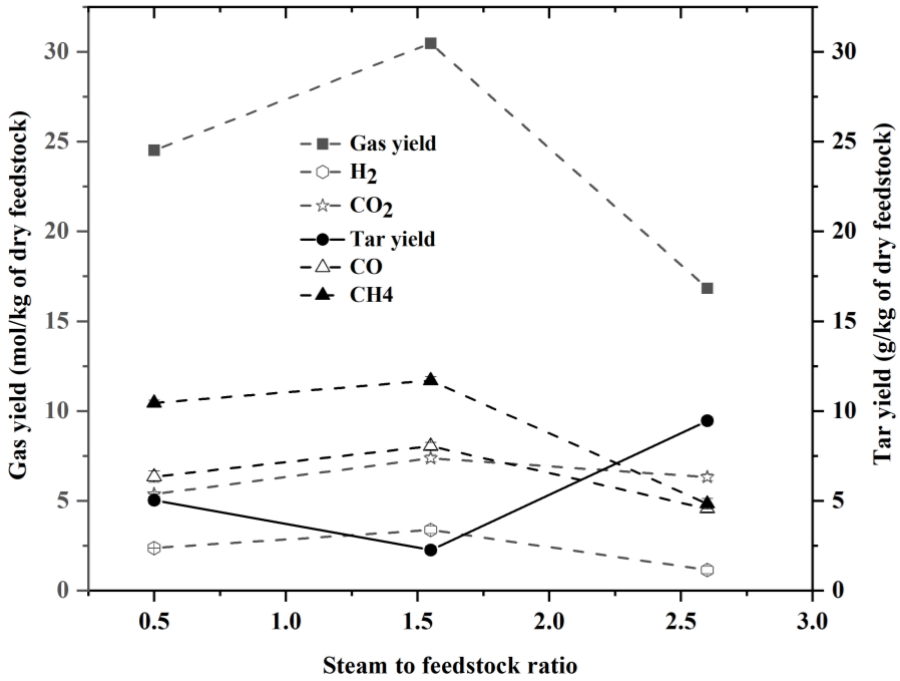

Figure 4.11. Effect of steam to feedstock ratio product gas yield and tar yield on steam gasification at a temperature of 1000 ^{0}C, and reaction time of 45 minutes

4.6.3 Effect steam to feedstock ratio on lower heating value

Figure 4.12 show the effect of steam to feedstock ratio of lower heating value on steam gasification yield. The steam to feedstock ratio was plotted against lower heating value at constant temperature of 1000 ^{0}C and reaction time of 45 minutes. The product gas products (H_2, CO, CO_2, and CH_4) yield increases as the steam to feedstock ratio increases from 0.5 to 1.55 and decreases as the steam to feedstock ratio further increase from 1.55 to 2.6 (see 4.6.2). The lower heating value also follow the same trend as it increases by about 16 % from 11.53 to 13.38 KJ/Nm^3 as the steam to feedstock ratio increases from 0.5 to 1.55, but later decrease sharply by 56 % from 13.38 to 5.83 KJ/Nm^3 as the steam to feedstock further increase to 2.6. This is because the lower heating value of the product gas is determined from the composition of the combustible gases such as H_2, CO and CH_4 in the product gas product.

Also, excess steam lowers the reaction temperature, and this results in low quality of product gas yield.

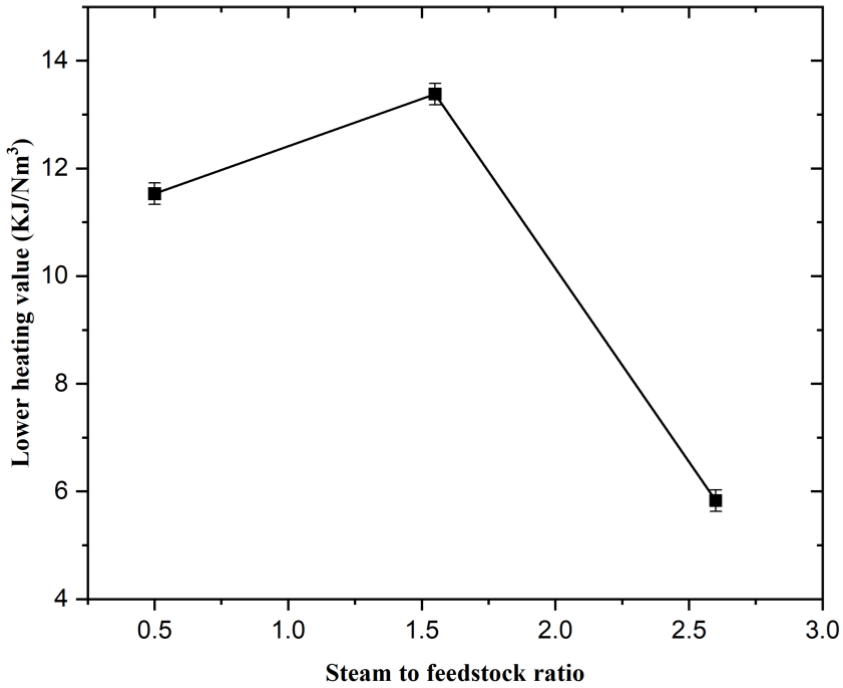

Figure 4.12. Effect of steam to feedstock ratio on the lower heating value of steam gasification at a temperature of 1000 ^{0}C, and reaction time of 45 minutes

4.6.4 Effect of steam to feedstock ratio on carbon gasification efficiency and cold gas efficiency

Figure 4.13 shows the effect of steam to feedstock ratio on carbon gasification and cold gas efficiency on steam gasification. The steam to feedstock ratio was plotted against the carbon gasification efficiency and the cold gas efficiency at constant temperature of 1000 ^{0}C, and reaction time of 45 minutes. The carbon gasification efficiency increases from 10.64 to 13.01 % as steam to feedstock ratio from 0.5 to 1.55 and later decreases from 13.01 to 7.53 % as the steam to feedstock further increases from 1.55 to 2.6. The cold gas efficiency increases from 13.38 to 15.54 % as the steam to feedstock increases from 0.5 to 1.55 and later decrease from 15.54 to 6.77 % as the steam to feedstock further increases from 1.55 to 2.6. This is because high temperature and longer reaction time promotes the breakdown of tar formed during the steam gasification. This condition improves the carbon conversion and cold gasification

efficiency of gasification process. However, higher steam to feedstock ratio can lower the gasification temperature, resulting into loss of chemical energy in form of tar [24].

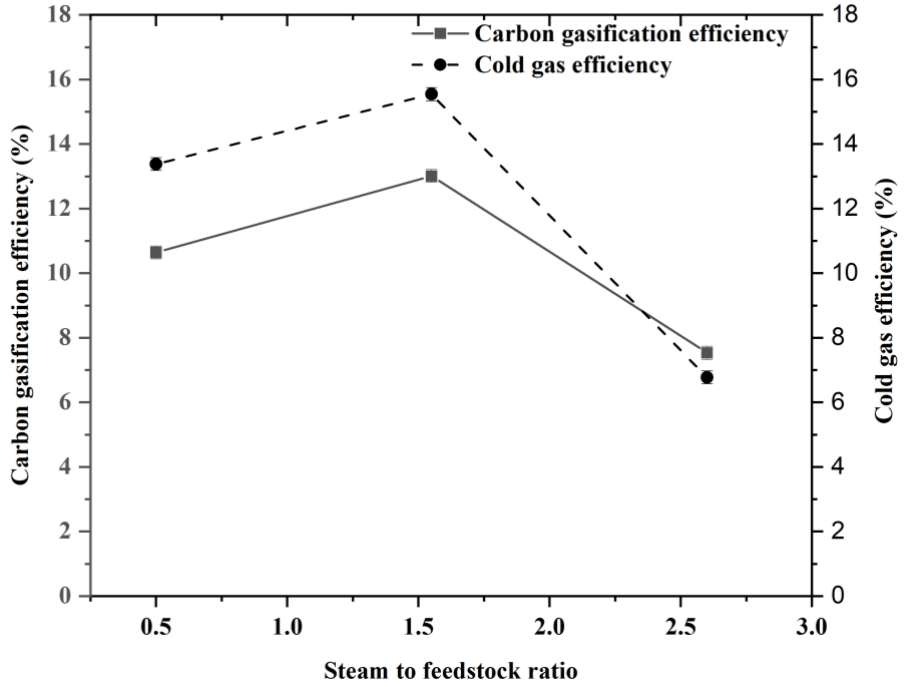

Figure 4.13. Effect of steam to feedstock ratio on carbon conversion and cold gas efficiency on steam gasification at a temperature of 1000 ^{0}C and reaction time 45 minutes

Chapter 5

Conclusions, Original Contributions, and Recommendations

5.1 Conclusions

This thesis reports the energy potential of excavated waste residue (EWR) from the City of Calgary Bio-cell. Based on the experimental results, the conclusions are drawn as follows:

The largest weight fraction of the EWR sample is soil, constituting about 25 % of the total EWR from the Calgary Bio-cell. The lower heating value of the EWR is 15.5 MJ/kg, moisture content is 42.4% wt, volatile matter is 46.7 % wt, and ash content is 41.4% wt.

The optimum conditions observed for product gas yield through steam gasification of the EWR sample are temperature 1000 ^{0}C, steam to feedstock ratio 0.5, and reaction time 45 minutes. Based on the analysis of variance (ANOVA), temperature and reaction time were the most significant factors affecting product gas production.

The product gas yield increases with an increase in the gasification temperature, while the tar yield decreases with an increase in the gasification temperature. The tar yield of the steam gasification process also decreases with gasification reaction time (*i.e.*, tar yield decreases as the gasification reaction time increases).

The product gas yield increases with an increase in the steam to feedstock ratio at the initial stage but later decrease with further increase in the steam to feedstock ratio. The tar yield of the steam gasification process also follows similar trend under the same condition.

The lower heating value (LHV) for the product gas product at the optimum condition is 11.53 KJ/Nm^3 while the carbon gasification efficiency and cold gas efficiency are 10.64% and 11.38% respectively.

5.2 Original Contributions

This thesis makes two significant contributions to the field of waste to energy (WtE). The contribution to knowledge of this thesis is specific to Calgary Bio-cell and this limit the

findings to only bioreactors operated under the similar processes and cold climate conditions as that of Calgary Bio-cell. The contributions to knowledge are as follows:

- The research method used in this thesis is one of the major contributions to the field of waste to energy because the ANOVA result was able to help end users determine the temperature and reaction time that are the most important to be considered in steam gasification of EWR
- The EWR from the city of Calgary Bio-cell is a low-quality fuel and as such gasification might not be an economically viable option of generating energy from EWR

5.3 Recommendation for Future Work

The following recommendation are suggested for future research based on the study of this thesis:

Co-gasification of EWR: Co-gasification is known to enhance the quality of the product gas as well as to improve the gasification performance. However, this thesis only focused on the gasification of the EWR sample alone. The EWR sample was not co-gasified with any other type of fuel due to the limited time of a master's research. Thus, future work can investigate the effect of co-gasification of the EWR sample with other types of fuel such as raw biomass, biochar, *etc.*, to enhance the quality of product gas product and improve the gasification performance

Higher temperature and other factors affecting the gasification performance: The factors affecting the gasification process includes temperature, pressure, feedstock size, reaction time, steam to feedstock ratio, and type of gasifier used. However, the factors considered in the thesis research were temperature, reaction time and steam to feedstock ratio due to our laboratory facility. The highest temperature considered in the study is 1000 ^{0}C due to the limitation of the horizontal lab-scale reactor used in this research work. Thus, future work can investigate the effects of other factors such pressure, type of gasifier, feedstock size, and higher temperature on the gasification performance.

Other value-added product potential of the EWR sample: This research work only focused on the thermochemical conversion of the EWR into energy. The char residue of the gasification process could be a source of valuable material due to its carbonaceous nature. Therefore, future work can investigate the potential of the char residue of the gasification process by converting other into other valuable products.

Copyright Permissions

License Details

This Agreement between Stephen Banjo ("You") and Elsevier ("Elsevier") consists of your license details and the terms and conditions provided by Elsevier and Copyright Clearance Center.

Print Copy

License Number	5337060863774
License date	Jun 27, 2022
Licensed Content Publisher	Elsevier
Licensed Content Publication	Energy Conversion and Management
Licensed Content Title	Waste management, waste resource facilities and waste conversion processes
Licensed Content Author	Ayhan Demirbas
Licensed Content Date	Feb 1, 2011
Licensed Content Volume	52
Licensed Content Issue	2
Licensed Content Pages	8
Type of Use	reuse in a thesis/dissertation
Portion	figures/tables/illustrations
Number of figures/tables/illustrations	1
Format	both print and electronic
Are you the author of this Elsevier article?	No
Will you be translating?	No
Title	Characterization of excavated landfill waste from Biocell site
Institution name	University of Waterloo
Expected presentation date	Sep 2022
Portions	Table 1, Image one page 1281
Requestor Location	Stephen Banjo 110 Fergus avenue Kitchener, ON N2A0K9 Canada Attn: Stephen Banjo
Publisher Tax ID	GB 494 6272 12
Total	**0.00 CAD**

License Details

This Agreement between Stephen Banjo ("You") and Elsevier ("Elsevier") consists of your license details and the terms and conditions provided by Elsevier and Copyright Clearance Center.

Print Copy

License Number	5344920937747
License date	Jul 09, 2022
Licensed Content Publisher	Elsevier
Licensed Content Publication	Journal of Cleaner Production
Licensed Content Title	The crucial role of Waste-to-Energy technologies in enhanced landfill mining: a technology review
Licensed Content Author	A. Bosmans,I. Vanderreydt,D. Geysen,L. Helsen
Licensed Content Date	Sep 15, 2013
Licensed Content Volume	55
Licensed Content Issue	n/a
Licensed Content Pages	14
Type of Use	reuse in a thesis/dissertation
Portion	figures/tables/illustrations
Number of figures/tables/illustrations	7
Format	both print and electronic
Are you the author of this Elsevier article?	No
Will you be translating?	No
Title	Characterization of excavated landfill waste from Biocell site
Institution name	University of Waterloo
Expected presentation date	Sep 2022
Portions	figure 1, Table 3, Table 4, Figure 5, Figure 6, Figure 7, Table 9
Requestor Location	Stephen Banjo 110 Fergus avenue Kitchener, ON N2A0K9 Canada Attn: Stephen Banjo
Publisher Tax ID	GB 494 6272 12
Total	**0.00 CAD**

CCC | Marketplace™

This is a License Agreement between Stephen Banjo ("User") and Copyright Clearance Center, Inc. ("CCC") on behalf of the Rightsholder identified in the order details below. The license consists of the order details, the Marketplace Order General Terms and Conditions below, and any Rightsholder Terms and Conditions which are included below.

All payments must be made in full to CCC in accordance with the Marketplace Order General Terms and Conditions below.

Order Date	09-Sep-2022	**Type of Use**	Republish in a thesis/dissertation
Order License ID	1267064-1	**Publisher**	ELSEVIER BV
ISSN	0959-6526	**Portion**	Chart/graph/table/figure

LICENSED CONTENT

Publication Title	Journal of cleaner production	**Rightsholder**	Elsevier Science & Technology Journals
Article Title	The crucial role of Waste-to-Energy technologies in enhanced landfill mining: a technology review	**Publication Type**	Journal
		Start Page	10
Date	01/01/1993	**End Page**	23
Language	English	**Volume**	55
Country	Netherlands		

REQUEST DETAILS

Portion Type	Chart/graph/table/figure	**Distribution**	Canada
Number of charts / graphs / tables / figures requested	11	**Translation**	Original language of publication
		Copies for the disabled?	No
Format (select all that apply)	Electronic	**Minor editing privileges?**	Yes
Who will republish the content?	Not-for-profit entity	**Incidental promotional use?**	No
Duration of Use	Life of current edition	**Currency**	CAD
Lifetime Unit Quantity	Up to 499		
Rights Requested	Main product		

NEW WORK DETAILS

References

[1] S. Mishra and R. K. Upadhyay, “Review on biomass gasification: Gasifiers, gasifying mediums, and operational parameters,” *Mater Sci Energy Technol*, vol. 4, pp. 329–340, Jan. 2021, doi: 10.1016/j.mset.2021.08.009.

[2] I. Hanif, “Impact of fossil fuels energy consumption, energy policies, and urban sprawl on carbon emissions in East Asia and the Pacific: A panel investigation,” *Energy Strategy Reviews*, vol. 21, pp. 16–24, Aug. 2018, doi: 10.1016/j.esr.2018.04.006.

[3] S. Nanda, J. Isen, A. K. Dalai, and J. A. Kozinski, “Gasification of fruit wastes and agro-food residues in supercritical water,” *Energy Convers Manag*, vol. 110, pp. 296–306, Feb. 2016, doi: 10.1016/j.enconman.2015.11.060.

[4] Zhongchao Tan, *Air Pollution and Greenhouse Gases*. Singapore: Springer Science, 2014.

[5] S. C. Wijayasekera, K. Hewage, O. Siddiqui, P. Hettiaratchi, and R. Sadiq, “Waste-to-hydrogen technologies: A critical review of techno-economic and socio-environmental sustainability,” *Int J Hydrogen Energy*, Dec. 2021, doi: 10.1016/j.ijhydene.2021.11.226.

[6] World Resources institute, “Climate Change,” *Environment and Climate change in Canada*, 2018.

[7] U. Shahzad, “The Need For Renewable Energy Sources ITEE Journal The Need For Renewable Energy Sources.”

[8] IEEE Power & Energy Society., *2010 Asia-Pacific Power and Energy Engineering Conference : proceedings : March 28-31, 2010, Chengdu, China*. IEEE, 2010.

[9] D. Zhang, G. Huang, Y. Xu, and Q. Gong, “Waste-to-energy in China: Key challenges and opportunities,” *Energies (Basel)*, vol. 8, no. 12, pp. 14182–14196, 2015, doi: 10.3390/en81212422.

[10] W. Sun, X. Wang, J. F. DeCarolis, and M. A. Barlaz, “Evaluation of optimal model parameters for prediction of methane generation from selected U.S. landfills,” *Waste Management*, vol. 91, pp. 120–127, May 2019, doi: 10.1016/j.wasman.2019.05.004.

[11] A. M. Costa, R. G. de S. M. Alfaia, and J. C. Campos, “Landfill leachate treatment in Brazil – An overview,” *Journal of Environmental Management*, vol. 232. Academic Press, pp. 110–116, Feb. 15, 2019. doi: 10.1016/j.jenvman.2018.11.006.

[12] O. K. M. Ouda, S. A. Raza, A. S. Nizami, M. Rehan, R. Al-Waked, and N. E. Korres, “Waste to energy potential: A case study of Saudi Arabia,” *Renewable and Sustainable Energy Reviews*, vol. 61. Elsevier Ltd, pp. 328–340, Aug. 01, 2016. doi: 10.1016/j.rser.2016.04.005.

[13] S. T. Tan, C. T. Lee, H. Hashim, W. S. Ho, and J. S. Lim, “Optimal process network for municipal solid waste management in Iskandar Malaysia,” in *Journal of Cleaner Production*, May 2014, vol. 71, pp. 48–58. doi: 10.1016/j.jclepro.2013.12.005.

[14] J. Havukainen *et al.*, “Environmental impact assessment of municipal solid waste management incorporating mechanical treatment of waste and incineration in Hangzhou, China,” *J Clean Prod*, vol. 141, pp. 453–461, Jan. 2017, doi: 10.1016/j.jclepro.2016.09.146.

[15] M. Cuberos Balda, T. Furubayashi, and T. Nakata, “Integration of WTE technologies into the electrical system for low-carbon growth in Venezuela,” *Renew Energy*, vol. 86, pp. 1247–1255, Feb. 2016, doi: 10.1016/j.renene.2015.09.052.

[16] L. P. Güereca, N. Torres, and C. R. Juárez-López, “The co-processing of municipal waste in a cement kiln in Mexico. A life-cycle assessment approach,” *J Clean Prod*, vol. 107, pp. 741–748, Nov. 2015, doi: 10.1016/j.jclepro.2015.05.085.

[17] M. D. Vaverková, “Landfill impacts on the environment— review,” *Geosciences (Switzerland)*, vol. 9, no. 10. MDPI AG, Oct. 01, 2019. doi: 10.3390/geosciences9100431.

[18] N. Wichai-utcha and O. Chavalparit, “3Rs Policy and plastic waste management in Thailand,” *Journal of Material Cycles and Waste Management*, vol. 21, no. 1. Springer Tokyo, pp. 10–22, Jan. 22, 2019. doi: 10.1007/s10163-018-0781-y.

[19] Z. Hameed *et al.*, “Gasification of municipal solid waste blends with biomass for energy production and resources recovery: Current status, hybrid technologies and innovative prospects,” *Renewable and Sustainable Energy Reviews*, vol. 136, Feb. 2021, doi: 10.1016/j.rser.2020.110375.

[20] N. Perera, D. van Everdingen, D. Davies, J. Hundal PEng, and J. Hettiaratchi, “Bioreactor Landfills-An Innovative Technology for Biostabilization of Municipal Solid Waste.”

[21] C. H. Hettiarachchi, J. N. Meegoda, J. Tavantzis, and P. Hettiaratchi, “Numerical model to predict settlements coupled with landfill gas pressure in bioreactor landfills,” *J Hazard Mater*, vol. 139, no. 3, pp. 514–522, Jan. 2007, doi: 10.1016/j.jhazmat.2006.02.067.

[22] C. A. Hunte, C. H. Hettiarachchi, J. N. Meegoda, and J. P. A. Hettiaratchi, “The City of Calgary Biocell Landfill: Data Collection and Settlement Predictions using a Multiphase Model,” 2012.

[23] J. N. Meegoda, H. Hettiarachchi, and P. Hettiaratchi, “Landfill design and operation,” in *Sustainable Solid Waste Management*, American Society of Civil Engineers (ASCE), 2016, pp. 577–604. doi: 10.1061/9780784414101.ch18.

[24] I. N. Zaini *et al.*, “Production of H2-rich syngas from excavated landfill waste through steam co-gasification with biochar,” *Energy*, vol. 207, Sep. 2020, doi: 10.1016/j.energy.2020.118208.

[25] R. Millati, R. B. Cahyono, T. Ariyanto, I. N. Azzahrani, R. U. Putri, and M. J. Taherzadeh, “Agricultural, industrial, municipal, and forest wastes: An overview,” in *Sustainable Resource Recovery and Zero Waste Approaches*, Elsevier, 2019, pp. 1–22. doi: 10.1016/B978-0-444-64200-4.00001-3.

[26] A. Demirbas, “Waste management, waste resource facilities and waste conversion processes,” *Energy Convers Manag*, vol. 52, no. 2, pp. 1280–1287, Feb. 2011, doi: 10.1016/j.enconman.2010.09.025.

[27] W. S. Ho, H. Hashim, J. S. Lim, C. T. Lee, K. C. Sam, and S. T. Tan, “Waste Management Pinch Analysis (WAMPA): Application of Pinch Analysis for greenhouse gas (GHG) emission reduction in municipal solid waste management,” *Appl Energy*, vol. 185, pp. 1481–1489, Jan. 2017, doi: 10.1016/j.apenergy.2016.01.044.

[28] A. Kan, “General characteristics of waste management: A review,” 2009. [Online]. Available: https://www.researchgate.net/publication/272677203

[29] M. Batayneh, I. Marie, and I. Asi, “Use of selected waste materials in concrete mixes,” *Waste Management*, vol. 27, no. 12, pp. 1870–1876, 2007, doi: 10.1016/j.wasman.2006.07.026.

[30] L. Rushton, “Health hazards and waste management,” *British Medical Bulletin*, vol. 68. pp. 183–197, 2003. doi: 10.1093/bmb/ldg034.

[31] R. Siddique, J. Khatib, and I. Kaur, “Use of recycled plastic in concrete: A review,” *Waste Management*, vol. 28, no. 10, pp. 1835–1852, 2008, doi: 10.1016/j.wasman.2007.09.011.

[32] V. W. Y. Tam and C. M. Tam, “A review on the viable technology for construction waste recycling,” *Resources, Conservation and Recycling*, vol. 47, no. 3. pp. 209–221, Jun. 2006. doi: 10.1016/j.resconrec.2005.12.002.

[33] S. Saheri, M. Aghajani Mir, N. Ezlin Ahmad Basri, R. Ara Begum, and N. Zalina Binti Mahmood, “Solid Waste Management by Considering Composting Potential in Malaysia Toward a Green Country,” 2009.

[34] A. Johari, H. Alkali, H. Hashim, S. I. Ahmed, and R. Mat, “Municipal solid waste management and potential revenue from recycling in Malaysia,” *Mod Appl Sci*, vol. 8, no. 4, pp. 37–49, 2014, doi: 10.5539/mas.v8n4p37.

[35] P. S. , G. S. P. , P. A. K. , A. M. K. , & S. S. Bundela, “Municipal solid waste management in Indian cities - A review,” *internation journa of Environmental Sciences*, vol. 1, no. 4, 2010.

[36] A. K. Pathak, M. M. Singh, and V. Kumar, “Composting of Municipal Solid Waste: a Sustainable Waste Management Technique in Indian Cities-a Review.” [Online]. Available: http://www.journalcra.com

[37] A. H. Molla, A. Fakhru’l-Razi, M. M. Hanafi, and M. Z. Alam, “Compost produced by solid state bioconversion of biosolids: A potential resource for plant growth and environmental friendly disposal,” *Commun Soil Sci Plant Anal*, vol. 36, no. 11–12, pp. 1435–1447, 2005, doi: 10.1081/CSS-200058487.

[38] M. Yeheyis, K. Hewage, M. S. Alam, C. Eskicioglu, and R. Sadiq, “An overview of construction and demolition waste management in Canada: A lifecycle analysis approach to sustainability,” *Clean Technologies and Environmental Policy*, vol. 15, no. 1. Springer Verlag, pp. 81–91, 2013. doi: 10.1007/s10098-012-0481-6.

[39] S.-S. Chung and C. W. H. Lo, “Evaluating sustainability in waste management: the case of construction and demolition, chemical and clinical wastes in Hong Kong.” [Online]. Available: www.elsevier.com/locate/resconrec

[40] S. Nanda and F. Berruti, “Municipal solid waste management and landfilling technologies: a review,” *Environmental Chemistry Letters*, vol. 19, no. 2. Springer Science and Business Media Deutschland GmbH, pp. 1433–1456, Apr. 01, 2021. doi: 10.1007/s10311-020-01100-y.

[41] P. T. Jones *et al.*, “Enhanced Landfill Mining in view of multiple resource recovery: A critical review,” *Journal of Cleaner Production*, vol. 55. pp. 45–55, Sep. 15, 2013. doi: 10.1016/j.jclepro.2012.05.021.

[42] L. Giroux, “State of Waste Management in Canada Prepared for: Canadian Council of Ministers of Environment.”

[43] H.-J. Ehrig, H.-J. Schneider, and V. Gossow, “Waste, 7. Deposition,” in *Ullmann’s Encyclopedia of Industrial Chemistry*, Wiley-VCH Verlag GmbH & Co. KGaA, 2011. doi: 10.1002/14356007.o28_o07.

[44] T. Narayana, “Municipal solid waste management in India: From waste disposal to recovery of resources?,” *Waste Management*, vol. 29, no. 3, pp. 1163–1166, Mar. 2009, doi: 10.1016/j.wasman.2008.06.038.

[45] J. P. A. Hettiaratchi, “New Trends in Waste Management: North American Perspective,” 2007.

[46] C. C. and A. M. Sunil Kumar, “Bioreactor landfill technology in municipal solid waste treatment: An overview,” *Crit Rev Biotechnol*, vol. 31, no. 1, pp. 77–97, 2011.

[47] J. Krook, N. Svensson, and M. Eklund, “Landfill mining: A critical review of two decades of research,” *Waste Management*, vol. 32, no. 3, pp. 513–520, Mar. 2012, doi: 10.1016/j.wasman.2011.10.015.

[48] P. T. Jones *et al.*, “Enhanced Landfill Mining in view of multiple resource recovery: A critical review,” *Journal of Cleaner Production*, vol. 55. pp. 45–55, Sep. 15, 2013. doi: 10.1016/j.jclepro.2012.05.021.

[49] M. Danthurebandara, S. van Passel, I. Vanderreydt, and K. van Acker, “Assessment of environmental and economic feasibility of Enhanced Landfill Mining,” *Waste Management*, vol. 45, pp. 434–447, Oct. 2014, doi: 10.1016/j.wasman.2015.01.041.

[50] M. Banar and A. Özkan, “Characterization of the municipal solid waste in Eskisehir City, Turkey,” *Environ Eng Sci*, vol. 25, no. 8, pp. 1213–1219, Oct. 2008, doi: 10.1089/ees.2007.0164.

[51] D. Khan, A. Kumar, and S. R. Samadder, “Impact of socioeconomic status on municipal solid waste generation rate,” *Waste Management*, vol. 49, pp. 15–25, Mar. 2016, doi: 10.1016/j.wasman.2016.01.019.

[52] P. T. Jones *et al.*, “Enhanced Landfill Mining in view of multiple resource recovery: A critical review,” *Journal of Cleaner Production*, vol. 55. pp. 45–55, Sep. 15, 2013. doi: 10.1016/j.jclepro.2012.05.021.

[53] A. Bosmans, I. Vanderreydt, D. Geysen, and L. Helsen, “The crucial role of Waste-to-Energy technologies in enhanced landfill mining: A technology review,” *J Clean Prod*, vol. 55, pp. 10–23, Sep. 2013, doi: 10.1016/j.jclepro.2012.05.032.

[54] A. Bosmans, I. Vanderreydt, D. Geysen, and L. Helsen, “The crucial role of Waste-to-Energy technologies in enhanced landfill mining: A technology review,” *J Clean Prod*, vol. 55, pp. 10–23, Sep. 2013, doi: 10.1016/j.jclepro.2012.05.032.

[55] I. N. Zaini, A. Nurdiawati, and M. Aziz, “Cogeneration of power and H2 by steam gasification and syngas chemical looping of macroalgae,” *Appl Energy*, vol. 207, pp. 134–145, Dec. 2017, doi: 10.1016/j.apenergy.2017.06.071.

[56] A. Khalid, M. Arshad, M. Anjum, T. Mahmood, and L. Dawson, “The anaerobic digestion of solid organic waste,” *Waste Management*, vol. 31, no. 8. pp. 1737–1744, Aug. 2011. doi: 10.1016/j.wasman.2011.03.021.

[57] A. Demirbas, “Biomass resource facilities and biomass conversion processing for fuels and chemicals.” [Online]. Available: www.elsevier.com/locate/enconman

[58] A. J. Ward, P. J. Hobbs, P. J. Holliman, and D. L. Jones, “Optimisation of the anaerobic digestion of agricultural resources,” *Bioresource Technology*, vol. 99, no. 17. pp. 7928–7940, Nov. 2008. doi: 10.1016/j.biortech.2008.02.044.

[59] G. C. Young, “Municipal Solid Waste to Energy Conversion Processes Economic, Technical, and Renewable Comparisons.”

[60] G. Maschio, C. Koufopanos, and A. Lucchesi, “Pyrolysis, a Promising Route for Biomass Utilization,” 1992.

[61] Y. Chhiti and M. Kemiha, “Thermal Conversion of Biomass, Pyrolysis and Gasification: A Review.” [Online]. Available: www.theijes.com

[62] S. A. Salaudeen, P. Arku, and A. Dutta, “Gasification of plastic solid waste and competitive technologies,” in *Plastics to Energy: Fuel, Chemicals, and Sustainability Implications*, Elsevier, 2018, pp. 269–293. doi: 10.1016/B978-0-12-813140-4.00010-8.

[63] N. Mahinpey and A. Gomez, “Review of gasification fundamentals and new findings: Reactors, feedstock, and kinetic studies,” *Chemical Engineering Science*, vol. 148. Elsevier Ltd, pp. 14–31, Jul. 12, 2016. doi: 10.1016/j.ces.2016.03.037.

[64] A. v Bridgwater, “A Catalysis in thermal biomass conversion.”

[65]. “Draft of a German Report with basic informations for a BREF-Document ‘Waste Incineration,’” 2001.

[66] S. Begum, M. G. Rasul, D. Cork, and D. Akbar, “An experimental investigation of solid waste gasification using a large pilot scale waste to energyplant,” in *Procedia Engineering*, 2014, vol. 90, pp. 718–724. doi: 10.1016/j.proeng.2014.11.802.

[67] C. Wu and P. T. Williams, “Pyrolysis-gasification of plastics, mixed plastics and real-world plastic waste with and without Ni-Mg-Al catalyst,” *Fuel*, vol. 89, no. 10, pp. 3022–3032, 2010, doi: 10.1016/j.fuel.2010.05.032.

[68] A. Klein and N. J. Themelis, “Energy Recovery from Municipal Solid Wastes by Gasification-asme/terms-of-use.” [Online]. Available: http://www.asme.org/about-asme/terms-of-use

[69] S. K. Sansaniwal, K. Pal, M. A. Rosen, and S. K. Tyagi, “Recent advances in the development of biomass gasification technology: A comprehensive review,” *Renewable and Sustainable Energy Reviews*, vol. 72. Elsevier Ltd, pp. 363–384, 2017. doi: 10.1016/j.rser.2017.01.038.

[70] J. Ren, J. P. Cao, X. Y. Zhao, F. L. Yang, and X. Y. Wei, “Recent advances in syngas production from biomass catalytic gasification: A critical review on reactors, catalysts, catalytic mechanisms and mathematical models,” *Renewable and Sustainable Energy Reviews*, vol. 116. Elsevier Ltd, Dec. 01, 2019. doi: 10.1016/j.rser.2019.109426.

[71] D. Hantoko, M. Yan, B. Prabowo, H. Susanto, X. Li, and C. Chen, “Aspen plus modeling approach in solid waste gasification,” in *Current Developments in Biotechnology and Bioengineering: Waste Treatment Processes for Energy Generation*, Elsevier, 2019, pp. 259–281. doi: 10.1016/B978-0-444-64083-3.00013-0.

[72] A. Kumar, K. Eskridge, D. D. Jones, and M. A. Hanna, “Steam-air fluidized bed gasification of distillers grains: Effects of steam to biomass ratio, equivalence ratio and gasification temperature,” *Bioresour Technol*, vol. 100, no. 6, pp. 2062–2068, Mar. 2009, doi: 10.1016/j.biortech.2008.10.011.

[73] S. Pang, “Fuel flexible gas production: Biomass, coal and bio-solid wastes,” in *Fuel Flexible Energy Generation: Solid, Liquid and Gaseous Fuels*, Elsevier Inc., 2016, pp. 241–269. doi: 10.1016/B978-1-78242-378-2.00009-2.

[74] C. Z. Zaman *et al.*, “Pyrolysis: A Sustainable Way to Generate Energy from Waste,” in *Pyrolysis*, InTech, 2017. doi: 10.5772/intechopen.69036.

[75] A. Kumar, D. D. Jones, and M. A. Hanna, “Thermochemical biomass gasification: A review of the current status of the technology,” *Energies*, vol. 2, no. 3. pp. 556–581, Sep. 2009. doi: 10.3390/en20300556.

[76] M. Sharma and R. Kaushal, “Advances and challenges in the generation of bio-based fuels using gasifiers: a comprehensive review,” *International Journal of Ambient Energy*, vol. 41, no. 14. Taylor and Francis Ltd., pp. 1645–1663, Dec. 05, 2020. doi: 10.1080/01430750.2018.1517687.

[77] C. Xu, J. Donald, E. Byambajav, and Y. Ohtsuka, “Recent advances in catalysts for hot-gas removal of tar and NH3 from biomass gasification,” *Fuel*, vol. 89, no. 8. Elsevier Ltd, pp. 1784–1795, 2010. doi: 10.1016/j.fuel.2010.02.014.

[78] V. S. Sikarwar, M. Zhao, P. S. Fennell, N. Shah, and E. J. Anthony, “Progress in biofuel production from gasification,” *Progress in Energy and Combustion Science*, vol. 61. Elsevier Ltd, pp. 189–248, 2017. doi: 10.1016/j.pecs.2017.04.001.

[79] F. Pinto, C. Franco, R. N. Andre, M. Miranda, I. Gulyurtlu, and I. Cabrita, “Co-gasi®cation study of biomass mixed with plastic wastes.”

[80] S. D. Anuar Sharuddin, F. Abnisa, W. M. A. Wan Daud, and M. K. Aroua, “A review on pyrolysis of plastic wastes,” *Energy Conversion and Management*, vol. 115. Elsevier Ltd, pp. 308–326, May 01, 2016. doi: 10.1016/j.enconman.2016.02.037.

[81] G. Chen, J. Andries, Z. Luo, and H. Spliethoff, “Biomass pyrolysis/gasification for product gas production: the overall investigation of parametric effects,” 2003. [Online]. Available: www.elsevier.com/locate/enconman

[82] J. Li, Y. Yin, J. Liu, and R. Yan, “Hydrogen-rich gas production from steam gasification of palm oil wastes using the supported nano-NiO/γ-Al2O3 catalyst,” in *2009 International Conference on Energy and Environment Technology, ICEET 2009*, 2009, vol. 1, pp. 185–189. doi: 10.1109/ICEET.2009.51.

[83] John. Scheirs and W. (Walter) Kaminsky, *Feedstock recycling and pyrolysis of waste plastics : converting waste plastics into diesel and other fuels*. J. Wiley & Sons, 2006.

[84] H. A. Choudhury, S. Chakma, and V. S. Moholkar, “Biomass Gasification Integrated Fischer-Tropsch Synthesis: Perspectives, Opportunities and Challenges,” in *Recent Advances in Thermochemical Conversion of Biomass*, Elsevier Inc., 2015, pp. 383–435. doi: 10.1016/B978-0-444-63289-0.00014-4.

[85] S. K. Sansaniwal, K. Pal, M. A. Rosen, and S. K. Tyagi, “Recent advances in the development of biomass gasification technology: A comprehensive review,” *Renewable and Sustainable Energy Reviews*, vol. 72. Elsevier Ltd, pp. 363–384, 2017. doi: 10.1016/j.rser.2017.01.038.

[86] A. K. Rajvanshi, “Biomass gasification.”

[87] G. Gautam, S. Adhikari, S. Thangalazhy-Gopakumar, C. Brodbeck, S. Bhavnani, and S. Taylor, “Tar analysis in syngas,” 2011.

[88] T. Srivastava, “Renewable Energy (Gasification),” 2013. [Online]. Available: http://www.ripublication.com/aeee.htm

[89] M. L. Valderrama Rios, A. M. González, E. E. S. Lora, and O. A. Almazán del Olmo, “Reduction of tar generated during biomass gasification: A review,” *Biomass and Bioenergy*, vol. 108. Elsevier Ltd, pp. 345–370, Jan. 01, 2018. doi: 10.1016/j.biombioe.2017.12.002.

[90] M. Siedlecki, R. Nieuwstraten, E. Simeone, W. de Jong, and A. H. M. Verkooijen, “Effect of magnesite as bed material in a 100 kWth steam-oxygen blown circulating fluidized-bed biomass gasifier on gas composition and tar formation,” *Energy and Fuels*, vol. 23, no. 11, pp. 5643–5654, Nov. 2009, doi: 10.1021/ef900420c.

[91] J. D. Morris, S. S. Daood, S. Chilton, and W. Nimmo, “Mechanisms and mitigation of agglomeration during fluidized bed combustion of biomass: A review,” *Fuel*, vol. 230. Elsevier Ltd, pp. 452–473, Oct. 15, 2018. doi: 10.1016/j.fuel.2018.04.098.

[92] R. Thomson, P. Kwong, E. Ahmad, and K. D. P. Nigam, “Clean syngas from small commercial biomass gasifiers; a review of gasifier development, recent advances and performance evaluation,” *International Journal of Hydrogen Energy*, vol. 45, no. 41. Elsevier Ltd, pp. 21087–21111, Aug. 21, 2020. doi: 10.1016/j.ijhydene.2020.05.160.

[93] R. Warnecke, “Gasification of biomass: comparison of fixed bed and uidized bed gasifier.” [Online]. Available: www.elsevier.com/locate/biombioe

[94] H. A. Choudhury, S. Chakma, and V. S. Moholkar, “Biomass Gasification Integrated Fischer-Tropsch Synthesis: Perspectives, Opportunities and Challenges,” in *Recent Advances in Thermochemical Conversion of Biomass*, Elsevier Inc., 2015, pp. 383–435. doi: 10.1016/B978-0-444-63289-0.00014-4.

[95] J. M. Wheeldon and D. Thimsen, “Economic evaluation of circulating fluidized bed combustion (CFBC) power generation plants,” in *Fluidized Bed Technologies for Near-Zero Emission Combustion and Gasification*, Elsevier Ltd., 2013, pp. 620–638. doi: 10.1533/9780857098801.2.620.

[96] D. Gray, “Major gasifiers for IGCC systems,” in *Integrated Gasification Combined Cycle (IGCC) Technologies*, Elsevier Inc., 2017, pp. 305–355. doi: 10.1016/B978-0-08-100167-7.00008-1.

[97] I. L. Motta, N. T. Miranda, R. Maciel Filho, and M. R. Wolf Maciel, “Biomass gasification in fluidized beds: A review of biomass moisture content and operating pressure effects,” *Renewable and Sustainable Energy Reviews*, vol. 94. Elsevier Ltd, pp. 998–1023, Oct. 01, 2018. doi: 10.1016/j.rser.2018.06.042.

[98] Y. Zhao *et al.*, “Experimental study on sawdust air gasification in an entrained-flow reactor,” in *Fuel Processing Technology*, Aug. 2010, vol. 91, no. 8, pp. 910–914. doi: 10.1016/j.fuproc.2010.01.012.

[99] H. Hofbauer and M. Materazzi, “Waste gasification processes for SNG production,” in *Substitute Natural Gas from Waste: Technical Assessment and Industrial Applications of Biochemical and Thermochemical Processes*, Elsevier, 2019, pp. 105–160. doi: 10.1016/B978-0-12-815554-7.00007-6.

[100] C. R. Cheeseman, S. Monteiro Da Rocha, C. Sollars, S. Bethanis, and A. R. Boccaccini, “Ceramic processing of incinerator bottom ash,” *Waste Management*, vol. 23, no. 10, pp. 907–916, 2003, doi: 10.1016/S0956-053X(03)00039-4.

[101] S. Burnley, R. Phillips, T. Coleman, and T. Rampling, “Energy implications of the thermal recovery of biodegradable municipal waste materials in the United Kingdom,” *Waste Management*, vol. 31, no. 9–10, pp. 1949–1959, 2011, doi: 10.1016/j.wasman.2011.04.015.

[102] C. G. López, A. Ni, J. C. Hernández Parrodi, B. Küppers, K. Raulf, and T. Pretz, “Characterization of landfill mining material after ballistic separation to evaluate material and energy recovery potential,” *Detritus*, vol. 8, no. December, pp. 5–23, Dec. 2019, doi: 10.31025/2611-4135/2019.13780.

[103] M. Quaghebeur *et al.*, “Characterization of landfilled materials: Screening of the enhanced landfill mining potential,” *J Clean Prod*, vol. 55, pp. 72–83, Sep. 2013, doi: 10.1016/j.jclepro.2012.06.012.

[104] T. Prechthai, M. Padmasri, and C. Visvanathan, “Quality assessment of mined MSW from an open dumpsite for recycling potential,” *Resour Conserv Recycl*, vol. 53, no. 1–2, pp. 70–78, Dec. 2008, doi: 10.1016/j.resconrec.2008.09.002.

[105] T. Kaartinen, K. Sormunen, and J. Rintala, “Case study on sampling, processing and characterization of landfilled municipal solid waste in the view of landfill mining,” *J Clean Prod*, vol. 55, pp. 56–66, Sep. 2013, doi: 10.1016/j.jclepro.2013.02.036.

[106] M. Quaghebeur *et al.*, “Characterization of landfilled materials: Screening of the enhanced landfill mining potential,” *J Clean Prod*, vol. 55, pp. 72–83, Sep. 2013, doi: 10.1016/j.jclepro.2012.06.012.

[107] C. G. López, A. Ni, J. C. Hernández Parrodi, B. Küppers, K. Raulf, and T. Pretz, “Characterization of landfill mining material after ballistic separation to evaluate material and energy recovery potential,” *Detritus*, vol. 8, no. December, pp. 5–23, Dec. 2019, doi: 10.31025/2611-4135/2019.13780.

[108] S. Nanda, J. Isen, A. K. Dalai, and J. A. Kozinski, “Gasification of fruit wastes and agro-food residues in supercritical water,” *Energy Convers Manag*, vol. 110, pp. 296–306, Feb. 2016, doi: 10.1016/j.enconman.2015.11.060.

[109] M. Zhai *et al.*, “Gasification characteristics of sawdust char at a high-temperature steam atmosphere,” *Energy*, vol. 128, pp. 509–518, 2017, doi: 10.1016/j.energy.2017.04.083.

[110] M. Wang, Q. Du, Y. Li, J. Xu, J. Gao, and H. Wang, “Effect of steam on the transformation of sulfur during demineralized coal pyrolysis,” *J Anal Appl Pyrolysis*, vol. 140, pp. 161–169, Jun. 2019, doi: 10.1016/j.jaap.2019.03.011.

[111] S. Yusup, Z. Khan, M. M. Ahmad, and N. A. Rashidi, “Optimization of hydrogen production in in-situ catalytic adsorption (ICA) steam gasification based on response surface methodology,” *Biomass Bioenergy*, vol. 60, pp. 98–107, Jan. 2014, doi: 10.1016/j.biombioe.2013.11.007.

[112] M. Uy and J. K. Telford, “Optimization by Design of Experiment Techniques.”

[113] M. Saidi, M. H. Gohari, and A. T. Ramezani, “Hydrogen production from waste gasification followed by membrane filtration: a review,” *Environmental Chemistry Letters*, vol. 18, no. 5. Springer, pp. 1529–1556, Sep. 01, 2020. doi: 10.1007/s10311-020-01030-9.

[114] M. He, B. Xiao, Z. Hu, S. Liu, X. Guo, and S. Luo, “Syngas production from catalytic gasification of waste polyethylene: Influence of temperature on gas yield and composition,” *Int J Hydrogen Energy*, vol. 34, no. 3, pp. 1342–1348, Feb. 2009, doi: 10.1016/j.ijhydene.2008.12.023.

[115] S. Nanda, A. K. Dalai, and J. A. Kozinski, “Supercritical water gasification of timothy grass as an energy crop in the presence of alkali carbonate and hydroxide catalysts,” *Biomass Bioenergy*, vol. 95, pp. 378–387, Dec. 2016, doi: 10.1016/j.biombioe.2016.05.023.

[116] N. Sophonrat, L. Sandström, I. N. Zaini, and W. Yang, “Stepwise pyrolysis of mixed plastics and paper for separation of oxygenated and hydrocarbon condensates,” *Appl Energy*, vol. 229, pp. 314–325, Nov. 2018, doi: 10.1016/j.apenergy.2018.08.006.

[117] F. Benedikt, J. Fuchs, J. C. Schmid, S. Müller, and H. Hofbauer, “Advanced dual fluidized bed steam gasification of wood and lignite with calcite as bed material,” *Korean Journal of Chemical Engineering*, vol. 34, no. 9, pp. 2548–2558, Sep. 2017, doi: 10.1007/s11814-017-0141-y.

[118] M. Materazzi, P. Lettieri, R. Taylor, and C. Chapman, “Performance analysis of RDF gasification in a two stage fluidized bed-plasma process,” *Waste Management*, vol. 47, pp. 256–266, 2016, doi: 10.1016/j.wasman.2015.06.016.

[119] I. N. Zaini, C. García López, T. Pretz, W. Yang, and P. G. Jönsson, “Characterization of pyrolysis products of high-ash excavated-waste and its char gasification reactivity

and kinetics under a steam atmosphere," *Waste Management*, vol. 97, pp. 149–163, Sep. 2019, doi: 10.1016/j.wasman.2019.08.001.

[120] F. Pinto *et al.*, "Gasification improvement of a poor quality solid recovered fuel (SRF). Effect of using natural minerals and biomass wastes blends," *Fuel*, vol. 117, no. PARTB, pp. 1034–1044, 2014, doi: 10.1016/j.fuel.2013.10.015.

[121] C. Zhou, W. Fang, W. Xu, A. Cao, and R. Wang, "Characteristics and the recovery potential of plastic wastes obtained from landfill mining," *J Clean Prod*, vol. 80, pp. 80–86, Oct. 2014, doi: 10.1016/j.jclepro.2014.05.083.

[122] J. Fermoso *et al.*, "Application of response surface methodology to assess the combined effect of operating variables on high-pressure coal gasification for H2-rich gas production," *Int J Hydrogen Energy*, vol. 35, no. 3, pp. 1191–1204, Feb. 2010, doi: 10.1016/j.ijhydene.2009.11.046.

[123] S. Nanda and F. Berruti, "Thermochemical conversion of plastic waste to fuels: a review," *Environmental Chemistry Letters*, vol. 19, no. 1. Springer Science and Business Media Deutschland GmbH, pp. 123–148, Feb. 01, 2021. doi: 10.1007/s10311-020-01094-7.

[124] D. Saebea, P. Ruengrit, A. Arpornwichanop, and Y. Patcharavorachot, "Gasification of plastic waste for synthesis gas production," in *Energy Reports*, Feb. 2020, vol. 6, pp. 202–207. doi: 10.1016/j.egyr.2019.08.043.

[125] D. Vamvuka and S. Sfakiotakis, "Effects of heating rate and water leaching of perennial energy crops on pyrolysis characteristics and kinetics," *Renew Energy*, vol. 36, no. 9, pp. 2433–2439, Sep. 2011, doi: 10.1016/j.renene.2011.02.013.

[126] L. Deng, T. Zhang, and D. Che, "Effect of water washing on fuel properties, pyrolysis and combustion characteristics, and ash fusibility of biomass," *Fuel Processing Technology*, vol. 106, pp. 712–720, Feb. 2013, doi: 10.1016/j.fuproc.2012.10.006.

Appendix A

Calibration of gas Chromatography

The gas chromatography was calibrated with similar composition of the gaseous mixture produce during the steam gasification process. The calibration mixture was ordered from Air Liquid Canada Inc based on the concentration and composition of the gasification product. The calibration mixture ordered from Air Liquid Canada Inc are Carbon monoxide (CO) 30%, Carbon dioxide (CO_2) 10%, Hydrogen (H_2)10%, Methane (CH_4) 20% and Nitrogen (N_2) was used to balance the concentration. Nitrogen was used to balance the calibration mixture because N_2 was only used to purge the gasification system before and after the gasification process.

The calibration curve was derived by correlating the peak area of the GC output from the calibration mixture and the peak area of the GC output from the steam gasification test. Figure A.1 (a) and (b) shows the GC output for the thermal conductivity detector (TCD), and the flame ionization detector for the calibration gas mixture. For the TCD (a), H_2 was the first gas to be identified followed by N_2, CO, CH_4 and CO_2 gas. For the FID (b), CH_4 was the only gas identified.

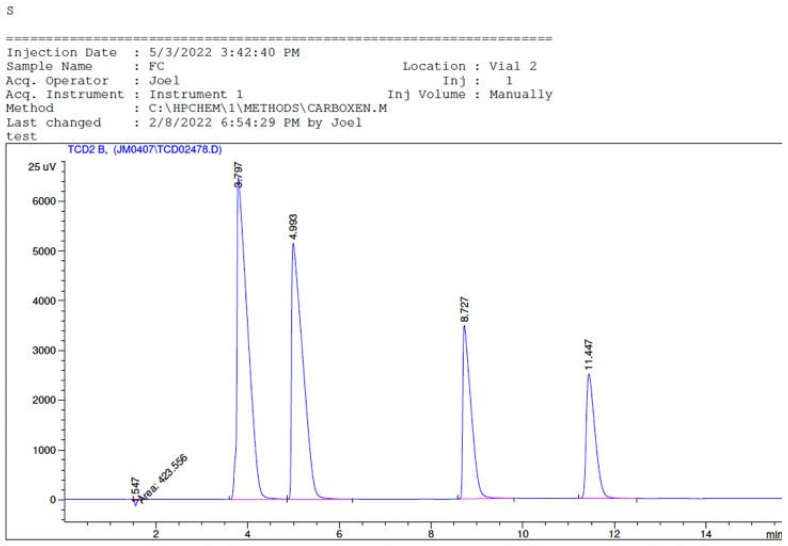

(a)

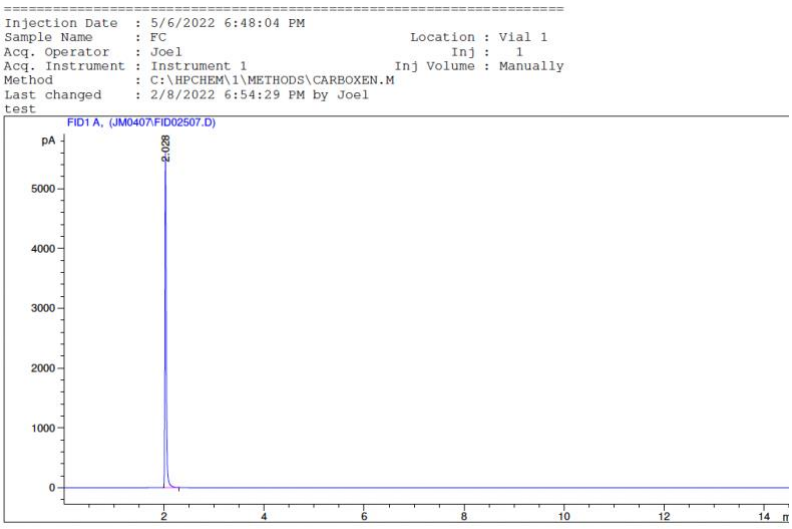

(b)

Figure A.1 (a) GC output for thermal conductivity detector (TCD), (b) GC output for flame ionization detector for the gas mixture.

Figure A.2 shows the calibration curve CO, CO_2, H_2, and CH_4. The GC output for the steam gasification test is linearly correlated with the GC output for the calibration mixture. The regression equation from the calibration curve was used to determine the concentration of the gaseous product of the steam gasification.

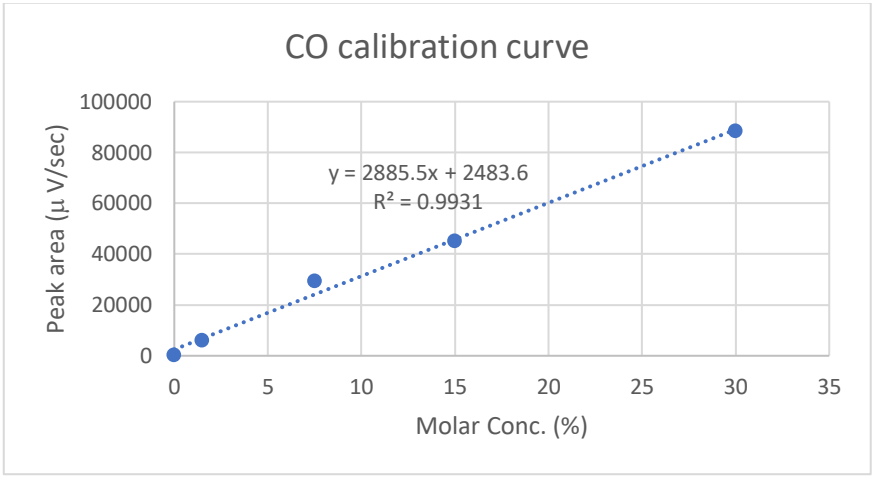

(a)

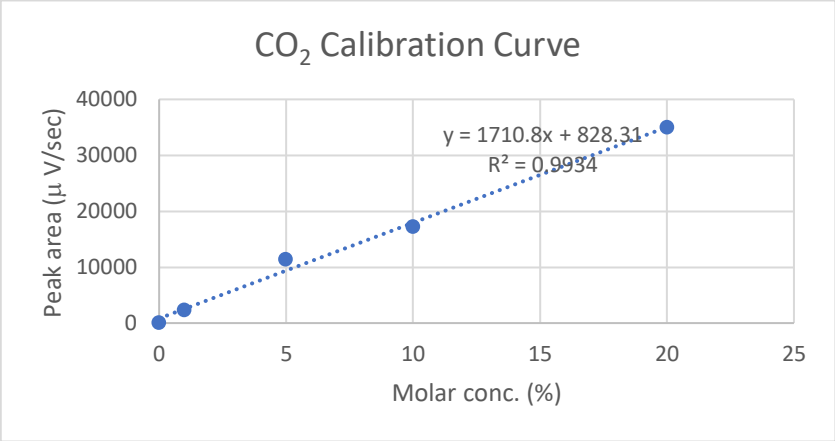

(b)

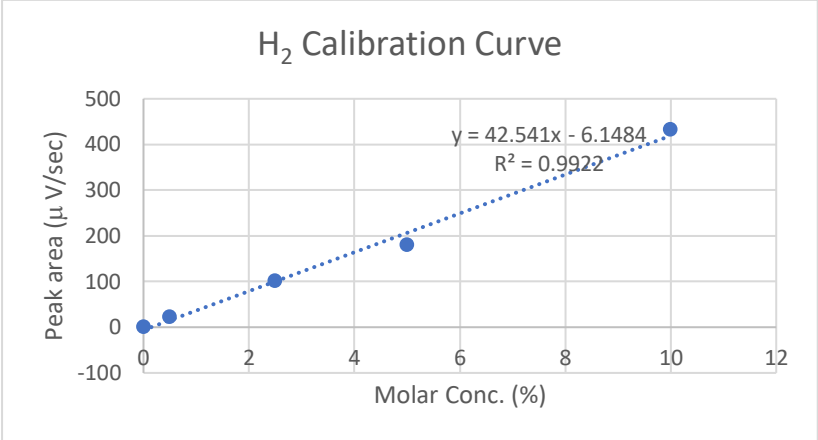

(c)

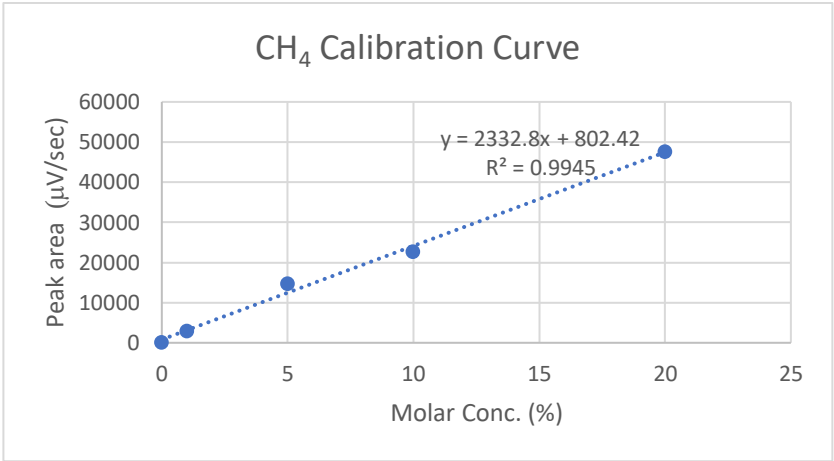

(d)

Figure A.2 (a) Calibration curve for CO, (b) Calibration curve for CO_2, (c) Calibration curve for H_2, (d) Calibration curve for CH_4.